



NUCLEAR WASTE
MANAGEMENT
ORGANIZATION

SOCIÉTÉ DE GESTION
DES DÉCHETS
NUCLÉAIRES

Phase 2 Geoscientific Preliminary Assessment

Lineament Interpretation

TOWNSHIP OF WHITE RIVER AND AREA, ONTARIO



APM-REP-01332-0210

APRIL 2017

This report has been prepared under contract to the NWMO. The report has been reviewed by the NWMO, but the views and conclusions are those of the authors and do not necessarily represent those of the NWMO.

All copyright and intellectual property rights belong to the NWMO.

For more information, please contact:

Nuclear Waste Management Organization

22 St. Clair Avenue East, Sixth Floor

Toronto, Ontario M4T 2S3 Canada

Tel 416.934.9814

Toll Free 1.866.249.6966

Email contactus@nwmo.ca

www.nwmo.ca

Phase 2 Geoscientific Preliminary Assessment

Lineament Interpretation, Township of White River and Area, Ontario

Report Prepared for
Nuclear Waste Management Organization



Report Prepared by



SRK Consulting (Canada) Inc.
SRK Project Number: 3CN020.004
NWMO Report Number: APM-REP-01332-0210
August 18, 2016
Reissued April 25, 2017

Phase 2 Geoscientific Preliminary Assessment, Lineament Interpretation, Township of White River, Ontario

Nuclear Waste Management Organization

22 St. Clair Avenue East, Sixth Floor
Toronto, Ontario, Canada
M4T 2S3
E-mail: contactus@nwmo.ca
Website: www.nwmo.ca
Tel: +1 416 934 9814
Fax: +1 416 934 9526

SRK Consulting (Canada) Inc.

1300, 151 Yonge Street
Toronto, Ontario, Canada
M5C 2W7
E-mail: toronto@srk.com
Website: www.srk.com
Tel: +1 416 601 1445
Fax: +1 416 601 9046

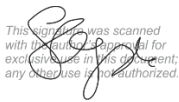
SRK Project Number: 3CN020.004

NWMO Report Number: APM-REP-01332-0210

August 18, 2016

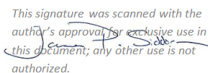
Reissued April 25, 2017

Authored by:


This signature was scanned with the author's approval for exclusive use in this document; any other use is not authorized.

Simon Craggs, MSc
Senior Consultant (Structural Geology)

Reviewed by:


This signature was scanned with the author's approval for exclusive use in this document; any other use is not authorized.

James Siddorn, PhD, PGeo
Principal Consultant (Structural Geology)
Practice Leader

Executive Summary

This technical report documents the results of an updated surficial and geophysical lineament interpretation study conducted as part of the Phase 2 Geoscientific Preliminary Assessment to further assess the suitability of the White River area to safely host a deep geological repository. This study follows the successful completion of the Phase 1 Geoscientific Desktop Preliminary Assessment (AECOM, 2014).

The purpose of the Phase 2 lineament interpretation was to provide an updated interpretation of the geological and structural characteristics of the bedrock units within the area identified in the Phase 1 desktop assessment. The assessment area considered for the lineament study includes the area covered by the newly acquired Phase 2 airborne surveys (SGL, 2017). The interpretation of lineaments was conducted using the new high-resolution airborne magnetic and digital elevation data (DEM), as well as high-resolution digital aerial imagery.

The lineament interpretation followed a systematic workflow involving three steps. The first step included an independent lineament interpretation by two individual interpreters for each data set and the assignment of a certainty level (low, medium, or high) of the interpreted lineaments. The second step involved the integration of the interpreted lineaments for each individual data set and a determination of reproducibility. The third and final step involved the integration of the lineament interpretations for the surficial data sets (DEM and digital aerial imagery) followed by the integration of the combined surficial data set with the aeromagnetic data set, with the determination of coincidence in each integration step. Over the course of these three steps, a comprehensive list of attributes for each lineament was compiled. The four key lineament attributes and characteristics used in the assessment include certainty, length, density, and orientation.

Geophysical lineaments were interpreted using the newly acquired high-resolution aeromagnetic data (SGL, 2017), which provides a significant improvement to the overall resolution and quality of aeromagnetic data compared with the available data interpreted during the Phase 1 preliminary assessment. Lineaments interpreted using the aeromagnetic data are typically less affected by the presence of overburden than surficial data sets, and more likely reflect potential structures at depth that may or may not have surficial expressions. The geophysical lineament interpretation identified 666 lineaments, including 261 brittle, 251 dyke, and 154 unclassified lineaments throughout the White River Phase 2 assessment area. The reproducibility assessment identified coincidence for 58% and a lack of coincidence for 42% of all geophysical lineaments, with 40% assigned the highest level of certainty (three), while 43% were assigned a moderate certainty value of two, and 17% were assigned a low certainty value of one. Brittle lineaments occur throughout the White River area, and are most abundant in the northeastern half of the study area. Brittle lineaments display a broad east-southeast, to south-southeast orientation, as well as a significant but less dominant north-south-trending orientation, and a minor northeast-trending orientation. Dyke lineaments occur throughout the White River area with a dominant southeast orientation, a subordinate north-northeast orientation, and a minor north-south orientation, which correspond to the Matachewan, Biscotasing, and Marathon dyke swarms, respectively. The density of the brittle and dyke lineaments is variable throughout the assessment area. Areas of higher brittle and dyke density correspond with clusters of northwest-trending dyke lineaments and where these clusters intersect with tight-spaced brittle lineaments and sporadic north- and northeast-trending dyke lineaments. Unclassified lineaments define semi-continuous, curvi-linear zones of ductile or brittle-ductile deformation in the Kabinakagami Lake greenstone belt, along the northern margin of the Strickland pluton, and within the Pukaskwa batholith, and the Anahareo pluton.

Surficial lineaments were interpreted using the high-resolution digital elevation data (DEM) from the airborne surveys, and high-resolution digital aerial imagery with a ground resolution cell of 0.4 m. Surficial lineaments were interpreted as linear traces along topographic features such as valleys, escarpments, and drainage patterns such as rivers, streams, and linear lakeshore lines. These linear traces may represent the expression of bedrock fractures on the land surface. However, it is uncertain what proportion of surficial lineaments represent actual geological structures and if so, whether the structures extend to significant depth. The observed distribution and density of surficial lineaments is highly influenced by the presence of overburden cover and water bodies, which can mask the surface expressions of potential fractures. The combination of interpreted DEM and digital aerial lineaments yielded 827 integrated surficial lineaments throughout the White River Phase 2 assessment area. The reproducibility assessment identified coincidence for 28% of the surficial lineaments and a lack of coincidence for 72% of all surficial lineaments, with 10% assigned the highest level of certainty (three), while

43% were assigned a moderate certainty value of two, and 47% were assigned a low certainty value of one. Surficial lineaments display a dominant, broad north-northeast to east-northeast orientation, and a broad, less significant southeast orientation. The dominant glacial flow direction was also from northeast to southwest, therefore care must be taken when evaluating northeast-trending surficial lineaments to ensure they are related to bedrock features. Surficial lineament density is variable throughout the assessment area. Zones of elevated lineament intersection density typically occur along or at the intersection of tight-spaced northwest-, and northeast-trending surficial lineaments, however, the highest surficial lineament intersection density is correlated with a set of curvi-linear lineaments near the centre of the assessment area, within the Pukaskwa batholith. Certain low density areas within the surficial data are the result of increased overburden masking lineaments, including the northwest of the assessment area near Gourlay Lake that is coincident with extensive organic terrain and glacial outwash deposits, and along the eastern border of the assessment area, west of Kabinakagami Lake that is coincident with extensive organic terrain and glaciolacustrine deposits

The integration of the geophysical and surficial lineament data sets resulted in the final integrated lineament data set. This data set identified 1225 lineaments, including 780 brittle, 249 dyke, and 196 unclassified lineaments through the White River Phase 2 assessment area. The reproducibility assessment between geophysical and surficial features revealed that 43% of the interpreted geophysical lineaments were also interpreted in at least one of the two surficial data sets. In general, reproducibility values for the final integrated data reveal a low coincidence between surficial and magnetic lineaments. Throughout the assessment area, only 9% of the final integrated lineaments were identified in all three data sets, and 24% of the final integrated lineaments were identified in two of the three data sets. Lineaments that were reproduced in all three data sets ($RA_2=3$), and lineaments with the highest certainty value (3) typically represent the longest lineaments (i.e., greater than 5 km). The orientation and distribution of brittle and dyke lineaments is similar to that documented for the geophysical lineaments with two dominant, broad east-southeast to south-southeast, and northeast trends, a subordinate north-south trend, and a minor east-northeast trend. The abundance of northeast-trending final integrated lineaments is due to the dominance of this trend in the integrated surficial data set. As with the geophysical and surficial data sets, the density of the final integrated brittle and dyke lineaments is variable throughout the assessment area. Areas of higher brittle and dyke density correspond to clusters of closely spaced lineaments, and the intersection of these lineament clusters. The distribution and density of unclassified lineaments is nearly identical as described for the geophysical lineaments and define semi-continuous, curvi-linear zones of ductile or brittle-ductile deformation in the Kabinakagami Lake greenstone belt, along the northern margin of the Strickland pluton, and within the Pukaskwa batholith, and the Anahareo pluton. Brittle lineaments of all orientations are observed to offset and truncate, and be offset and truncated by all other brittle and dyke lineament orientations. The complexity and inconsistency of the structural relationships observed between all brittle lineaments suggest a protracted deformation history that likely includes multiple generations of brittle reactivation.

Table of Contents

Executive Summary	i
Table of Contents	iv
List of Tables	vi
List of Figures (in order following text)	vi
1 Introduction.....	8
1.1 Scope of Work and Work Program.....	8
1.2 Assessment Area.....	9
1.3 Qualifications of SRK and SRK Team.....	9
2 Summary of Geology	11
2.1 Geological Setting.....	11
2.2 Bedrock Geology	11
2.2.1 Strickland Pluton	12
2.2.2 Pukaskwa Batholith.....	12
2.2.3 Anahareo Pluton	13
2.2.4 Black-Pic Batholith	14
2.2.5 Foliated Tonalite Suite	15
2.2.6 Mafic Dykes	15
2.3 Structural History	16
2.3.1 Mapped Structures.....	18
2.4 Metamorphism	19
2.5 Quaternary Geology.....	20
3 Methodology	21
3.1 Source Data Description	21
3.1.1 High-resolution Aeromagnetic Data	21
3.1.2 Digital Elevation Model	22
3.1.3 High-resolution Digital Aerial Imagery	22
3.2 Lineament Interpretation Workflow.....	22
3.2.1 Step 1: Lineament Interpretation and Certainty Level	25
3.2.2 Step 2: Lineament Reproducibility Assessment 1 (RA_1).....	26
3.2.3 Step 3: Coincidence Assessment (RA_2).....	27
3.2.4 Lineament Trends	29
3.2.5 Lineament Length	29
3.2.6 Lineament Density	30
4 Lineament Interpretation Results.....	31
4.1 Geophysical Lineaments (RA_1).....	31
4.2 Surficial Lineaments.....	33
4.2.1 DEM Lineaments (RA_1).....	33
4.2.2 FRI Digital Aerial Imagery Lineaments (RA_1).....	35
4.3 Integrated Surficial Lineaments (RA_2).....	36
4.4 Integrated Final Lineaments (RA_2)	37
5 Discussion	39
5.1 Lineament Reproducibility (RA_1) and Coincidence (RA_2)	39
5.2 Lineament Trends	41
5.2.1 Relationship between Lineament Sets and Regional Stress Field.....	42
5.3 Lineament Length	43

5.4	Density.....	44
5.4.1	Lineament Density	44
5.4.2	Lineament Intersection Density	46
5.5	Lineament Truncation and Relative Age Relationships	47
5.5.1	Mapped Structure and Lineament Relationships.....	49
6	Summary of Results.....	51
7	References	54
	APPENDIX A – Additional Supporting Figures	61
	APPENDIX B – Summary of Lineament Statistics	67
	Figures	71

List of Tables

Table 1: Bounding Coordinates of the Phase 2 Lineament Assessment Area in the White River Area, Ontario	9
Table 2: Geological and Structural History of the White River Area (adapted from AECOM, 2014a)	17
Table 3: FRI Digital Aerial Imagery Band Ranges and Resolution.....	22
Table 4: Attribute Table Fields Populated for the Lineament Interpretation	24
Table 5: Summary of Geophysical Lineament Orientations for the White River Area	32
Table 6: Summary of DEM Lineament Orientations for the White River Area	33
Table 7: Summary of FRI Lineament Orientations for the White River Area	35
Table 8: : Summary of Integrated Surficial Lineament (RA_2) Orientations for the White River Area.....	37
Table 9: Summary of Integrated Final Lineament (RA_2) Orientations for the White River Area.....	38

List of Figures (in order following text)

Figure 1: Location and Overview of the White River Area	
Figure 2: Bedrock Geology of the White River Area	
Figure 3: Terrain Features of the White River Area	
Figure 4: Pole Reduced Magnetic Data (First Vertical Derivative) of the White River Area	
Figure 5: Digital Elevation Data of the White River Area	
Figure 6: Forest Resource Inventory Digital Aerial Imagery of the White River Area	
Figure 7: Form Lines from Pole Reduced Magnetic Data of the White River Area	
Figure 8: Interpreted Lineaments from Pole Reduced Magnetic Data of the White River Area	
Figure 9: Interpreted Lineaments from Digital Elevation Data of the White River Area	
Figure 10: Interpreted Lineaments from Forest Resource Inventory (FRI) Imagery of the White River Area	
Figure 11: Interpreted Lineaments from Surficial Data of the White River Area	
Figure 12: Interpreted Lineaments from Pole Reduced Magnetic Data of the White River Area	
Figure 13: Select Final Integrated Lineaments of the White River Area	
Figure 14: Interpreted Brittle and Dyke Lineaments from Pole Reduced Magnetic Data (by Length) of the White River Area	
Figure 15: Interpreted Lineaments (by Length) from Surficial Data of the White River Area	
Figure 16: Final Integrated Lineaments (by Length) of the White River Area	
Figure 17: Lineament Density for Interpreted Brittle and Dyke Lineaments from Pole Reduced Magnetic Data of the White River Area	
Figure 18: Lineament Density for All Interpreted Lineaments from Pole Reduced Magnetic Data of the White River Area	
Figure 19: Lineament Density for Interpreted Lineaments from Surficial Data of the White River Area	

Figure 20: Lineament Density for Final Integrated Brittle and Dyke Lineaments of the White River Area

Figure 21: Lineament Density for All Final Integrated Lineaments of the White River Area

Figure 22: Lineament Intersection Density for Interpreted Brittle and Dyke Lineaments from Pole Reduced Magnetic Data of the White River Area

Figure 23: Lineament Intersection Density for All Interpreted Lineaments from Pole Reduced Magnetic Data of the White River Area

Figure 24: Lineament Intersection Density for Interpreted Surficial Lineaments of the White River Area

Figure 25: Lineament Intersection Density for Final Integrated Brittle and Dyke Lineaments of the White River Area

Figure 26: Lineament Intersection Density for All Final Integrated Lineaments of the White River Area

Figure 27: Lineament Relative Age Relationships of the White River Area

1 Introduction

This technical report documents the results of an updated geophysical and surficial lineament interpretation study conducted as part of the Phase 2 Geoscientific Preliminary Assessment to further assess the suitability of the White River area to safely host a deep geological repository. This study follows the successful completion of a Phase 1 Geoscientific Desktop Preliminary Assessment (NWMO, 2014; AECOM, 2014a and b), which identified several potentially suitable areas warranting further studies, such as high-resolution geophysical surveys and geological mapping.

The purpose of the Phase 2 lineament interpretation was to provide an updated interpretation of the geological and structural characteristics of the bedrock units within the potentially suitable areas identified in the Phase 1 desktop assessment. The assessment area considered for the lineament study includes the area covered by newly acquired Phase 2 airborne geophysical surveys (SGL, 2017).

The interpretation of geophysical lineaments was conducted using newly acquired high-resolution airborne magnetic data (SGL, 2017). The interpretation of surficial lineaments was conducted using newly acquired digital elevation data (SGL, 2017) and high-resolution digital aerial imagery of the area (Forest Resource Inventory digital aerial imagery: OMNR, 2009).

1.1 Scope of Work and Work Program

The scope of work for this study included the completion of a structural lineament interpretation of remote sensing data for the White River area in northeastern Ontario (Figure 1). The lineament study involved the interpretation of remotely-sensed data sets, including surficial (digital elevation and digital aerial imagery) and geophysical (magnetic) data sets (SGL, 2017) for the White River area. The investigation interpreted lineament locations and orientations in terms of their potential impact as bedrock structural features (e.g., individual fractures or fracture zones) and evaluated their relative timing relationships within the context of the local and regional geological setting. For the purpose of this report, a lineament was defined as “a linear or curvi-linear geophysical, DEM or surficial feature.” The approach undertaken in this lineament investigation was based on the following:

- Lineaments were interpreted using newly acquired high-resolution aeromagnetic and digital elevation data (SGL, 2017), and purchased high-resolution digital aerial imagery (Forest Resource Inventory digital aerial imagery; OMNR, 2009);
- Lineament interpretations for each data set were made by two specialist interpreters using a standardized workflow;
- Lineaments were interpreted as having an unclassified, brittle, or dyke character by each interpreter;
- Lineaments were analyzed based on an evaluation of the quality and limitations of the available data sets;
- Lineaments were evaluated using: age relationships; reproducibility tests, particularly the coincidence of lineaments identified by different interpreters; coincidence of lineaments interpreted from different data sets; and comparison to literature and mapped geology;
- Classification was applied to indicate the significance of lineaments based on certainty, length, and reproducibility.

These elements help to address the issues of uncertainty, subjectivity and reproducibility normally associated with lineament investigations. Their incorporation into the methodology increases the confidence in the resulting lineament interpretation.

1.2 Assessment Area

The area used for the lineament assessment and interpretation includes one rectangular area, totalling approximately 1140 square kilometres (km²) within the White River area (Figure 1). The approximate coordinates defining the boundaries of the Phase 2 assessment area are listed in Table 1 (UTM NAD83, Zone 16N).

Table 1: Bounding Coordinates of the Phase 2 Lineament Assessment Area in the White River Area, Ontario

X UTM	Y UTM
650,623	5,393,783
657,835	5,379,970
677,000	5,379,930
677,000	5,425,000
650,625	5,425,000

1.3 Qualifications of SRK and SRK Team

The SRK Group comprises more than 1,400 professionals, offering expertise in a wide range of resource engineering disciplines. The independence of the SRK Group is ensured as it holds no equity in any project it investigates and its ownership rests solely with its staff. Consequently, SRK can provide its clients with conflict-free and objective recommendations on crucial issues. SRK has a proven track record in undertaking independent assessments of mineral resources and mineral reserves, project evaluations and audits, technical reports and independent feasibility evaluations to bankable standards on behalf of exploration and mining companies, and financial institutions worldwide. Through its work with a large number of major international mining companies, the SRK Group has established a reputation for providing valuable consultancy services to the global mining industry.

The lineament interpretation and the compilation of this report were completed by Mr. Simon Craggs and Ms. Anna Fonseca, PGeo. Dr. James P. Siddorn, PGeo served as a technical advisor and reviewed lineament interpretations and drafts of this report prior to their delivery to the NWMO as per SRK internal quality management procedures.

Following is a brief description of the qualifications and roles of the project team members.

Mr. Simon Craggs, MSc is a Senior Consultant (Structural Geology) who specializes in regional mapping, detailed analysis of fracture/fluid flow mechanics, and the structural controls on epithermal ore deposit formation. Mr. Craggs has conducted several structural interpretations for vein-type precious metal deposits in poly-deformed terranes across Canada. He recently completed structural lineament interpretations for the Phase 1 Schreiber (SRK, 2013a), Manitouwadge (SRK, 2014a), and White River (SRK, 2014b) areas for the NWMO. In this study, Mr. Craggs was the lead interpreter and the report author.

Ms. Anna Fonseca, MSc, PGeo is a Principal Consultant (Geology) and has more than 20 years of international experience in geological mapping at various scales. She has conducted structural

lineament interpretations of remote sensing data sets for the Rice Lake Greenstone Belt of the Superior Province and of the Yaramoko project area in Burkina Faso. She recently completed Phase 2 structural lineament interpretations for the Ignace study area (SRK, 2015c) for the NWMO. In this study, Ms. Fonseca was the second interpreter.

Dr. James Siddorn, PGeo is a Practice Leader (Structural Geology) and specialist in applied structural interpretation of remotely sensed data combined with the structural analysis of ore deposits. Dr. Siddorn has conducted numerous detailed interpretations of magnetic and electromagnetic data sets for gold and diamond exploration, and rock mechanics/hydrogeological engineering studies. He oversaw the Phase 1 structural lineament interpretations for the Schreiber (SRK, 2013a), Ear Falls (SRK, 2013b), White River (SRK, 2014b), and Manitouwadge (SRK, 2014a) areas, as well as the Phase 2 structural lineament interpretations for the Creighton (SRK, 2015a), Schreiber (SRK, 2015b), and Ignace (SRK, 2015c) areas. In this study, Dr. Siddorn was the senior reviewer.

Mr. Jason Adam is an Associate Consultant (GIS) who has a broad experience in GIS (geographical information systems). Mr. Adam provided GIS support for the study, mainly in the preparation of figures, under the direction of Mr. Craggs.

2 Summary of Geology

Details of the geology of the White River area were described in the Phase 1 Geoscientific Desktop Preliminary Assessment (AECOM, 2014a). The following sections provide brief descriptions of the geologic setting, bedrock geology, structural history and mapped structures, metamorphism and Quaternary geology of the White River area. The focus of the following sections are the bedrock units identified during Phase 1 as being potentially suitable to host a deep geological repository and the important structural features in the area.

2.1 Geological Setting

The White River area is located within the Archean Superior Province of northern Ontario. The Superior Province is a stable craton created from a collage of ancient plates and accreted juvenile arc terranes that were progressively amalgamated over a period of more than 2 Ga (e.g., Percival et al., 2006). The Superior Province covers an area of approximately 1,500,000 km² and is divided into subprovinces, including the Wawa Subprovince within which the White River area is located.

The Wawa Subprovince comprises multiple units of volcanic and associated metasedimentary rocks (greenstone belts) separated by extensive granitic plutons and batholiths. These greenstone belts typically occur in elongate, narrow, geometries and represent volumetrically a relatively minor percentage of the rocks. The surrounding granitic bodies are composed primarily of tonalite to granodiorite, and represent the vast majority of the rocks present throughout the White River area.

Four generations of Paleoproterozoic diabase dyke swarms, ranging in age from ca. 2.473 to 2.101 Ga intrude all bedrock units in the White River area (Hamilton et al., 2002; Buchan and Ernst, 2004; Halls et al., 2006).

2.2 Bedrock Geology

The White River area is situated within the Wawa Subprovince, which is a volcano-sedimentary-plutonic terrane bounded to the east by the Kapuskasing structural zone and to the north by the metasedimentary-dominated Quetico Subprovince. The Wawa Subprovince is composed of well-defined greenstone belts of metamorphosed volcanic rocks and associated metasedimentary rocks, separated by granitoid rock units.

There are two semi-linear to arcuate zones of greenstone belts within the Wawa Subprovince, the northern of which includes the Shebandowan, Schreiber-Hemlo, White River-Hornepayne, Dayohessarah, and Kabinakagami greenstone belts (Figure 2). The southern zone comprises the Michipicoten, Mishibishu, and Gamitagama greenstone belts, which are located west of the Kapuskasing structural zone, well southeast of the White River area. The Dayohessarah greenstone belt and the western portion of the Kabinakagami belt are within the White River area (Figure 2). A small portion of the Schreiber-Hemlo belt is located along the western boundary of the White River area, while the Michipicoten greenstone belt is situated approximately 25 kilometres to the southeast. The Dayohessarah and Kabinakagami greenstone belts have been interpreted by Williams et al. (1991) and Stott (1999) as being part of a once continuous supracrustal belt now represented by the White River-Hornepayne and the Black River assemblage of the Schreiber-Hemlo belts.

The granitoids that separate the greenstone belts comprise 20 to 30 percent of the landmass of the Wawa Subprovince, and consist of massive, foliated and gneissic tonalite-granodiorite, which is cut by massive to foliated granodiorite and granite. The majority of the granitoids were emplaced during or after the deposition of the greenstone belts with which they are associated (Williams et al., 1991). The granitoids in the White River Phase 2 assessment area include the Strickland and Anahareo plutons, the Pukaskwa batholith and to a lesser extent the Black-Pic batholith.

Several generations of Paleo- and Meso-proterozoic diabase dyke swarms, ranging in age from 2.473 to 1.14 Ga, cut all bedrock units in the White River area. The most prominent of these dyke swarms include the northwest-trending Matachewan swarm, ca. 2.473 Ga (Buchan and Ernst, 2004); the northeast-trending Biscotasing dyke swarm, ca. 2.167 Ga (Hamilton et al., 2002); and the north-trending Marathon dyke swarm ca. 2.121 Ga (Buchan et al., 1996; Hamilton et al., 2002). Less numerous dykes belonging to the west-northwest trending Sudbury (ca. 1.238 Ga; Krogh et al., 1987) and northeast-trending Abitibi (ca. 1.14 Ga; Ernst and Buchan, 1993) dyke swarms also crosscut the area.

The main geological units of interest occurring in the White River area are further described below.

2.2.1 Strickland Pluton

The Strickland pluton occurs in the northern portion of the White River area bordering the Dayohessarah and Kabinakagami greenstone belts. The pluton extends to the northeast of the study area, occupies an area of approximately 600 km² and has maximum dimensions (including areas beyond the study area) of 34 kilometres north-south and 55 kilometres east-west (Figure 2). Stott (1999) described the Strickland pluton as a relatively homogeneous, quartz porphyritic granodiorite; although, near the outer margin of the pluton, adjacent to the greenstone belt, granodiorite to tonalite and diorite are present. In the area west of the Kabinakagami greenstone belt, Siragusa (1977) noted that massive quartz monzonite (i.e., monzogranite in modern terminology) intrudes the granodioritic and trondhjemitic rocks in the form of medium-grained to pegmatitic dykes and small sills and irregular bodies.

Some degree of post-emplacement deformation and metamorphism of the Strickland pluton is indicated by the observed presence of fine- to medium-grained titanite and the widespread presence of hematite-filled fractures and weak alteration of silicate minerals (Stott, 1999). Stott (1999) noted that the pluton is petrographically similar to the ca. 2.697 Ga Dotted Lake batholith located in the northwestern corner of the White River area and suggested that these plutons are members of an intrusive suite commonly found along the margins of greenstone belts in this part of the Wawa Subprovince.

No readily available information regarding the thickness of the Strickland pluton was found, although, it may extend to a significant depth.

2.2.2 Pukaskwa Batholith

The Pukaskwa batholith (also referred to as the Pukaskwa gneissic complex) is a large, regionally-extensive intrusion covering an area of at least 5,000 km² in the Wawa Subprovince (Figure 2). Mapping of the intrusion in the White River area was completed at a reconnaissance scale resulting in crudely defined boundaries of the batholith (Milne et al., 1972; Santaguida, 2001). As mapped by Santaguida (2001), the batholith is bounded to the north by the Strickland pluton, the Danny Lake stock and the Black-Pic batholith. The Pukaskwa batholith surrounds the western extent of the Anahareo pluton.

The Pukaskwa batholith extends over the central portion of the White River area (Figure 2) and is described as comprising foliated tonalite and gneissic tonalite suites (Santaguida, 2001). Regionally, the Pukaskwa batholith is a multi-phased intrusion emplaced over an extended time period (Stott, 1999; Beakhouse and Lin, 2006; Beakhouse et al., 2011).

Knowledge of the Pukaskwa batholith is primarily obtained from regional studies conducted to the west, in the vicinity of the Hemlo greenstone belt. An investigation of the batholith by Beakhouse et al. (2011) identified a number of lithologic associations (rock groupings) based on petrological and geochemical characteristics, three of which were volumetrically significant. The oldest association and most abundant of the three are a group of gneissic, well-foliated tonalite to granodioritic rocks. The gneissic nature of these rocks is a composite fabric formed by flattening or transposition of heterogeneities, metamorphic segregation or partial melting, and emplacement of sheet-like intrusive phases controlled by pre-existing anisotropy (Beakhouse et al., 2011). This lithologic association is interpreted to represent rocks derived from melting of a mafic crust and emplaced during the period ca. 2.720 to 2.703 Ga (Corfu and Muir, 1989; Jackson et al., 1998; Stott, 1999; Beakhouse et al., 2011; Lin and Beakhouse, 2013). It is likely that the foliated tonalite and gneissic tonalite suites as described by Santaguida (2001) in the White River area are part of this rock group.

The Pukaskwa batholith's second lithologic association, emplaced in the period between ca. 2.703 and 2.686 Ga, consists of foliated granodiorite to quartz-monzodiorite that is widespread but volumetrically limited (Beakhouse et al., 2011). Corfu and Muir (1989) reported a weakly foliated granodiorite from the Pukaskwa batholith having an inferred magmatic crystallization age of ca. 2.688 Ga. Geochemical analysis indicates that the rocks of the lithological association were derived from, or due to some sort of interaction with, an ultramafic source. These rocks cut the older lithologic association described above and have a weakly to moderate foliation which is generally subparallel to parallel to pre-existing rock units. The geometrical, age and field relationships are interpreted as indicative of a syn-tectonic emplacement of the second lithologic association of the Pukaskwa batholith (Beakhouse et al., 2011). Following the emplacement of the syn-tectonic phases, the Pukaskwa batholith was uplifted as a regional dome structure relative to flanking greenstone belts at approximately 2.680 Ga and synchronous with ongoing regional sinistral transpressive deformation (Beakhouse et al., 2011; Lin and Beakhouse, 2013).

The youngest lithologic association comprises a group of granodioritic to granitic units that form large, homogeneous plutons and small dykes. The geochemical signature of the rocks suggests that they are derived from melting of older intermediate to felsic crust (Beakhouse et al., 2011). The rocks are dated at ca. 2.667 Ga and, therefore, are interpreted as late to post-tectonic (Davis and Lin, 2003; Beakhouse et al., 2011).

No readily available information regarding the thickness of the Pukaskwa batholith was found, however, its size and the geological history of the region suggest it may extend to a significant depth.

2.2.3 Anahareo Pluton

The Anahareo pluton (informal name adopted in this report) is a large felsic intrusion of which approximately 690 km² is located within the southern and southeastern parts of the White River area (Figure 2). The pluton extends west of the study area and has maximum dimensions (including areas beyond the study area) of over 51 kilometres north-south and 71 kilometres east-west. The intrusion was mapped by Siragusa (1977, 1978) as being dominantly granodiorite and quartz monzonite (i.e., monzogranite in modern terminology). Distal from the contact with the Kabinakagami greenstone belt, these rock types are relatively uniform and appear to represent multi-phase intrusions. Migmatites of trondhjemitic composition, the least dominant granitic rock within the intrusion, are

present along the pluton's boundaries and as syntectonic intrusive sheets that locally exhibit a variably developed cataclastic fabric (Siragusa, 1978).

Quartz monzonite is the youngest recognized phase of the Anahareo pluton and commonly intrudes the granodioritic and trondhjemitic rocks in the form of large, coarse-grained pegmatitic dykes, sills and discordant bodies of variable size (Siragusa, 1977; 1978). This phase of the pluton is described as massive, which prompted Siragusa (1978) to suggest that these young intrusive phases post-date the major period of tectonism in the White River area. However, no geochronological information is currently available to test this interpretation and the age of the pluton is unknown.

No detailed information is available regarding the thickness of the Anahareo pluton.

2.2.4 Black-Pic Batholith

The Black-Pic batholith is a regionally-extensive intrusion that encompasses roughly 3,000 km² within the Wawa Subprovince and underlies only a very small portion along the northern boundary of the White River area (Figure 2). It is bounded to the south by the Strickland Pluton, the Pukaskwa batholith, and the Danny Lake stock, and to the east by the Dayohessarah greenstone belt.

The Black-Pic batholith comprises a multi-phase suite that includes hornblende-biotite, monzodiorite, foliated tonalite, and pegmatitic granite with subordinate foliated diorite, granodiorite, granites, and crosscutting aplitic to pegmatitic dykes (Williams and Breaks, 1989; Zaleski and Peterson, 1993). In the White River area, the batholith is described as a gneissic tonalite in a compilation map of Santaguida (2001); however, Fenwick (1967), similarly to Milne (1968), mapped the batholith as uniform, biotite granitic gneiss and biotite granite that becomes gneissic near the boundary with the Dayohessarah greenstone belt (noting that the terminology used was before Streckeisen's [1976] standard classification). Fenwick (1967) also noted the occurrence of migmatites (noting that terminology used was prior to either Mehnert's (1968) or Sawyer's (2008) classifications) composed of highly altered remnants of pre-existing volcanic and sedimentary rocks mixed with variable amounts of granitic material. The migmatites occur as either a breccia type, in which fragments of the older rocks are cemented by dykes; and veins of granitic rock or a banded type, in which layers of the older material alternate with layers of granitic material.

Several generations of intrusions are present within the Black-Pic batholith, yielding geochronological ages ranging from ca. 2.720 Ga (Jackson et al. 1998) for the earliest recognized rock unit to ca. 2.689 Ga for a late-stage monzodioritic unit (Zaleski et al., 1999). In addition, there are also younger granitic phases within the Black-Pic batholith which, despite a lack of geochronological information, are thought to be part of the regional suite of ca. 2.660 Ga, post-tectonic "Algonian granites" (Zaleski et al., 1999). Within the batholith, intrusive relationships are typically destroyed and only metamorphic textures and associated mineral assemblages are preserved. Inclusions of relatively melanocratic members of the suite occur as foliated inclusions within later, leucocratic members (Williams and Breaks, 1989, 1996).

The foliation pattern recognized within the Black-Pic batholith was interpreted to define regional scale domal structures characterized by broad antiforms and tight synforms (Williams and Breaks, 1989; Lin and Beakhouse, 2013). At least one such smaller-scale structure potentially exists to the west of White River Phase 2 assessment area, immediately north of the Danny Lake stock where semi-circular faults outline the position of a possible dome several kilometres in width.

Structurally deeper levels of the tonalite suite in the Black-Pic batholith are strongly foliated with a subhorizontal planar fabric that exhibits a poorly developed, north-trending rodding and mineral-elongation lineation (Williams and Breaks, 1989). Upper structural levels of the tonalite suite are cut

by abundant granitic sheets of pegmatite and aplite, and are more massive (Williams and Breaks, 1989; Zaleski and Peterson, 1993). Just to the north of the White River area are zones of migmatized volcanic rocks, and zones of massive granodiorite to granite embodied in the Black-Pic batholith. The contact between these rocks and the tonalitic rocks of the Black-Pic batholith is gradational with extensive sheeting of the tonalitic unit (Williams and Breaks, 1989; Williams et al., 1991).

No readily available information regarding the thickness of the batholith is available, however, its size and the geological history of the region suggest it may extend to a significant depth.

2.2.5 Foliated Tonalite Suite

On the southeast side of Kabinakagami Lake, Santaguida (2001) outlined two packages of foliated tonalite suite rock, bisected by greenstone, that occur between the Kabinakagami greenstone belt and the Anahareo pluton (Figure 2). The tonalite packages extends over a distance of 29 kilometres north-south and 25 kilometres east-west, but only a small amount occurs within the White River area. This suite of rocks is similar to the Anahareo pluton mapped by Siragusa (1977; 1978). Siragusa (1977) described outcrops of the foliated tonalite suite within the White River area as consisting of biotite trondhjemite, trondhjemite, granodiorite, and biotite granodiorite. Biotite trondhjemite is the dominant granitic rock in contact zones between the granitic and supracrustal rocks of the Kabinakagami greenstone belt and also occurs as syntectonic intrusive sheets concordant to the foliations observed in the metavolcanic rocks. The biotite trondhjemite appears as strongly gneissic, grey to brownish grey, medium-grained rock and is locally porphyritic owing to the presence of eye-shaped quartz and feldspar porphyroblasts (Siragusa, 1977).

No absolute age is available for this foliated tonalite suite, although, it may be of the same age as other lithologically similar intrusions in the region. No information is available regarding the thickness of the suite.

2.2.6 Mafic Dykes

Four generations of Paleoproterozoic and Mesoproterozoic diabase dyke swarms crosscut the White River area (Figure 2), including:

- Northwest-trending Matachewan Suite dykes (ca. 2.473 Ga; Buchan and Ernst, 2004). This dyke swarm is one of the largest in the Canadian Shield and most predominant of all dyke swarms recognized in the White River area. Individual dykes are generally up to 10 m wide, and have vertical to subvertical dips. The Matachewan dykes comprise mainly quartz diabase dominated by plagioclase, augite and quartz (Osmani, 1991).
- Northeast-trending Biscotasing Suite dykes (ca. 2.167 Ga; Hamilton et al., 2002). These dykes are not considered to be numerous in the White River area.
- North-trending Marathon Suite dykes (ca. 2.121 Ga; Buchan et al., 1996; Hamilton et al., 2002). These form a fan-shaped distribution pattern around the northern, eastern, and western flanks of Lake Superior, and are fairly minor in the White River area. The dykes vary in orientation from northwest to northeast, and occur as steep to subvertical sheets, typically a few m to tens of m thick, but occasionally up to 75 m thick (Hamilton et al., 2002). The Marathon dykes comprise quartz diabase (Osmani, 1991) dominated by equigranular to subophitic clinopyroxene and plagioclase.
- West-northwest-trending Sudbury Suite dykes (ca. 1.238 Ga; Krogh et al., 1987). These dykes are not considered to be numerous in the White River area.

The four dyke swarms in the White River area are generally distinguishable by their unique strike directions, crosscutting relationships and, to a lesser extent, by the amplitude of the associated, magnetic anomalies.

2.3 Structural History

Information on the structural history of the White River area is based predominantly on insights derived from structural investigations of the White River and Dayohessarah greenstone belts (Polat, 1998; Zaleski et al., 1994; Peterson and Zaleski, 1999), and the Hemlo gold deposit and surrounding region (Muir, 2003). Additional studies by Lin (2001), Percival et al. (2006), and Williams and Breaks (1996) have also contributed to the structural understanding of the area. The aforementioned studies were performed at various scales and from various perspectives. Consequently, the following summary of the structural history of the White River area should be considered as a best-fit model that incorporates relevant findings from all studies. The structural history of the White River area is described below and summarized in Table 2.

On the basis of overprinting relationships between different structures, Polat et al. (1998) suggested that the Schreiber-Hemlo greenstone belt underwent at least two main episodes of deformation. These deformation events can be correlated with observations from Peterson and Zaleski (1999) and Muir (2003), who reported at least five and six generations of structural elements, respectively. Two of these generations of structures account for most of the ductile strain, and although others can be distinguished on the basis of crosscutting relationships, they are likely the products of progressive deformation events.

Table 2: Geological and Structural History of the White River Area (adapted from AECOM, 2014a)

Approximate Time Period (years before present)	Geological Event
2.89 to 2.77Ga	Progressive growth and early evolution of the Wawa-Abitibi terrane by collision, and ultimately accretion, of distinct geologic terranes
	<ul style="list-style-type: none"> - ca. 2.720 Ga: Onset of volcanism and subordinate sedimentation associated with the formation of the Dayohessarah and Kabinakagami greenstone belts - ca. 2.720 Ga: Emplacement of oldest recognized phase of Black-Pic batholith - ca. 2720-2.703 Ga: Emplacement of oldest lithologic association of Pukaskwa batholith - ca. 2703-2.686 Ga: Emplacement of second lithologic association of Pukaskwa batholith - ca. 2.697 Ga: Intrusion Dotted Lake pluton, and possibly of Strickland pluton - ca. 2.689 Ga: Emplacement of younger recognized phase of Black-Pic batholith - ca. 2.677 Ga: Emplacement of Bremner pluton
2.770 – 2.673 Ga	<ul style="list-style-type: none"> - ca. 2.719 to 2.673 Ga: Four periods of ductile-brittle deformation (D₁-D₄): <ul style="list-style-type: none"> D₁: ca. 2.719 – 2.691 Ga D₂: ca. 2.691 – 2.683 Ga → Main phase of coalescence of the Wawa and Quetico subprovinces (Corfu and Stott, 1996) D₃: ca. 2.682 – 2.679 Ga → Sinistral transpressive deformation, structural domal uplift of Pukaskwa batholith D₄: ca. 2.679 – 2.673 Ga - ca.2.688 to 2.675: Regional metamorphism
2.675 and 2.669 Ga	Peak metamorphism of regional greenstone belts
< 2.673 Ga	Two phases of brittle deformation (D ₅ -D ₆)
2.667 Ga	Youngest lithologic association of Pukaskwa batholith
2.5 to 2.1 Ga	<ul style="list-style-type: none"> - ca. 2.5 Ga: Supercontinent fragmentation and rifting in Lake Superior area, development of Southern Province - ca. 2.473 Ga: Emplacement of the Matachewan dyke swarm - ca. 2.167 Ga: Emplacement of Biscotasing dyke swarm - ca. 2.121 Ga: Emplacement of the Marathon dyke swarm
1.9 to 1.7 Ga	Penokean Orogeny in Lake Superior and Lake Huron areas; possible deposition and subsequent erosion in the White River area
1.238 Ga	- ca. 1.238 Ga emplacement of the Sudbury dyke swarm
1.150 to 1.090 Ga	<ul style="list-style-type: none"> Rifting and formation of the Midcontinent Rift - ca. 1.14 Ga: Emplacement of the Abitibi dyke swarm
540 to 355 Ma	Possible coverage of the area by marine seas and deposition of carbonate and clastic rocks subsequently removed by erosion
145 to 66 Ma	Possible deposition of marine and terrestrial sediments of Cretaceous age, subsequently removed by erosion
2.6 to 0.01 Ma	Periods of glaciation and deposition of glacial sediments

Integration of the structural histories detailed in Williams and Breaks (1996), Polat et al. (1998), Peterson and Zaleski (1999), Lin (2001), and Muir (2003) suggest that six deformation events occurred within the White River area. The first four deformation events (D₁-D₄) are associated with

ductile and brittle-ductile deformation. D_5 and D_6 were associated with a combination of brittle deformation and fault propagation through all rock units in the White River area. The main characteristics of each deformation event are summarized below.

The earliest recognizable deformation phase (D_1) is associated with rarely preserved small-scale isoclinal (F_1) folds, ductile shear zones that truncate stratigraphy, and a general lack of penetrative foliation development. Peterson and Zaleski (1999) reported that an S_1 foliation is only preserved locally in outcrop and in thin section. D_1 deformation is poorly constrained to between ca. 2.719 and ca. 2.691 Ga (Muir, 2003).

D_2 structural elements include prevalent open to isoclinal F_2 folds, an axial planar S_2 foliation, and L_2 mineral elongation lineations (Peterson and Zaleski, 1999). Muir (2003) interpreted D_2 to have resulted from progressive north-northeast to northeast directed compression that was coincident with the intrusion of various plutons. The S_2 foliation is the dominant meso- to macro-scale fabric evident regionally. Ductile flow of volcano-sedimentary rocks between more competent batholiths may also have occurred during D_2 deformation. This generation of deformation is constrained to between ca. 2.691 and ca. 2.683 Ga (Muir, 2003).

D_3 deformation was the result of northwest-southeast shortening during regional dextral transpression. D_3 structural elements include macroscale F_3 folds, including the regional scale isoclinal fold developed within the Manitouwadge greenstone belt, and local shear fabrics that exhibit a dextral sense of motion and overprint D_2 structures (Peterson and Zaleski, 1999; Muir, 2003). D_3 deformation did not develop an extensive penetrative axial planar and (or) crenulation cleavage. D_3 deformation is constrained to between ca. 2.682 and ca. 2.679 Ga (Muir, 2003).

D_4 structural elements include isolated northeast-plunging F_4 kink folds with a Z-asymmetry, and associated small-scale fractures and faults overprinting D_3 structures. D_3 - D_4 interference relationships are best developed in the Manitouwadge greenstone belt and in rocks of the Quetico Subprovince. D_4 deformation is roughly constrained to between ca. 2.679 and ca. 2.673 Ga (Muir, 2003).

Details of structural features associated with the D_5 and D_6 deformation events are limited in the literature to brittle and brittle-ductile faults of various scales and orientations (Lin, 2001; Muir, 2003). Within the Hemlo greenstone belt, Muir (2003) suggested that local D_5 and D_6 faults offset the Marathon and Biscotasing dyke swarms (all ca. 2.2 Ga), and as such, suggested that in the Hemlo region D_5 and D_6 faults propagated after ca. 2.2 Ga. However, since there are no absolute age constraints on specific events, the entire D_5 - D_6 interval of brittle deformation can only be constrained to a post-2.673 Ga timeframe that may include many periods of post-Archean tectonic re-activation.

2.3.1 Mapped Structures

In the White River area five unnamed faults are indicated on public domain geological maps that are considered to be associated with D_5 - D_6 brittle deformation. (Fenwick, 1966; Siragusa, 1977, 1978; Stott, 1995a, b, c; Santaguida, 2001; OGS, 2011; Figure 2). The longest unnamed fault parallels the axis of Esnagi Lake in the southeast corner of the area (Siragusa, 1978). A northeast-trending mapped fault is located crossing the western margin of the White River area and is mapped as juxtaposing the Pukaskwa batholith against the Strickland pluton. A northwest-trending mapped brittle fault is located at the southern extent of Nameigos Lake that is shown offsetting the Kabinakagami Lake greenstone belt with a dextral strike-separation. A northwest-trending mapped fault is located within the Anahareo pluton, southwest of Anahareo Lake. A mapped west-northwest trending fault is located at the northern extent of Nameigos Lake that is shown as truncating the Pukaskwa batholith against the Strickland pluton and the Kabinakagami Lake greenstone belt.

In the Kabinakagami Lake greenstone belt, Siragusa (1977) reported that it is likely that a northeast-trending strike-slip fault with horizontal displacement of 240 m is present in a narrow valley, to the north of the inlet of the Kabinakagami River.

Fenwick (1967) and Siragusa (1977) noted that lineaments parallel the trend of two sets of diabase dykes, which strike either northeast or northwest, and assumed that the lineaments formed from the weathering of diabase dykes or from vertical joints.

2.4 Metamorphism

Studies on metamorphism in Precambrian rocks across the Canadian Shield have been summarized in a few publications since the 1970s (e.g., Fraser and Heywood, 1978; Kraus and Menard, 1997; Menard and Gordon, 1997; Berman et al., 2000; Easton, 2000a; 2000b; and Berman et al., 2005) and the thermochronological record for large parts of the Canadian Shield is documented in a number of studies (Berman et al., 2005; Bleeker and Hall, 2007; Corrigan et al., 2007; and Pease et al., 2008).

The Superior Province of the Canadian Shield largely preserves low-pressure–high-temperature Neoproterozoic (ca. 2.710–2.640 Ga) metamorphic rocks. The relative timing and grade of regional metamorphism in the Superior Province corresponds to the lithological composition of the subprovinces (Easton, 2000a; Percival et al., 2006). Subprovinces comprising volcano-sedimentary assemblages and synvolcanic to syntectonic plutons (i.e., granite-greenstone terranes) are affected by relatively early lower greenschist to amphibolite facies metamorphism. Subprovinces comprising both metasedimentary- and migmatite-dominated lithologies, such as English River and Quetico, and dominantly plutonic and orthogneissic domains, such as Winnipeg River, are affected by relatively late middle amphibolite to granulite facies metamorphism (Breaks and Bond, 1993; Corfu et al., 1995). Subgreenschist facies metamorphism in the Superior Province is restricted to limited areas, notably within the central Abitibi greenstone belt (e.g., Jolly, 1978; Powell et al., 1993).

In general, most of the Canadian Shield preserves a complex episodic history of Neoproterozoic metamorphism overprinted by Paleoproterozoic tectonothermal events culminating at the end of the Grenville orogeny ca. 950 Ma. The distribution of contrasting metamorphic domains in the Canadian Shield is a consequence of relative uplift, block rotation, and erosion resulting from Neoproterozoic orogenesis, subsequent local Proterozoic orogenic events and broader epeirogeny during later Proterozoic and Phanerozoic eons.

All Precambrian rocks of the White River area display some degree of metamorphism. The Dayohessarah greenstone belt is typically characterized by amphibolite facies metamorphism (Stott, 1999). This amphibolite facies metamorphic grade may be a manifestation of an amphibolite grade contact metamorphic aureole bordering the Strickland pluton (Stott, 1999). Little information regarding the metamorphic grade of the exposed rocks of the Kabinakagami greenstone belt is available in the reviewed literature. Based on ages obtained from metamorphic monazites, Zaleski et al. (1995; 1999) suggested that near-peak metamorphism of the White River-Hornepayne greenstone belt occurred between 2.675 and 2.669 Ga. It can be inferred that the Dayohessarah and Kabinakagami belts may have been subjected to metamorphism during this period, as the age constraints given by Zaleski et al. (1994; 1999) correspond well with the 2.675 ± 1 and 2.661 ± 1 Ga periods of regional metamorphism recognized by Schandl et al. (1991).

Typical metamorphic grades in plutonic rocks within the White River area are variable from non-metamorphosed to amphibolite grade in metamorphic contact aureoles. No evidence to date suggest that rocks in the White River area were affected by thermal overprints related to post-Archean events.

2.5 Quaternary Geology

Quaternary geology of the White River area is described in detail in the remote sensing and terrain evaluation completed as part of the Phase 1 Desktop Preliminary Assessment (AECOM, 2014b). An overview of the relevant Quaternary features are presented in Figure 2, and summarized below.

The Quaternary sediments, commonly referred to as drift, soil, or overburden, in the White River area comprise glacial and post-glacial materials that overlie the bedrock. All glacial landforms and related materials are associated with the Wisconsinan glaciation, which began approximately 115,000 years ago (Barnett, 1992). Geddes et al. (1985) and Geddes and Kristjansson (1986) reported that glacial striae in the White River area reveal an early north to south ice movement that was followed by a strong, regional flow oriented approximately 220 degrees (°). Bedrock erosional features indicate that ice flow, likely in the waning stage of glacial cover, was influenced by local topographic conditions as demonstrated by striae measurements ranging from 180° to 245°.

Till thickness is variable and while depths of several m are present locally, thicknesses are typically less than 3 m (A. Bajc, pers. comm., 2013). Gartner and McQuay (1980a, 1980b) reported that the till is seldom more than 1 metre thick on the crests of the hills, but can thicken to 5 m or more on the flanks and in the valleys between the bedrock hills. For large parts of the White River area drift thickness over bedrock is limited and the ground surface reflects the bedrock topography (Geddes and Kristjansson, 1986). Over the majority of the area bedrock outcrops are common and the terrain is classified, for surficial purposes, as a bedrock-drift complex, i.e., thin drift cover that only locally achieves thicknesses that mask or subdue the bedrock topography (Figure 3). Valleys and lowland areas typically have extensive and thicker surficial deposits that frequently have a linear outline.

Glaciofluvial outwash deposits in the White River area occur as northeast trending areas of limited relief along the esker-kame complexes and within the larger modern drainage systems, such as the Gum, Kwinkwaga, Shabotik, and White rivers to the west of the study area. Smaller deposits, occupying topographic lows and bedrock valleys, are scattered across the area. The thickness of the outwash deposits are likely to be variable, but may be substantial where they are proximal to ice-contact stratified drift (ICSD) features. Deposits are generally well-sorted and consist predominantly of stratified sand with a low clast content; however, locally they are coarser-grained and gravel-rich (Geddes and Kristjansson, 1986).

Glaciolacustrine sediments in the area consist of fine sand, silt, and minor clay deposited in shallow lakes within bedrock controlled basins (Figure 3). The largest of these deposits is located proximal to Nameigos Lake (Gartner and McQuay, 1980a, 1980b). Other small deposits, typically occur towards the northeast of the area (Geddes and Kristjansson, 2009).

Bogs and organic-rich alluvial deposits, consisting of sand, silt and organic debris, are present along several of the water courses in the White River area (Figure 3). These deposits tend to be relatively narrow (<200 m), although their width can increase notably proximal to lakes. Larger expanses of organic terrain, some of several square kilometres in size, are present in the northeast and northwestern parts of the White River area near Nameigos and Gourlay lakes, respectively. These deposits may be developed on finer-grained glaciolacustrine deposits and/or outwash that occupy lowland areas. Smaller occurrences of organic terrain exist in bedrock-controlled basins throughout the White River area.

3 Methodology

The structural lineament interpretation of the White River area was based on high-resolution remote sensing data sets, including a high-resolution airborne magnetic survey contracted by the NWMO to Sander Geophysics Limited (SGL, 2017), digital elevation data (DEM) collected during the airborne magnetic survey (SGL, 2017), and high-resolution Ontario Ministry of Natural Resources Forest Resources Inventory (FRI) digital aerial imagery procured from Land Information Ontario (OMNR, 2009).

3.1 Source Data Description

All data were assessed for quality, enhanced, and reviewed before use in the lineament interpretation. The geophysical data were used to evaluate potential deeper bedrock structures, and were instrumental in identifying potential bedrock structures beneath areas of surficial cover. Furthermore, the geophysical data were instrumental in establishing the age relationships among the different lineament sets. Topographic (DEM) and FRI digital aerial imagery data sets were used to identify surficial lineaments expressed in the topography, drainage, and vegetation. For this study, the best resolution data available was used for the lineament interpretation.

3.1.1 High-resolution Aeromagnetic Data

Sander Geophysics Limited (SGL) completed a fixed-wing high-resolution airborne magnetic survey in the White River area (SGL, 2017; Figure 4).

The airborne survey in the White River area included a total of 14,383 km of flight lines covering a surface area of more than 1,100 km². Flight operations were conducted out of the Municipal Airport (CYMG), in Manitouwadge, Ontario, using a Cessna 208B Grand Caravan. Data were acquired along traverse lines flown in a north-south direction spaced at 100 m, and control lines flown east-west spaced at 500 m. The survey was flown at a target altitude of 80 m above ground level, with an average ground speed of 100 knots (approximately 185 km/h). The survey acquisition parameters are listed below:

- Traverse line spacing of 100 m
- Traverse line azimuth of 000 - 180°
- Control line spacing of 500 m
- Control line azimuth of 090 - 270°
- Grid cell size of 25 m
- Targeted sensor height of 80 m
- Acquisition date of July 31 to October 6, 2015

Acquired data were processed by SGL (SGL, 2017) and provided to SRK as GRD files. The following products of the high resolution airborne magnetic survey were available for this structural lineament interpretation:

- Reduction to the pole of the total magnetic intensity
- First vertical derivative of the reduction to the pole of the total magnetic intensity
- Second vertical derivative of the reduction to the pole of the total magnetic intensity
- Tilt derivative of the reduction to the pole of the total magnetic intensity

The reduced to pole total magnetic intensity, first and second vertical derivatives, and tilt derivative grids were converted to ERS images, shaded by intensity, and the data ranges and colour were enhanced in ERMapper to highlight potential structures. Ultimately, a series of compressed raster images was created in ERMapper for use in ArcGIS.

3.1.2 Digital Elevation Model

Digital elevation data (DEM) were collected during the magnetic survey conducted by SGL (SGL, 2017). The survey acquisition parameters are identical to those described for the high-resolution magnetic data in Section 3.1.1.

DEM data were processed by SGL and provided to SRK as GRD files. The data grid was then converted to an ERS image, and the data ranges, hill shading (using sun angles of 000°, 045°, and 315°), and colour ranges of the DEM were enhanced in ERMapper to highlight potential structures (Figure 5). Compressed raster images were created in ERMapper for use in ArcGIS.

3.1.3 High-resolution Digital Aerial Imagery

High resolution digital aerial imagery was obtained from the Ontario Ministry of Natural Resources Forest Resources Inventory (FRI) (OMNR, 2009).

Digital aerial imagery was collected using a Leica ADS40 Airborne Digital Sensor. The ADS40 sensor captures multispectral bands simultaneously at the same true resolution, and therefore produces a four-band, truly co-registered and equal resolution imagery (not pan sharpened) from the data acquisition. The spectral ranges and spatial resolution of each band are listed in Table 3.

Prior to release to the public, the imagery tiles were run through a bidirectional reflectance distribution function (BRDF) process to remove atmospheric distortions associated with sun angles. Subsequently, blocks of orthorectified tile imagery were compiled and processed to be normalized using the brightest and darkest values within the multi-date acquisition. Each image consists of a mosaic of 5-by-5-kilometre orthorectified tiles of four-band data.

A natural colour composite of the FRI digital aerial imagery was created in ArcGIS and utilized for the lineament interpretations (Figure 6).

Table 3: FRI Digital Aerial Imagery Band Ranges and Resolution

Band	Range (nm)	Resolution (m)
Panchromatic	465 - 680	0.2
Blue	428 - 492	0.4
Green	533 - 587	0.4
Red	608 - 662	0.4

3.2 Lineament Interpretation Workflow

The structural lineament assessment of the White River area was conducted to identify the location and orientation of potential individual fractures or fracture zones and to evaluate their relative timing relationships within the context of the local and regional geological setting.

Lineaments were interpreted using a workflow designed to address issues of subjectivity and reproducibility that are inherent to any lineament interpretation. The workflow followed a set of detailed guidelines using the high-resolution airborne geophysical (magnetic) and high-resolution surficial (DEM and FRI digital aerial imagery) data sets described above. Throughout the report the term geophysical lineaments refers to structures interpreted from the high-resolution magnetic data. The interpretation guidelines involved three steps:

- Step 1: Independent lineament interpretation by two individual interpreters for each data set and assignment of certainty level (1, 2, or 3 representing low, medium and high certainty);
- Step 2: Integration of lineament interpretations for each individual data set and first determination of reproducibility;
- Step 3: Integration of lineament interpretations for the surficial data sets (DEM and digital aerial imagery) followed by integration of the combined surficial data set with the geophysical data set, with determination of coincidence in each integration step.

Each identified lineament feature was classified in an attribute table in ArcGIS. The description of the attribute fields used is included in Table 4. Fields 1 to 9, and Fields 19 and 20 were populated during Step 1. Fields 10 and 11 were populated during Step 2. Fields 12 to 18 were populated during Step 3.

The interpreted geophysical and final integrated lineaments were classified into four general categories based on a working knowledge of the structural history and bedrock geology of the White River area. These categories include form lines, unclassified, brittle and dyke lineaments, described as follows:

- **Form lines:** Features interpreted to represent the internal fabric of the rock units (including sedimentary or volcanic layering, tectonic foliation or gneissosity, and magmatic foliation). Form lines are typically characterized by semi-continuous linear to curvi-linear magnetic highs that appear to define the grain of the rock units. See Figure A1 for example.
- **Unclassified lineaments:** Linear to curvi-linear features that do not exhibit characteristics to easily form an interpretation, and are therefore unclassified. Possible interpretations may include ductile shear zones (intensification of foliation across a narrow zone) or brittle-ductile shear zones (intensification of foliation across a narrow zone with associated fracturing). Unclassified structures were typically characterized by curvi-linear magnetic lows and commonly truncated or offset the internal fabric of the rock (i.e., form lines). Alternatively, these unclassified structures may represent the internal fabric of the rock (foliation or gneissosity), in particular in domains where they are subparallel to the form lines, or possible brittle structures. Additional field investigations are required to determine the true nature of these lineaments. See Appendix A: Figure A2 for example.
- **Brittle lineaments:** Features interpreted as fractures (joints or joint sets, faults or fault zones, and veins or vein sets). This category also includes brittle partings interpreted to represent discontinuous re-activation parallel to the ductile fabric (e.g., form lines). Brittle lineaments are commonly characterized by continuous magnetic lows, offsets of magnetic highs, offset of form lines, and offset of unclassified lineaments, and breaks in topography and vegetation. At the desktop stage of the investigation, this category also includes features of unknown affinity. See Figure A4 for example.
- **Dyke lineaments:** Features interpreted as dykes, on the basis of their distinct character (e.g., scale orientation, geophysical signature and topographic expression). Dykes were dominantly interpreted from the magnetic data set, and are typically characterized by continuous linear magnetic highs. The interpretation of dykes is also combined with pre-existing knowledge of the bedrock geology of the study area. See Figure A3 for example.

A detailed description of the three workflow steps and the methodology for determining the associated attribute fields for each interpreted lineament is provided below.

Table 4: Attribute Table Fields Populated for the Lineament Interpretation

ID	Attribute	Brief Description
1	Rev_ID	Reviewer initials
2	Feat_ID	Feature identifier
3	Data_typ	Data set used (MAG, DEM, FRI)
		Type of feature used to identify each lineament
		Digital Aerial Imagery:
		A. Lineaments drawn along straight or curved lake shorelines
		B. Lineaments drawn along straight or curved changes in intensity or texture (i.e., vegetation)
		C. Lineaments drawn down centre of thin rivers or streams
		D. Lineaments drawn along a linear chain of lakes
		E. Other (if other, define in comments)
4	Feat_typ	Digital Elevation Model:
		A. Lineaments drawn along straight or curved topographic valleys
		B. Lineaments drawn along straight or curved slope walls
		C. Other (if other, define in comments)
		Airborne Geophysics (magnetic and electromagnetic data):
		A. Lineaments drawn along straight or curved magnetic high
		B. Lineaments drawn along straight or curved magnetic low
		C. Lineaments drawn along straight or curved steep gradient
		D. Other (if other, define in comments)
5	Name	Name of feature (if known)
6	Certain	Value describing the interpreters confidence in the feature being related to bedrock structure (1-low, 2-medium or 3-high)
7	Length*	Length of feature is the sum of individual lengths of mapped polylines and is expressed in kilometres
		Width of feature; this assessment is categorized into 5 bin classes:
8	Width**	A. < 100 metres
		B. 100 – 250 metres
		C. 250 – 500 metres
		D. 500 – 1,000 metres
		E. > 1,000 metres
9	Azimuth	Lineament orientation expressed as degree rotation between 0 and 180 degrees
10	Buffer_RA_1	Buffer zone width for first reproducibility assessment (in metres)
11	RA_1	Feature value (1 or 2) based on reproducibility assessment
12	Buffer_RA_2	Buffer zone width for coincidence assessment (in metres)
13	RA_2	Feature value (1, 2 or 3) based on coincidence assessment
14	MAG	Feature identified in geophysical data set (Y or Blank)
15	DEM	Feature identified in DEM data set (Y or Blank)
16	SAT	Feature identified in satellite imagery data set (Y or Blank)
17	F_Width	Final interpretation of the width of feature
18	Rel_age	Interpretation of relative age of feature, in accord with regional structural history
19	Comment	Comment field for additional relevant information on a feature
20	Object	Geological element identified, e.g., form lines, unclassified lineament, brittle lineament, dyke lineament.

* The length of each interpreted feature is calculated based on the sum of all segment lengths that make up that lineament.

** The width of each interpreted feature is determined by expert judgment and utilization of a GIS-based measurement tool. Width determination takes into account the nature of the feature as assigned in the Feature type (Feat_typ) attribute.

3.2.1 Step 1: Lineament Interpretation and Certainty Level

To accommodate the generation of the best possible unbiased lineament interpretation, two individual interpreters followed an identical process for structural lineament analysis during Step 1. The first step of the lineament interpretation was to have each individual interpreter independently produce GIS lineament maps, and detailed attribute tables, for each of the three data sets. Step 1 of the structural lineament analysis was conducted up to a scale of 1:25,000 and followed a designated workflow.

The interpretation of magnetic data followed a two-step process. The first step involved the drawing of form lines (Figure 7). Form lines were drawn along linear to curvi-linear magnetic highs as seen in the high-resolution first vertical derivative magnetic data. Locally, where the magnetic contrast was low, the tilt angle derivative data were used to enhance magnetic features. The form lines were interpreted to trace the geometry of stratigraphy, or tectonic foliation within metavolcanic and metasedimentary rocks, and the internal fabric (foliation or magmatic layering) within granitoid batholiths and gneissic rocks. Magnetic highs associated with dykes (i.e., linear crosscutting magnetic highs in orientations identified in the literature as dyke orientations) were not included in this process.

Form line construction highlighted discontinuities between form lines (e.g., form lines intersecting or truncating) that may represent structures (faults, folds), unconformities, or intrusive contacts. The process of drawing form lines was instrumental in highlighting other lineaments in the magnetic data.

The second step involved drawing a structural base layer that represented all interpreted lineaments regardless of interpreted age, type (e.g., unclassified, brittle or dyke), or kinematics. Evidence for lineaments was derived from several sources in the magnetic data, including discontinuities between form lines, offset of magnetic units, or the presence of linear magnetic lows or highs. The first vertical derivative magnetic data was used mainly with the tilt angle derivative data to further enhance this interpretation.

The lineament interpretation of DEM data involved tracing linear or curvi-linear features along topographic valleys, slope walls, and any other relevant features that were visible in a colour shaded DEM derived from the airborne geophysical survey data. Similarly, the lineament interpretation of digital aerial imagery involved tracing linear or curvi-linear features along visible shore lines, changes in colour intensity or texture (e.g., vegetation), linear rivers and streams, and along linear chains of features associated with lakes that were visible in the FRI imagery. Particular care was taken for lineaments that were coincident with eskers in the FRI data. Unless there was clear evidence for a surficial lineament to be associated with a bedrock feature, lineaments that were coincident with eskers were not drawn.

Lineaments from each of the data sets were assigned attributes by each interpreter to characterize what type of feature the lineament corresponded to, the interpreter's certainty that the lineament represented a bedrock structure, and the approximate width of the topographic feature.

Lineaments identified in the DEM and or the digital aerial imagery that were interpreted to be related to glacial events were excluded from the lineament interpretation data set. The following criteria were utilized to decide whether a DEM or digital aerial imagery lineament should be excluded:

- The lineament coincided with a mapped ice-flow feature, moraine, or esker;

- The lineament was parallel to known eskers or moraines and was marked by narrow, curving ridges;
- The lineament was parallel to the local ice flow direction and was accompanied by drumlin-shaped hills in the DEM data set.

The Step 1 lineament analysis resulted in the generation of one interpretation for each data set (e.g., magnetic, DEM, digital aerial imagery) for each interpreter, resulting in a total of six individual GIS layer-based interpretations. Where evident, lineament segments were merged, and lineament lengths calculated, resulting in final lineament lengths that corresponded to the sum of all merged segments.

During Step 1, identified lineaments were attributed with Fields 1 to 9, and Fields 19 and 20 (Comment and Object attribute) as listed in Table 4.

3.2.2 Step 2: Lineament Reproducibility Assessment 1 (RA_1)

During Step 2, individual lineament interpretations produced by each interpreter were compared for each data set (e.g., two individual DEM lineament interpretations). This included a reproducibility assessment based on the coincidence, or lack thereof, of the interpreted lineaments within a data set specific buffer zone. The two individual lineament interpretations for each data set were then integrated and a single interpretation was generated for each data set (Figure 7 to Figure 10). A discussion of the parameters used during this step follows.

Buffer Size Selection

Buffer sizes for lineaments in each data set were based on the magnetic grid resolution. The buffer size was determined using trial-and-error over a selected portion of the lineament interpretation. A buffer size of five times the grid cell resolution (25 m) was selected as it provided a balanced result for assessing reproducibility. A buffer of 125 m (either side of the lineament) was generated for the magnetic data. Given that the DEM data were extracted from the same survey, the same buffer size was applied to the DEM data. A 125-metre buffer was also applied to the digital aerial imagery data in order to be consistent with the magnetic and DEM buffer size.

The buffer size widths were included in the attribute fields of each interpretation file (Table 4). The buffers were used as an initial guide to determine coincidence between lineaments, with the expert judgement of the interpreter ultimately determining which lineaments were coincident.

Reproducibility Assessment

The generation of an integrated lineament interpretation for each data set, including the reproducibility assessment, followed a three-step process:

- Lineament buffers were generated for both individual Step 1 interpretations. The lead interpreter's Step 1 lineaments were then overlain on top of these buffers, and all lineaments that occurred within overlapping buffers were carried forward and copied into a new file for Step 2. These lineaments were attributed with a reproducibility value (RA_1; Table 4) of two in the Step 2 attribute table. In addition, if two lineaments were deemed coincident, the highest certainty value from either lineament was carried forward. During this process, based upon insight gained from analyzing the separate interpretations together, the geometry of the lineament that was carried forward was occasionally adapted to better reflect the underlying data.
- The remaining lineaments in the lead Step 1 interpretation were then manually analyzed by both interpreters on the basis of the available imagery for each data set. In some instances, this included adapting the shape and extent of individual lineaments to increase the accuracy

of spatial location or length of the lineament, and carrying the adapted lineament forward into the Step 2 interpretation file. These lineaments were attributed a RA_1 value of one in the Step 2 attribute table. Where it was determined by the two interpreters that these features were not representative of potential bedrock structure, they were removed from the data set.

- Finally, the second Step 1 lineament interpretation was overlain on top of the Step 2 integrated file, and all remaining lineaments in the second interpreter's Step 1 interpretation were then manually analyzed by both interpreters on the basis of the available imagery for each data set. In some instances, this included adapting the shape and extent of individual lineaments to increase the accuracy of spatial location or length of the lineament, and carrying the adapted lineament forward into the Step 2 interpretation file. These lineaments were attributed a RA_1 value of one in the Step 2 attribute table. All remaining lineaments that were attributed a certainty value of one were analyzed by both interpreters, and removed if it was determined that these features were not representative of potential bedrock structures.

As specified above, the decision on whether or not to adapt the shape and extent of an individual lineament, or whether the lineament was carried forward to the next step was based on analysis of the specified lineament with the available dataset and a discussion between the two interpreters. If a lineament was drawn continuously by one interpreter but as individual, spaced, or disconnected segments by the other interpreter, the longer lineament, or the lineament that most accurately represented the underlying feature was carried forward to the Step 2 interpretation with a RA_1 value of two.

The resulting Step 2 interpretations for each data set (e.g., magnetics, DEM, and FRI digital aerial imagery) were then slightly refined to avoid any structurally inconsistent or geologically improbable relationships. Any modifications of lineaments were minor, took place within the limits of the assigned buffer zone, and respected the underlying data.

3.2.3 Step 3: Coincidence Assessment (RA_2)

During Step 3, the integrated lineament interpretations for each data set were amalgamated into one final interpretation. First, lineaments derived from the DEM and digital aerial imagery were merged to produce an integrated surficial lineament data set. Subsequently, the geophysical lineaments were integrated with the integrated surficial lineaments to produce a final integrated interpretation. A discussion of the parameters used during this step follows below.

Surficial Lineament Integration

The FRI digital aerial imagery data have a resolution of 40 cm while the DEM data have a resolution of approximately 25 m. Furthermore, the orientation of minor and intermediate topographic features as identified in the DEM can be ambiguous due to the resolution of the data, while these features could be drawn with greater precision from the FRI digital aerial imagery. Therefore, lineaments derived from the FRI data were used as the lead data set, and lineaments drawn from DEM data were used as the secondary data set.

A buffer of 125 m (five times the resolution of the DEM data) was generated around the DEM lineaments and the FRI lineaments were overlain on top of this buffer. Similar to the procedure in RA_1, all lineaments that occurred within overlapping buffers were carried forward and copied into a new file. These lineaments were attributed with a RA_2 reproducibility value of two (RA_2; Table 4). In addition, if two lineaments were deemed coincident, the highest certainty value from either lineament was carried forward. During this process, based upon insight gained from analyzing the separate interpretations together, the geometry of the lineament that was carried forward was occasionally adapted within the boundaries of the buffer to better reflect the underlying data.

All remaining lineaments were then manually analyzed by both interpreters on the basis of the available imagery for each data set. In some instances, this included minor adaptations to the shape and extent of individual lineaments, within the limitations of the buffer, to increase the accuracy of spatial location, length of the lineament, and (or) preserve structural relationships. All these lineaments were then carried over and attributed with an RA_2 value of one in the attribute table (RA_2; Table 4). No lineaments were removed or significantly modified at this stage of the integration.

Final Lineament Integration

The geophysical data supplied important information regarding structures in the subsurface. Therefore, for this step of the interpretation, the lineaments derived from geophysical data were given precedence over lineaments derived from surficial data, since the latter primarily provided information regarding the surface expression of potential structures.

On this premise, all lineaments derived from the magnetic data were included in the final interpretation. A buffer of 125 m (five times the resolution of the geophysical and DEM data) was generated around the integrated surficial lineaments, and the geophysical lineaments were overlain on top of this buffer. This buffer size was included as an attribute field for all interpreted lineaments (Buffer RA_2; Table 4). Similar to the procedure in RA_1, all lineaments that occurred within overlapping buffers were carried forward and copied into a new file. These lineaments were attributed with a RA_2 reproducibility value of two or three, depending on how many surficial data sets they were observed in (RA_2; Table 4). During this process, based upon insight gained from analyzing the separate interpretations together, the geometry of the lineament that was carried forward was occasionally adapted within the boundaries of the buffer to better reflect the underlying data.

The following rules were applied for determining coincidence between the data set specific lineament maps:

- If any coincidence of lineaments occurred between the two lineament data sets, the longest lineament was carried forward and attributed as derived from two (or more) data sets, regardless of the length of overlap between the lineaments. This meant that if any part of a lineament derived from one data set was identified in another data set, it was considered that this lineament was reproduced. In addition, if two lineaments were deemed coincident, the highest certainty value from either lineament was carried forward.
- A lineament derived from DEM and (or) FRI digital aerial imagery data that occurred within the buffer of a lineament derived from geophysical data was attributed as reproduced in the relevant data sets, if the orientation of the lineaments did not deviate significantly.
- Short (less than 500 m) discontinuous DEM and FRI digital aerial imagery data lineaments that were at low angles to geophysical data lineaments but extended outside the geophysical lineament buffer were considered to be coincident.
- Short (less than 500 m) DEM and FRI digital aerial imagery data lineaments that were at high angles to geophysical data lineaments, largely overlapped with the buffer zone from the geophysical data lineament, and had no further continuity (i.e., singular elements), were carried forward to the final interpretation. This was done on the basis that these short segments may represent a bedrock structure, and as such, should be contained within the final integrated data set.

All remaining lineaments were then manually analyzed by both interpreters on the basis of the available imagery for each data set. In some instances, this included minor adaptations to the shape and extent of individual lineaments, within the limitations of the buffer, to increase the accuracy of

spatial location, length of the lineament, and or preserve structural relationships. All these lineaments were then carried over and attributed with an RA_2 value of one (or two if observed in both surficial data sets) in the attribute table (RA_2; Table 4). No lineaments were removed or significantly modified at this stage of the integration. This resulted in a combined interpretation with lineaments derived from the magnetic and surficial data sets.

During this process, each lineament was attributed with a text field highlighting in which data sets it was identified. The final reproducibility value (RA_2; Table 4) was then calculated as the sum of the number of data sets in which each lineament was identified, i.e., a value of 1 to 3.

Subsequently, the relative age of each lineament was interpreted and populated in the attribute table (Rel_Age; Table 4). This incorporated a working knowledge of the structural history of the White River area, combined with an understanding of the characteristics in each lineament population (e.g., unclassified, brittle, dyke). The structural history of the area is described in Section 2.3 based on the existing literature.

3.2.4 Lineament Trends

An analysis of lineament trends revealed different sets of structures, which can then be related to the known structural history of the area. Lineament orientations were assessed for each data set as a whole, within individual subareas, and within distinct geological units, to determine the dominant lineament trends, and potential conjugate sets.

Lineament orientations (azimuth) were calculated using ET EasyCalculate 10, an add-in extension to ArcGIS. This add-in provides a function (polyline_GetAzimuth.cal) that calculates the azimuth of each polyline at a user-specified point and populates an assigned attribute field. SRK used the mid-point of each interpreted lineament to calculate the azimuth. A limitation is acknowledged, however, for calculating a single orientation for curvi-linear structures.

Rose diagrams are circular or semi-circular histograms that depict orientation (azimuthal) data and frequency for each data bin. The histogram peaks show the frequency of occurrence of lineament orientations within each bin. Rose diagrams were produced in Spheristat, with frequencies divided into 10-degree bins, and weighted by length. The length weighting uses a linear function directly related to the lineament length, whereby a lineament with a length of 2 kilometres will have twice the weighting of a lineament with a length of 1 kilometre.

3.2.5 Lineament Length

Lineament lengths were calculated using a simple geometrical calculation of the total length of the polyline in ArcGIS. The length distribution of the various integrated data sets was analyzed through a comparison of summary statistics, histograms, and cumulative frequency plots. Histograms and summary statistics were computed using the Stanford Geostatistical Modelling Software (SGeMS). Histogram bins were computed using arbitrary 500-metre bins.

There is no information available on the depth extent into the bedrock of the lineaments interpreted for the White River area. In the absence of available information, the interpreted length can be used as a proxy for the depth extent of the identified structures (Nur, 1982). A preliminary assumption may be that the longer interpreted lineaments in the White River area may extend to greater depths than the shorter interpreted lineaments. However, this is highly dependent on the style and structural history of a given lineament.

3.2.6 Lineament Density

Lineament density analyses were conducted using the ArcGIS Analysis and Spatial Analyst toolsets, and included creating lineament line density plots and lineament intersection point density plots for the magnetic, surficial, and final integrated lineament data sets.

Lineament line density of all interpreted lineaments in the White River area was determined by examining the statistical density of individual lineaments using ArcGIS Spatial Analyst. A grid cell size of 50 m and a search radius of 1.25 km (equivalent to half the size of the longest boundary of the minimum area size of a potential repository siting area) were used. The spatial analysis used a circular search radius examining the lengths of polylines intersected within the circular search radius around each grid cell.

The lineament intersection point density of all intersecting lineaments in the White River area was determined by extracting all points where two or more lineaments intersected, and then calculating the statistical density of these intersection points. Lineament intersections were extracted using the ArcGIS Analysis Tools Intersect function. The density distribution of these points was then calculated in ArcGIS Spatial Analyst by defining a neighbourhood around each raster cell centre, calculating the number of points that fall within the neighbourhood, and dividing by the area of the neighbourhood. A grid cell size of 50 m and a search radius of 1.25 km (equivalent to half the size of the longest boundary of the minimum area size of a potential siting area) were used.

4 Lineament Interpretation Results

The following section describes the results of the lineament interpretation for the White River area based on analysis of the geophysical and surficial (DEM, FRI digital aerial imagery) data sets. Lineaments interpreted and integrated from the various data sets are presented below and in Figure 7 to Figure 13. A summary of lineament statistics is presented in Appendix B.

4.1 Geophysical Lineaments (RA_1)

The interpretation of magnetic data allows for the identification of form lines, unclassified, brittle, and dyke lineaments. Form lines traced from the magnetic data set are shown in Appendix A: Figure A1 and Figure 7, and are interpreted to represent the internal fabric of the rock units, including the geometry of the stratigraphy of the greenstone belts or the internal fabric (foliation and magmatic layering) within plutonic and gneissic rocks. Discontinuities between form lines highlight potential brittle-ductile, and brittle structures (potential shear zones and/or fractures), unconformities, or intrusive contacts. Therefore, they constitute an essential data component that should be used along with the first vertical derivative of the magnetic data for interpreting unclassified and brittle lineaments. A brief discussion of form lines is included in this report to provide context to the lineament interpretation, but were not included in the statistical analyses of the lineament data sets.

Within the White River Phase 2 lineament assessment area, a total of 666 geophysical lineaments were interpreted and classified as brittle lineaments, dyke lineaments and unclassified lineaments. Each of these lineaments were identified and merged by the two interpreters based on interpretation from the geophysical data (Figure 8). Of the total number of geophysical lineaments 261 were interpreted as brittle lineaments, 251 were interpreted as dyke lineaments and 154 were interpreted as unclassified lineaments. The length of all geophysical lineaments ranges from 0.19 to 40.53 km, with a median of 2.68 km and a mean of 4.20 km. Of the total geophysical lineaments, the reproducibility assessment between two interpreters identified coincidence for 383 lineaments (58%; RA_1 = 2) and a lack of coincidence for 283 lineaments (42%; RA_1 = 1). For the brittle lineaments, the reproducibility assessment between two interpreters identified coincidence for 138 lineaments (53%; RA_1 = 2) and a lack of coincidence for 123 lineaments (47%; RA_1 = 1). For the dyke lineaments, the reproducibility assessment between two interpreters identified coincidence for 174 lineaments (69%; RA_1 = 2) and a lack of coincidence for 77 lineaments (31%; RA_1 = 1). For the unclassified lineaments, the reproducibility assessment between two interpreters identified coincidence for 71 lineaments (46%; RA_1 = 2) and a lack of coincidence for 83 lineaments (54%; RA_1 = 1).

Of the 666 lineaments interpreted, 264 (40%) were assigned the highest level of certainty (three), while 288 (43%) were assigned a moderate certainty value of two, and 114 (17%) were assigned a low certainty value of one. The certainty value reflects the certainty that the interpreted lineament represents a bedrock feature. For the 261 brittle lineaments, 74 (28%) were assigned the highest level of certainty (three), while 130 (50%) were assigned a certainty value of two, and 57 (22%) were assigned a lower certainty value of one. For the 251 dyke lineaments the certainty increased, with 165 (66%) assigned the highest level of certainty (three), 67 (27%) assigned a certainty value of two, and 19 (8%) were assigned a lower certainty value of one. For the 154 unclassified lineaments, 25 (16%) were assigned the highest level of certainty (three), while 91 (59%) were assigned a certainty value of two, and 38 (25%) were assigned a lower certainty value of one. Appendix B presents a summary of geophysical lineaments statistics. All brittle, dyke and unclassified lineaments were included in the statistical analyses, and are shown in Appendix A: Figures A3 and A4, and Figure 8.

Azimuth data weighted by length for the interpreted brittle lineaments display a broad east-southeast, to south-southeast orientation (two high confidence peaks at 128° and 113°, and one medium to high confidence peak at 148°), as well as a significant but less dominant north-south-trending orientation (one medium to low confidence peak at 010°), and a minor northeast-trending orientation (see rose diagram inset in Figure 8 and Table 5). These orientations are similar to those of the dyke lineaments discussed below, which include an abundance of southeast-trending brittle lineaments that are typically long. The north- and northeast-trending brittle lineaments tend to comprise both long and continuous lineaments, as well as short and segmented lineaments. In general, the style of the different orientations of brittle lineaments (i.e., length, continuity, etc.) closely resembles the style of the dyke lineaments in the equivalent orientations. The range in orientations is well replicated between the Strickland and Anahareo plutons, and the Pukaskwa batholith; however, the north- and northeast-trending interpreted brittle lineaments appear more dominant in the Anahareo pluton (Figure 8).

Azimuth data weighted by length for the interpreted dyke lineaments display a dominant southeast orientation (one high confidence peak at 135°), a subordinate north-northeast orientation (one medium to low confidence peak at 030°), and a minor north-south orientation (see rose diagram inset in Figure 8 and Table 5). The southeast dyke lineament orientation corresponds to the Matachewan dyke set which tend to be continuous and can occur in swarms or clusters that manifest as multiple tight-spaced dyke lineaments. Minor north- and north-northeast-trending dyke lineaments are also common and correspond to the Marathon and Biscotasing dyke sets, respectively. The north-northeast-trending Biscotasing dyke lineaments are continuous and long, but less abundant than Matachewan dykes and often occur as single isolated dyke lineaments. North-trending Marathon dyke lineaments are less-frequent and are commonly segmented and disjointed. In addition, few interpreted east-southeast trending dyke lineaments that have orientations consistent with the Sudbury dyke swarm occur in the assessment area but tend to be rare. These east-southeast trending dyke lineaments are relatively short and discontinuous, and are not well defined in the rose diagram. The range in dyke lineament orientations is well replicated between the Strickland and Anahareo plutons, and the Pukaskwa batholith.

Azimuth data weighted by length for the interpreted unclassified lineaments display a broad east-northeast orientation (two high confidence peaks at 062° and 078°), and an east-southeast orientation (one medium to high confidence peak at 107°), as well as several other minor orientations including north-northeast (one medium to low confidence peak at 032°) (see rose diagram inset in Figure 8 and Table 5). The range in orientations is broadly replicated within the Strickland and Anahareo plutons, and the Pukaskwa batholith. A north-trending orientation is also apparent in the unclassified lineaments within the Strickland pluton and the Pukaskwa batholith.

Table 5: Summary of Geophysical Lineament Orientations for the White River Area

Lineament Type	Orientation Set	Peak (deg)	Range (deg)	Frequency (%)	Confidence
Brittle	SE-NW	128	123 - 139	13.8	High
	ESE-WNW	113	102 - 120	13.2	High
	SSE-NNW	148	142 - 152	9.4	Medium - High
	N-S	010	003 - 016	6.5	Medium - Low
Dyke	SE-NW	135	124 - 145	28.4	High
	NNE-SSW	030	024 - 035	5.9	Medium - Low
Unclassified	ENE-WSW	078	070 - 089	14.2	High
	ENE-WSW	062	054 - 068	12.2	High
	ESE-WNW	107	102 - 119	9.5	Medium - High
	NNE-SSW	032	026 - 039	6.1	Medium - Low

4.2 Surficial Lineaments

Surficial lineaments include lineaments interpreted from the DEM and FRI digital aerial imagery data sets, and are shown on Figure 9 and Figure 10, respectively. Unlike the lineaments identified from the magnetic data, surficial lineaments cannot be easily differentiated into unclassified, brittle, or dyke lineaments based solely upon their expression in surficial data. Therefore, all surficial lineaments are classified only by the data set from which they were identified (i.e., DEM lineament and FRI lineament). An overview of the results of the surficial lineament interpretation is provided below.

4.2.1 DEM Lineaments (RA_1)

A total of 425 DEM lineaments were interpreted within the White River Phase 2 lineament assessment area. These comprise lineaments that were identified and merged by the two interpreters based on interpretation from the DEM data (Figure 9). Of the 425 lineaments interpreted, 67 (16 %) were assigned the highest level of certainty (three), while 215 (50%) were assigned a moderate certainty values of two, and 143 (34%) were assigned a low certainty value of one. The certainty value reflects the certainty that the interpreted lineament represents a bedrock feature. The length of all DEM lineaments ranges from 0.38 to 15.98 km, with a median of 2.42 km and a mean of 3.09 km. Of the total DEM lineaments, 262 lineaments were coincident between the two interpreters (62%; RA_1 = 2) and there was a lack of coincidence for 163 lineaments (38%; RA_1 = 1). Appendix B presents a summary of statistical analyses for the interpreted DEM lineaments.

Azimuth data weighted by length for the interpreted DEM lineaments display a broad north-northeast to east-northeast orientation (two high confidence peaks at 033° and 053°, and one medium to low confidence peak at 075°), and subordinate southeast (one medium to low confidence peak at 133°) and north-south orientations (one medium to low confidence peak at 000°) (see rose diagram inset in Figure 9). The range in orientations is well replicated between the Strickland and Anahareo plutons, and the Pukaskwa batholith. Throughout the White River area, north-northeast to east-northeast-trending DEM lineaments are typically abundant and continuous. However, the northeast orientation of the DEM lineaments is also coincident with the dominant trend of the glacial flow direction (Figure 2). Southeast-trending DEM lineaments are moderately abundant, variable in length, and continuous. North-south trending DEM lineaments are less abundant, and are typically discontinuous.

The abundance of DEM lineaments is directly influenced by the degree of topography in a given area, i.e., areas with subdued topography and a lack of elevation contrast impede the interpretation of topographic lineaments. This can be observed where low relief regions (coloured blue in Figure 9) have a relatively low number of interpreted DEM lineaments, such as in the northwest portion of the assessment area, northeast of Gourlay Lake (Figure 9).

Table 6: Summary of DEM Lineament Orientations for the White River Area

Lineament Type	Orientation Set	Peak (deg)	Range (deg)	Frequency (%)	Confidence
DEM	NNE-SSW	033	023 - 043	11.8	High
	NE-SW	053	045 - 066	9.7	High
	ENE-WSW	075	070 - 080	6.4	Medium - Low
	SE-NW	133	122 - 144	6.2	Medium - Low
	N-S	000	355 - 005	5.7	Medium - Low

4.2.2 FRI Digital Aerial Imagery Lineaments (RA_1)

A total of 670 FRI lineaments were interpreted within the White River Phase 2 lineament assessment area. These comprise lineaments that were identified and merged by the two interpreters based on interpretation from the FRI digital aerial imagery data (Figure 10). Of the 670 lineaments interpreted, 40 (6 %) were assigned the highest level of certainty (three), while 261 (39%) were assigned a moderate certainty value of two, and 369 (55%) were assigned a low certainty value of one. The certainty value reflects the certainty that the interpreted lineament represents a bedrock feature. The length of all FRI lineaments ranges from 0.16 to 14.23 km, with a median of 1.06 km and a mean of 1.43 km. Of the total FRI lineaments, the reproducibility assessment identified coincidence for 493 lineaments (74%; RA_1 = 2) and a lack of coincidence for 177 lineaments (26%; RA_1 = 1). The high coincidence and low certainty is attributed to the abundance of short lineaments defined by linear lake shores and narrow streams that were identified by both interpreters. However due to the nature of FRI dataset and the typically shorter lineament lengths, a high number of these FRI lineaments were attributed lower certainties. Appendix B presents a summary of statistical analyses for the interpreted FRI lineaments.

Azimuth data weighted by length for the interpreted FRI lineaments display a broad north-northeast to east-northeast orientation (one high confidence peak at 035°, one medium to high confidence peak at 015°, and one medium confidence peak at 062°), and a broad east-southeast to southeast orientation (two medium to high confidence peaks at 140° and 125°, and one medium confidence peak at 115°) (see rose diagram inset in Figure 10 and Table 7). In the Anahareo pluton the northeast lineament trend is dominant, while the Strickland pluton has dominant east-southeast, southeast, and north-northeast trends. The Pukaskwa batholith has a dominant southeast lineament trend.

Throughout the White River area, each of the lineament orientation sets are dominated by fairly short lineaments traces with a few isolated longer lineaments. The northeast orientation is also coincident with the dominant trend of the glacial flow direction (Figure 3). The abundance of lineaments tends to be directly influenced by the exposure of bedrock and quality of surficial features in a given area. Areas characterized by well-defined lake boundaries, breaks in vegetation, linear rivers, etc., often yield numerous FRI lineaments, versus areas with extensive overburden and subdued surficial features, which impede the interpretation of digital aerial imagery lineaments. This can be observed where regions of subdued surficial features (such as northwest of Anahareo Lake, northeast of Gourlay Lake, and northeast of Nameigos Lake seen in Figure 10) typically have a relatively low number of interpreted FRI lineaments. Unlike the DEM or geophysical lineaments, the lineaments observed in the FRI imagery are often short and discontinuous due to the way in which bedrock features are expressed in digital aerial imagery.

Table 7: Summary of FRI Lineament Orientations for the White River Area

Lineament Type	Orientation Set	Peak (deg)	Range (deg)	Frequency (%)	Confidence
DEM	NE-SW	035	028 - 049	9.3	High
	SE-NW	140	132 - 151	8.1	Medium - High
	SE-NW	125	120 - 129	8	Medium - High
	NNE-SSW	015	009 - 020	7.9	Medium - High
	ESE-WNW	115	113 - 117	7.3	Medium
	ENE-WSW	062	055 - 067	7.1	Medium

4.3 Integrated Surficial Lineaments (RA_2)

The lineaments interpreted based on DEM and FRI digital aerial imagery data were integrated into a single set of surficial lineaments following the methodology outlined in Section 3. Similar to the interpretation of DEM and FRI lineaments, surficial lineaments cannot be differentiated into unclassified, brittle, and dyke lineaments based solely upon their expression in surficial data, and are, therefore, all classified as surficial lineaments. The integrated surficial lineaments are shown in **Error! Reference source not found. 11** on the mapped bedrock geology based on the Ontario Geological Survey (OGS 2011). The figure also shows mapped faults and mapped dykes, based on either field mapping evidence or an interpretation from historic aeromagnetic data. An overview of the results of the integrated surficial lineaments is provided below and summarized in Appendix B.

The integration of DEM and FRI lineaments yielded a total of 827 surficial lineaments (Figure 11). The merging of DEM and FRI lineaments commonly resulted in lineaments of new lengths, and in some cases an individual lineament may appear either shorter or longer than its original interpreted length. The length of all surficial lineaments ranges from 0.17 to 17.18 km, with a median of 1.45 km and a mean of 2.12 km. Of the 827 integrated surficial lineaments, 85 (10 %) were assigned the highest level of certainty (three), while 351 (43%) were assigned a moderate certainty value of two, and 391 (47%) were assigned a low certainty value of one. The certainty value reflects the certainty that the interpreted lineament represents a bedrock feature. A total of 232 lineaments (28%; RA_2 = 2) were coincident in both the DEM and FRI data sets whereas 595 lineaments only occurred in one of the two data sets (72%; RA_2 = 1).

Azimuth data weighted by length for the integrated surficial lineaments display a broad north-northeast to east-northeast orientation (one high confidence peak at 033°, and one medium confidence peak at 064°), and a broad southeast orientation (one medium confidence peak at 124°) (see rose diagram inset in Figure 11). In general, these orientations match those observed in the individual interpretations (DEM and FRI; Figures 9 and 10). The range in orientations is well replicated between the Strickland and Anahareo plutons, and the Pukaskwa batholith. The longer surficial lineaments tend to be largely inherited from the integrated DEM lineaments, whereas many of the shorter and discontinuous surficial lineaments are inherited from the FRI imagery lineaments. Variation in lineament lengths from the DEM and FRI lineament data sets is due to the way in which bedrock features manifest in these respective data sets.

In general, the northeast-trending surficial lineaments are most abundant and show a wide variability in their lengths. This orientation is consistent with the dominant trend of glaciation (Figure 3). Overall, the abundance of surficial lineaments tends to be directly influenced by the intensity of surficial features in a given area, i.e., presence of topographic relief, vegetation changes, linear lakeshores, etc. In areas of subdued surficial features, fewer and shorter lineaments were interpreted and integrated into the surficial lineament data set. These areas include: the area northwest of Anahareo Lake that is coincident with abundant glacial outwash deposits; the northwest portion of the assessment area near Gourlay Lake that is coincident with extensive organic terrain and glacial outwash deposits; and, the eastern border of the assessment area, west of Kabinakagami Lake that is coincident with extensive organic terrain and glaciolacustrine deposits (Figure 11).

Table 8: Summary of Integrated Surficial Lineament (RA_2) Orientations for the White River Area

Lineament Type	Orientation Set	Peak (deg)	Range (deg)	Frequency (%)	Confidence
Integrated	NNE-SSW	033	022 - 047	10.2	High
Surficial	ENE-WSW	064	060 - 073	7.0	Medium
Lineaments	SE-NW	124	115 - 150	6.4	Medium

4.4 Integrated Final Lineaments (RA_2)

The final integrated lineament data set produced by merging all lineaments interpreted from the geophysical (Figure 12) and surficial (DEM and aerial imagery, Figure 11) data is presented in Figure 13. Based upon the geophysical interpretation, and the geological understanding of the area, the final integrated lineaments were differentiated into brittle, dyke and unclassified lineaments. An overview of the results of the final integrated lineaments is provided below, summarized in Appendix B, and presented in Figure 13.

The integration of geophysical and surficial lineament sets produced a total of 1,225 final integrated lineaments (Figure 13), of which 780 are classified as brittle lineaments, 249 as dyke lineaments and 196 as unclassified lineaments. The length of all final integrated lineaments ranges from 0.17 to 40.53 kilometres, with a median of 2.06 kilometres and a mean of 3.29 kilometres. Of the 1,225 final integrated lineaments, 336 (28 %) were assigned the highest level of certainty (three), while 518 (42%) were assigned a certainty value of two, and 371 (30%) were assigned a certainty value of one. The certainty value reflects the certainty that the interpreted lineament represents a bedrock feature. The reproducibility assessment identified coincidence in all three data sets for 105 lineaments (9%; RA_2 = 3), and coincidence in two out of three data sets for 297 lineaments (24%; RA_2 = 2) and 43% of the interpreted geophysical lineaments were also interpreted in at least one of the two surficial data sets. A total of 823 (67%) lineaments were not coincident with any other data set (RA_2 = 1).

Azimuth data weighted by length for the interpreted integrated brittle lineaments displays dominant, broad east-southeast to south-southeast (two high confidence peaks at 128° and 113°, and one medium to low confidence peak at 149°), and northeast trends (one high confidence peak at 038°), a subordinate north-south orientation (one medium to low confidence peak at 008°), and a minor east-northeast orientation (see rose diagram inset in Figure 13 and Table 9). Interpreted brittle lineaments in the Strickland pluton and Pukaskwa batholith replicate these trends well, while interpreted brittle lineaments in the Anahareo pluton display a dominant northeast trend, with subordinate southeast, north, and east-northeast trends present. Both the east-southeast- to south-southeast-, and northeast-trending brittle lineaments are abundant, and tend to be long and continuous relative to lineaments in other orientations. The north-trending brittle lineaments tend to display a more variable length, which results from the interpreted trace of the lineaments terminating against the northeast and southeast trending lineaments.

In general, the azimuth data weighted by length for the interpreted integrated dyke lineaments display a dominant southeast orientation (one high confidence peak at 133°), with a subordinate north-northeast orientation (one medium to low confidence peak at 030°), and a minor north-south orientation (see rose diagram inset in Figure 13 and Table 9). The southeast-trending lineaments are interpreted to correspond to dykes of the Matachewan swarm. The southeast-trending dyke lineaments are the most continuous, and typically occur in clusters that manifest as multiple tight-

spaced dyke lineaments. Minor north-south, and northeast-trending orientations are also present that are interpreted to correspond to dykes of the Marathon, and Biscotasing swarms, respectively. The northeast-trending dyke lineaments are continuous and long, but less abundant than Matachewan dykes, and often occur as single isolated dyke lineaments. The north-trending dyke lineaments are sporadic, and are commonly segmented and disjointed. Although rare, few interpreted dyke lineaments are associated with the Sudbury dyke swarm, which are east-southeast-trending, are relatively short and discontinuous, and are not well defined in the rose diagram in Figure 13. The range in dyke lineament orientations is well replicated within the Strickland and Anahareo plutons, and the Pukaskwa batholith.

Azimuth data weighted by length for the interpreted unclassified lineaments display a range of trends including a dominant, broad east-west to east-northeast trend (two high confidence peaks at 080° and 068°), a north-northeast trend (one medium to high confidence peak at 032°), an east-southeast trend (one medium confidence peak at 110°), and a minor north-south trend (see rose diagram inset in Figure 13 and Table 9).

In terms of their spatial distribution, both dyke and brittle lineaments are abundant in the northeastern half of the study area, while dykes are more significantly abundant than brittle lineaments in the southwestern half of the study area. Unclassified lineaments tend to be spatially associated with the margins of the Strickland pluton and the Pukaskwa batholith, and with the Kabinakagami greenstone belt.

Table 9: Summary of Integrated Final Lineament (RA_2) Orientations for the White River Area

Lineament Type	Orientation Set	Peak (deg)	Range (deg)	Frequency (%)	Confidence
Brittle	SE-NW	128	123 - 137	9.3	High
	ESE-WNW	113	109 - 117	8.5	High
	NE-SW	038	027 - 047	8.2	High
	SSE-NNW	149	145 - 153	6.3	Medium - Low
	N-S	008	002 - 016	5.9	Medium - Low
Dyke	SE-NW	133	125 - 147	28.8	High
	NNE-SSW	030	025 - 036	6.2	Medium - Low
Unclassified	E-W	080	075 - 086	13.3	High
	ENE-WSW	068	058 - 072	12.5	High
	NNE-SSW	032	025 - 041	10.2	Medium - High
	ESE-WNW	110	097 - 119	8.1	Medium

5 Discussion

This lineament interpretation provides an understanding of potential structures within the bedrock units of the White River Phase 2 lineament assessment area. The results of the lineament interpretation, including lineament reproducibility, orientation, length, and density are discussed below. The relationship of the integrated lineament data sets relative to the regional structural history and their relative ages are also discussed.

5.1 Lineament Reproducibility (RA_1) and Coincidence (RA_2)

Lineament reproducibility and coincidence are assessed in several steps during the analysis (as outlined in Section 3). First, the two individual interpretations for each data set were integrated to produce single data set specific (RA_1) interpretations. During this step, the reproducibility (RA_1 value) of each lineament was assessed (Section 3.2.2). Secondly, the individual data set interpretations were integrated to produce the final integrated (RA_2) data set. During this step, the coincidence (RA_2 value) between lineaments identified in the various data sets was evaluated (Section 3.2.3). A breakdown of all reproducibility and coincidence values is presented in Section 4 and Appendix B.

The evaluation of RA_1 data for all lineament types (geophysical, DEM, and FRI) reveals a moderate to high reproducibility between interpreters for the geophysical lineaments (58% of lineaments RA_1=2), the DEM lineaments (62% of lineaments RA_1=2), and the FRI lineaments (74% of lineaments RA_1=2). The higher reproducibility between interpreters for the FRI lineaments relative to the other data sets is largely attributed to the abundance of well-defined rivers, streams, and linear lake edges in the assessment area that were identified by both interpreters.

Reproducibility values (RA_1) vary between geophysical lineaments types, with unclassified lineaments having the lowest reproducibility (46% of unclassified lineaments RA_1=2), and dyke lineaments having the highest reproducibility (69% of dyke lineaments RA_1=2). The lower reproducibility of unclassified geophysical lineaments can be attributed to the subtle magnetic signature of the curvi-linear unclassified lineaments that can inhibit their identification. The high reproducibility for dyke lineaments is expected, as their geophysical signatures are typically well-defined (long, continuous magnetic highs), and are therefore easily interpreted. Low lineament reproducibility values are the result of differences in the individual lineament interpretations from each interpreter for the same data set, and can be attributed to the judgement and subjectivity of the expert carrying out the interpretation.

Coincidence between lineaments identified from the DEM and FRI data sets was evaluated for the second reproducibility assessment (RA_2). Overall, a total of 28% of the surficial lineaments were interpreted in both the DEM and FRI data sets. The coincidence between lineaments of these data sets is in part explained by the fact that lineaments interpreted from the FRI imagery and the DEM data represent surficial expressions of the same bedrock feature. For example, a lineament drawn along a stream channel shown on the FRI imagery is expected to be coincident with a lineament that captures the trend of the associated topographic valley expressed in the DEM data. The lack of coincidence between the two surficial data sets may be the result of several factors, including, the difference in resolution, and the different styles in which structures manifest in the DEM and FRI data sets. The DEM data were collected during the magnetic survey (25-metre grid cell size), with a much lower resolution than the FRI imagery (0.4 m resolution). Therefore, a structure that is apparent in the FRI imagery may not be apparent in the DEM data. Alternatively, a structure present

in the DEM data may be represented as multiple structures within the higher resolution FRI data. In addition, certain structures observed in the DEM data may be obscured by vegetation in the FRI data, and conversely, structures defined by a change in vegetation in the FRI data may not have a topographic expression in the DEM data.

The coincidence assessment (RA_2) between geophysical and surficial features revealed that 43% of the interpreted geophysical lineaments were also interpreted in at least one of the two surficial data sets. When considering the entire final integrated lineament data set, only 9% of the final integrated lineaments were identified in all three data sets, and 24% of the final integrated lineaments were identified in two of the three data sets.

The remaining 67% of the lineaments lack any coincidence (RA_2=1) and were only identified in a single data set. The final integrated lineament data set can be further assessed to identify coincidence between data sets for each of the specific types of lineaments (i.e., brittle, dyke and unclassified). For the 780 of brittle lineaments interpreted in the final integrated lineament data set, 12% of the lineaments were identified in all three data sets, and 25% of the lineaments were identified in two of the three data sets. The remaining 63% of the lineaments lack any coincidence and were only identified in a single data set. In particular, almost half (47%) of the brittle lineaments that are lacking coincidence with any other data set are derived from the FRI data.

In addition, it is apparent that interpreted dyke lineaments from the geophysical data set also had some sort of surficial lineament expression. Considering the 249 dyke lineaments interpreted, 15% of these lineaments were coincident with at least one of the two surficial data sets, and 8% were interpreted in both surficial data sets.

For the 196 unclassified lineaments interpreted in the final integrated lineament data set, 12% of the lineaments were identified in all three data sets, and 25% were identified in two of the three data sets. The remaining 63% of the lineaments lack any coincidence and were only identified in a single data set. Of the total number of unclassified lineaments, 75% of these lineaments were interpreted using the geophysical data set.

The lack of coincidence between different sets of lineaments may be attributed to multiple factors, including:

- Deeper structures identified in the geophysical data may not have a surficial expression
- Certain structures identified in the geophysical data may have a subdued or no surficial expression
- Surface expression of geophysical lineaments may be masked by the presence of overburden (e.g., large river valleys covered by Quaternary sediments)
- Structures identified in the surficial data may not extend to significant depths and therefore may not be recognizable in the magnetic data
- Structures identified in the surficial data may not possess sufficient magnetic susceptibility contrast to be recognized in the magnetic data

Considering the above factors, it is necessary to objectively analyze the results of the RA_2 assessment with the understanding that RA_2 = 1 does not necessarily imply a low degree of confidence that the specified lineament represents a true bedrock structure.

Lineaments that were coincident in two or three data sets were commonly long and continuous. Within the geophysical data, these lineaments were defined by continuous magnetic lows or highs, whereas in the surficial data sets, these lineaments were defined by continuous topographic valleys, long linear lakes, and vegetation changes.

5.2 Lineament Trends

Lineament orientations within the White River Phase 2 assessment area can be observed visually (Figure 7 to Figure 13), and via length weighted azimuth plots (see rose diagram insets in Figure 7 to Figure 13). A summary of lineament orientation data for the assessment area is presented in Appendix A and Figure A5.

Lineaments identified from both the geophysical and surficial data sets within the White River area tend to reveal four general lineament orientation sets: southeast, northeast, and east-northeast, with an additional minor north-south trend (Figure A5 and Figure 7 to Figure 13). Of these lineament orientations, the southeast- and northeast-trending lineaments tend to be broadly distributed but are well-defined in all lineament data sets. The east-northeast trending lineaments are most prominently observed in the geophysical lineament data set where they are attributed as unclassified lineaments.

Length weighted orientation data for the geophysical lineaments tend to exhibit a dominant but broad southeast-trending lineament orientation, with minor north-south and north-northeast, to northeast orientations (Figure 12). These geophysical lineaments can also be subdivided into orientation sets based on the lineament type (i.e. brittle, dyke, unclassified lineaments). The dyke lineament orientations exhibit a dominant southeast orientation (one high confidence peak at 135°), a subordinate north-northeast orientation (one medium to low confidence peak at 030°), and a minor north-south orientation, which can be attributed to the Matachewan, Biscotasing, and Marathon dyke swarms, respectively. The southeast-trending Matachewan dyke lineaments are most prominent, followed by sporadic north-trending Marathon and northeast-trending Biscotasing dyke lineaments. East-southeast-trending Sudbury dyke lineaments are rare and occur in the southern half of the study area and are not easily distinguished from the Matachewan dykes in the rose diagram plots. The southeast-trending dyke lineaments often occur as clusters of tightly spaced dyke lineaments, separated by kilometre-scale zones without interpreted dyke lineaments. In contrast, interpreted dyke lineament orientations attributed to the Marathon, Biscotasing, and Sudbury swarms are typically widely spaced and distributed throughout the assessment area. The orientation of brittle lineaments interpreted in the geophysical data show similar general trends as the dykes, but their orientation sets tend to display a broad east-southeast, to south-southeast orientation (two high confidence peaks at 128° and 113°, and one medium to high confidence peak at 148°), as well as a significant but less dominant north-south-trending orientation (one medium to low confidence peak at 010°), and a minor northeast-trending orientation.

For the most part, the interpreted surficial lineaments tend to exhibit broad orientation trends similar to those of the geophysical lineaments (Figure 11 and Figure A5); the main difference is that surficial lineaments have a dominant north-northeast to east-northeast orientation (one high confidence peak at 033°, and one medium confidence peak at 064°), and a broad, less significant southeast orientation (one medium confidence peak at 124°). As with the interpreted geophysical brittle lineaments, some of the surficial lineament trends are coincident with orientations of the Matachewan, Marathon, and Biscotasing dyke swarms. Despite the abundance of the dominant northeast-trending surficial lineaments, some of these lineaments are oriented parallel to prominent glacial landforms (see in Figure 3) and may in fact represent the trend of glacial features. Although an effort was made to avoid interpreting glacially derived linear features (e.g., eskers, etc.) as tectonic lineaments, the coincidence in orientation suggests using caution when interpreting the nature of northeast-trending surficial lineaments. Despite this uncertainty, the northeast-trending surficial lineaments are also coincident with a broad distribution of northeast-trending brittle and dyke geophysical lineaments.

As expected, the final integrated brittle lineaments (Figure 13) generally show similar trends as seen in the geophysical and surficial data sets, but with two dominant, broad east-southeast to south-southeast (two high confidence peaks at 128° and 113°, and one medium to low confidence peak at 149°), and northeast trends (one high confidence peak at 038°), a subordinate north-south orientation (one medium to low confidence peak at 008°), and a minor east-northeast. The orientations of the interpreted brittle lineaments from the final integrated lineaments are mostly consistent with the orientations of interpreted dyke lineaments derived from the geophysical data set (Figure 12). Although their lineament orientation sets display a similar trend, the frequency/length of lineaments within the dominant peaks differ between the interpreted dyke lineaments and the brittle lineaments. In general, it seems as though brittle lineaments subparallel to the Matachewan dyke swarm tend to be better expressed in the geophysical data, whereas brittle lineaments that are subparallel to the Biscotasing dyke swarm seem to be better expressed in the surficial data sets. Brittle lineaments interpreted to be subparallel to the Marathon and Sudbury dyke swarms tend to have a weaker expression in both the geophysical and surficial data sets.

Significant east-northeast (two high confidence peaks at 062° and 078°) and east-southeast orientations (one medium to high confidence peak at 107°), as well as several other minor orientations including north-northeast (one medium to low confidence peak at 032°) were observed within the geophysical data and have been attributed mainly to the unclassified lineament set. These unclassified lineaments are best seen within the Kabinakagami Lake greenstone belt (Figure 7), however, were also identified throughout the White River assessment area. Unclassified lineaments within the Strickland pluton and the Pukaskwa batholith are curvi-linear and tend to replicate the shape of the intrusion margins. An exception to this is towards the northeast of the White River area, where unclassified lineaments show a dominant east-west trend within the Strickland pluton. Within the Anahareo pluton, the unclassified lineaments define a narrow zone of anastomosing, sporadically folded, east-northeast trending structures. The curvi-linear nature of these lineaments will have an impact on the distribution or spread of orientations interpreted in a rose diagram.

The abundance, length, and through-going nature of the southeast- and northeast-trending brittle and surficial lineaments, suggest that these lineament trends represent the most significant regional orientation of brittle structures. Overall, these trends appear to correlate well with regional fault systems, with mapped brittle faults in the surrounding area generally showing the same northwest and northeast orientations. These correlations are described in further detail in Section 5.5.1.

5.2.1 Relationship between Lineament Sets and Regional Stress Field

The principal neotectonic stress orientation in central North America is generally oriented approximately east-northeast (63 degrees \pm 28 degrees; Zoback, 1992) although anomalous stress orientations have also been reported in the mid-continent that include a 90-degree change in azimuth of the maximum compressive stress axis (Brown et al., 1995) and a north-south maximum horizontal compressive stress (Haimson, 1990). Local variations, and other potential complicating factors involved in characterizing crustal stresses, including the effect of shear stress by mantle flow at the base of the lithosphere (Bokermann, 2002; Bokermann and Silver, 2002), the degree of coupling between the North American plate and the underlying mantle (Forte et al., 2010), the effects of crustal depression and Holocene rebound, and the influence of the thick lithospheric mantle root under the Canadian Shield, make it premature to correlate the regional neotectonic stress orientation with the orientation of interpreted lineaments.

However, it is possible to broadly speculate on the potential behavior of the identified lineaments if they were to be reactivated by the regional east-northeast neotectonic stress regime. Four dominant orientations of lineaments were interpreted: northwest, north, northeast, and east to east-northeast. Should the identified lineaments be reactivated under the current stress regime, the northwest and

north oriented lineaments would likely reactivate as reverse dip-slip to oblique-slip faults depending on their strike and dip, and the northeast and east to east-northeast oriented lineaments would likely reactivate as strike-slip to oblique-slip faults.

5.3 Lineament Length

Interpreted geophysical, surficial and final integrated lineaments classified by length are presented in Figures 14, 15 and 16. The distributions of lineament lengths are displayed on histograms and cumulative frequency plots (see inset plots on Figures 14-16). On these plots, the x-axis represents the bin lengths for the lineaments (km), and the left y-axis represents the percentage of the total number of interpreted lineaments contained within that length bin. The blue line represents the cumulative frequencies expressed as a fraction between 0 and 1, which can be considered equivalent to probability. The probability is labeled on the right y-axis of the plot. Length statistics are summarized in Appendix A: Figure A6, and Appendix B. Lineament lengths displayed and reported in the figures, statistics tables, and histogram plots only reflect the length of the portion of the lineament that is contained within the individual lineament assessment block. Therefore, the lineament lengths do not necessarily reflect the full length of all lineaments, as lineaments were only traced within the assessment area and could extend beyond its borders.

Overall, lineament lengths for the geophysical brittle and dyke, surficial, and final integrated lineaments display a similar distribution, with the distribution of lengths skewed toward shorter lineaments in the surficial lineaments data set (Figure 15). For each of the lineament data sets the majority of lineaments tend to have lengths less than 5 km. Approximately 77% of the geophysical brittle and dyke lineaments and approximately 93% of the surficial lineaments have lengths that are less than 5 km. The geophysical brittle and dyke lineaments contain a higher number of long lineaments relative to the integrated surficial lineaments. This is most apparent for lineaments in the 5-10 kilometre range, which were less commonly interpreted from the surficial data sets (Figure 14 to Figure 16, and Appendix A: Figure A6).

The comparison of median and mean values for all geophysical, integrated surficial, and final integrated lineaments reveals a roughly similar length distribution as described above (Appendix B). The geophysical lineaments exhibit the longest overall mean (4.20 km) and median (2.68 km), whereas the integrated surficial lineaments exhibit the shortest mean (2.12 km) and median (1.45 km). The final integrated lineaments exhibit an intermediate mean (3.29 km) and median (2.06 km), as would be expected as these lineament are the result of the combination of the slightly longer geophysical and slightly shorter surficial lineaments.

The difference in length between lineaments interpreted from geophysical and surficial data sets can in part be explained by the nature of the lineaments interpreted from each data set. From the geophysical data, lineaments are typically characterized by long continuous magnetic lows or highs (dykes, for example). Conversely, surficial lineaments are typically characterized by a combination of breaks in topography, vegetation and bedrock, and elongated lakes. These surficial features are not as continuous as the lineaments interpreted from geophysical data, often due to their interruption by overburden. This resulted in the interpretation of shorter surficial lineaments relative to the geophysical lineaments.

Analysis of lineament length relative to coincidence values for all final integrated lineaments indicates that lineaments coincident in all three data sets (RA_2=3) are typically longer (mean = 8.27 km, median = 6.12 km) than lineaments reproduced in two (RA_2=2; mean = 4.20 km, median = 3.01 km) or only one (RA_2_1; mean = 2.33 km, median = 1.53 km) data sets (Appendix B). This is to be expected, as lineaments observed in all three data sets may represent significant bedrock structures.

Similarly, an analysis of lineament length relative to certainty values for the final integrated lineaments indicate that lineaments with the highest certainty value (3), are typically longer (mean = 6.48 km, median = 4.52 km), than those with certainty values of 2 (mean = 2.51 km, median = 2.11 km) and 1 (mean = 1.48 km, median = 1.18 km) (Appendix B). Again, this is to be expected as lineaments assigned the highest certainty lineaments are most likely to represent significant bedrock structures.

Lineament lengths relative to the dominant lineament orientations suggest that longer lineaments tend to be evenly distributed in all of the dominant lineament orientations. As expected, both geophysical and surficial lineaments trending in northwest, and northeast orientations seem to contain relatively similar amounts of longer lineaments. Of these long lineaments, most of them correspond to long and continuous dykes of the Matachewan and Biscotasing dyke swarms. Although it is apparent that the northeast trending set of surficial lineaments tend to have a higher number of longer lineaments, as noted previously, this orientation of surficial lineament is also coincident with the orientation of glaciation.

Although there is no information available on the depth extent of the interpreted lineaments for the White Phase 2 assessment area, the length information described above can be used as a proxy for depth extent. Therefore, a preliminary assumption may be that the longer interpreted lineaments may extend to greater depths than the shorter interpreted lineaments.

5.4 Density

Analyses of lineament and lineament intersection density were conducted for the White River Phase 2 assessment area as described in Section 3.2.6, and are presented in Figure 17 to Figure 21 (lineament density) and Figure 22 to Figure 27 (lineament intersection density).

5.4.1 Lineament Density

An analysis of lineament density for each data set is presented below and in Figure 17 to Figure 21. Locally, lineament density appears to be lower at the margins of the assessment area. This arises as lineaments are only traced to the margins of the assessment area, and when generating density plots, this can result in an apparent low lineament density around the border of the area.

Geophysical Lineament Density

As the nature of unclassified lineaments is unknown at this stage (potential to represent ductile shear zones, brittle-ductile shear zones or the internal fabric of the rock units, etc), density analyses for these lineaments were conducted separately. Figure 17 shows the lineament density of the brittle and dyke lineaments, and Figure 18 includes the unclassified lineaments in the calculation of lineament density.

Throughout the White River area, lineament density analyses of brittle and dyke lineaments reveal a relatively uniform lineament density, with few discrete zones of elevated and lower lineament density throughout. In particular, areas of highest lineament density are located north of Nameigos Lake within the Strickland pluton, and west of Anahareo Lake in the Anahareo pluton (Figure 17). In general, the majority of the areas of elevated lineament density tend to occur in areas with clusters of northwest-trending dyke lineaments and where these clusters intersect with tight-spaced brittle lineaments and sporadic north- and northeast-trending dyke lineaments. Areas of lowest lineament density are located in the area around Gourlay Lake within the Strickland pluton, and north of Anahareo Lake in the Anahareo pluton (Figure 17). In addition, a broad low lineament density area

is most pronounced in the zone within the gneissic tonalite suite of the Pukaskwa batholith, located between the two plutons.

By including the unclassified lineaments in the density calculation, the distribution of lineament density becomes elevated within discrete areas where unclassified lineaments were interpreted. In particular, a high density of unclassified lineaments are interpreted within the Kabinakagami Lake greenstone belt on the eastern side of the assessment area. Within this rock unit the unclassified lineaments are curvi-linear and tightly spaced, and maintain a strong east-northeast orientation. Although the area within the Pukaskwa batholith previously displayed an apparent low lineament density, including the unclassified lineaments in the lineament density calculation enhances the density; however the nature of these lineaments remains uncertain. In addition, unclassified lineaments interpreted as a narrow east-northeast-trending zone extending from the southern part of the Kabinakagami greenstone belt tend to increase the lineament density within a broad zone north of Anahareo Lake in the Anahareo pluton (Figure 18). Lastly, several short and discontinuous unclassified lineaments located along the northern boundary of the Strickland pluton tend to slightly elevate the lineament density in this area.

Surficial Lineament Density

Lineament density plots for the surficial lineaments show variable lineament density, with broad but well-defined areas of lower density (Figure 19). The lowest surficial lineament density areas tend to be located in broad areas along the northern boundary of the assessment area within the Strickland pluton and Kabinakagami Lake greenstone belt. Smaller lower density areas are sporadically distributed throughout the assessment area. It is noted however, that the density of surficial lineaments may be in part related to the presence or absence of overburden. In order to properly assess surficial lineament density, it is necessary to take into account the location of surficial features (broad river valleys, large water features, glacial overburden, etc.), as the ability to interpret surficial lineaments is limited in these areas. Large organic terrain, glaciolacustrine sediments, and glacial outwash deposits are present northeast of Gourel Lake and proximal to Nameigos Lake (Figure 3), and as such few surficial lineaments were interpreted in these areas, and the corresponding lineament density is low. In areas where bedrock is readily exposed, zones of elevated lineament density occur along or at the intersection of tight-spaced northwest- and northeast-trending surficial lineaments. The area displaying the highest surficial lineament density is correlated with a set of curvi-linear lineaments near the centre of the assessment area, within the Pukaskwa batholith, and is correlated with a series of ridges, streams, and aligned lakes. This area is also consistent with the high density of unclassified lineaments interpreted from the geophysical data.

Final Integrated Lineament Density

The final integrated lineaments result from the integration of the geophysical and surficial lineaments. Therefore, these lineaments can be classified into brittle and dyke lineaments and a set of unclassified lineaments. Similar to the geophysical lineament density analyses, unclassified lineaments were analyzed separately and are presented on separate figures. Figure 20 shows the lineament density of the brittle and dyke lineaments from the final integrated lineament data set, and Figure 21 includes the unclassified lineaments in the calculation of lineament density.

Lineament density analyses of the final integrated brittle and dyke lineaments reveal a variable lineament density with multiple well defined zones of elevated lineament density (Figure 20). Similar to the other data sets, zones of higher lineament density correspond to tight-spaced northeast, north-, and northwest-trending brittle and dyke lineaments, and the intersection of these lineament orientations. The areas of highest lineament density occur in broad zones located throughout most of the Strickland pluton, and throughout much of the Anahareo pluton. The Kabinakagami Lake greenstone belt displays a lower lineament density when considering the interpretation of only dyke and brittle lineaments. Outside of the Kabinakagami Lake greenstone belt, the lowest lineament

density occurs in the centre of the assessment area within the Pukaskwa batholith, and proximal to Anahareo Lake in the Anahareo pluton. Neither of these areas are coincident with extensive overburden, however, both areas are coincident with abundant unclassified lineaments. Additional areas of lower lineament density are located north of Gourlay Lake and southwest of Beaton Lake. Each of these areas tend to be relatively small, with the exception of the area north of Gourlay Lake which is coincident with the significant organic deposit.

By adding the unclassified lineaments to the final lineament density calculation, the density becomes elevated within broad zones where the pervasive unclassified lineaments are interpreted (Figure 21). In particular, a high density of unclassified lineaments is interpreted within the Kabinakagami Lake greenstone belt on the eastern side of the assessment area. In addition, unclassified lineaments interpreted as a narrow east-northeast-trending zone extending from the southern part of the Kabinakagami greenstone belt tend to increase the lineament density within a broad zone north of Anahareo Lake in the Anahareo pluton. Although the area within the Pukaskwa batholith was previously displayed an apparent low lineament density, including the unclassified lineaments in the lineament density calculation enhances the density; however the nature of these lineaments remains uncertain. Lastly, several short and discontinuous unclassified lineaments located along the northern boundary of the Strickland pluton tend to slightly elevate the lineament density in this area

5.4.2 Lineament Intersection Density

An analysis of lineament intersection density for each data set is presented below and in Figure 22 to Figure 26.

Geophysical Lineament Intersection Density

As the character of the unclassified lineaments is unknown at this stage, two separate lineament intersection density analyses were conducted. Figure 22 shows lineament intersection density of only brittle and dyke lineaments interpreted in the geophysical data. Figure 23 incorporates the distribution of unclassified lineaments into this lineament intersection density analyses.

Lineament intersection density for the final integrated brittle and dyke lineaments is generally higher than the lineament intersection density calculated for the geophysical brittle and dyke lineaments, however, areas of elevated lineament intersection density are typically coincident between both datasets, such as north of Nameigos Lake and west of Anahareo Lake. Elevated lineament intersection density is typically due to the intersection of clusters of northwest-trending dyke lineaments and where these clusters intersect with tight-spaced brittle lineaments and sporadic north- and northeast-trending dyke lineaments (Figure 22). Similar to the lineament density analysis of geophysical brittle and dyke lineaments, zones of slightly elevated brittle and dyke lineament intersection density occur north of Nameigos Lake (proximal to an inlier of gneissic tonalite within the Strickland pluton), and west of Anahareo Lake. When also considering unclassified lineaments (Figure 23), additional zones of elevated intersection density are present, particularly north of Anahareo Lake in the Anahareo pluton, and towards the northwest of the assessment area at the northern margin of the Strickland pluton. These areas of elevated density are the result of the intersection of northwest- and northeast-trending brittle and dyke lineaments with east-northeast trending unclassified lineaments. In areas where numerous unclassified lineaments occur at a high angle to the dominant northeast- and northwest-trending brittle and dyke lineaments (i.e., north of Anahareo Lake), lineament intersection density is elevated.

Surficial Lineament Intersection Density

Lineament intersection density for the integrated surficial lineaments (Figure 24) is typically low and uniform throughout the White River area. Zones of elevated lineament intersection density typically

occur along or at the intersection of tight-spaced northwest-, and northeast-trending surficial lineaments, however, the highest surficial lineament intersection density is related to a set of curvi-linear lineaments near the centre of the assessment area, within the Pukaskwa batholith. The density of surficial lineaments is in part related to the presence of overburden. In order to properly assess surficial lineament density, it is necessary to take into account the location of surficial features (river valleys, glacial till cover, etc.), as the ability to interpret surficial lineaments was limited in these areas. Large expanses of organic terrain, glaciolacustrine sediments, and glacial outwash deposits are present northeast of Gourlay Lake and proximal to Nameigos Lake, and as such few surficial lineaments were interpreted in the areas, and lineament intersection density is low.

Final Integrated Lineament Intersection Density

As the character of final integrated unclassified lineaments may be variable (between brittle-ductile shear zones, and the internal fabric of the rock units), two separate lineament intersection density analyses were conducted, one including only final integrated brittle and dyke lineaments, and the other including all final integrated brittle, dyke and unclassified lineaments. Results of these analyses are presented in Figure 25 and Figure 26, respectively.

Lineament intersection density is variable with multiple well defined zones of low and high lineament intersection density throughout the White River area, and lineament intersection density of all final integrated brittle and dyke lineaments closely resembles lineament density of the same final integrated lineaments. Elevated lineament intersection density is typically due to the intersection of clusters of northwest-trending dyke lineaments and where these clusters intersect with tight-spaced brittle lineaments and sporadic north- and northeast-trending dyke lineaments (Figure 25). Similar to the lineament density analysis of all final integrated brittle and dyke lineaments, zones of slightly elevated brittle and dyke lineament intersection density occur throughout most of the Strickland pluton (with the exception of proximal to the north margin of the pluton in the northwest of the assessment area, and northeast of Nameigos Lake), and throughout much of the Anahareo pluton. Outside of the Kabinakagami Lake greenstone belt, the lowest lineament intersection density occurs in the northwest of the assessment area near the northern margin of the Strickland pluton, in the centre of the assessment area (within the Pukaskwa batholith), and west of Anahareo Lake in the Anahareo pluton. When also considering unclassified lineaments (Figure 26), additional zones of elevated intersection density are present, particularly north of Anahareo Lake in the Anahareo pluton, and near the centre of the assessment area, within the Pukaskwa batholith that is correlated with a series curvi-linear lineaments. These areas of elevated density are the result of the intersection of northwest- and northeast-trending brittle and dyke lineaments with typically east-northeast trending unclassified lineaments. In areas where numerous unclassified lineaments occur at a high angle to the dominant northeast- and northwest-trending brittle and dyke lineaments (i.e., north of Anahareo Lake), lineament intersection density is elevated.

5.5 Lineament Truncation and Relative Age Relationships

The structural history of the White River area, outlined in Section 2.2, provides a framework that may aid in constraining the relative age relationships of the interpreted bedrock lineaments. Previous work in and around the White River area identified six regionally distinguishable deformation episodes (D_1 – D_6) that are inferred to have overprinted the bedrock geological units of the area. The lineament interpretation is roughly consistent with regional observations; however, certain deformation events described in the literature could not be distinguished in the interpreted lineaments (D_1), and other deformation events could not be separated and were therefore grouped together (i.e., D_2 to D_4 , and D_5 and D_6).

As summarized in Section 2.3, D_1 is characterized by a lack of penetrative fabric and rarely preserved isoclinal folds between ca. 2.719 and ca. 2.691 Ga, and D_2 - D_4 includes all unclassified

lineaments, and is characterized by steep-dipping foliations, isoclinal folds, and thrust faults, primarily observed within the greenstone belts, but also identified in the Pukaskwa batholith and the Strickland and Anahareo plutons, and dated between ca. 2.691 and ca. 2.673 Ga.

Details of structural features associated with the D₅ and D₆ deformation events are limited in the literature to brittle and brittle-ductile faults of various scales and orientations (Lin, 2001; Muir, 2003). Within the Hemlo greenstone belt, certain D₅ and D₆ faults offset the Marathon and Biscotasing dyke swarms (all ca. 2.2 Ga; Muir, 2003), and as such, D₅ and D₆ faults in the Hemlo region propagated after ca. 2.2 Ga. However, since there are no absolute age constraints on specific events, the entire D₅-D₆ interval of brittle deformation can only be constrained to a post-2.673 Ga timeframe that may include many periods of re-activation attributable to any of several post-Archean tectonic events. In addition, while no evidence was observed for dyke emplacement postdating brittle deformation, the lack of constraint on the age of fault development does not preclude this possibility.

Of the 1,225 final integrated lineaments, 196 were attributed as unclassified lineaments, 780 were classified as brittle lineaments, and 249 as dyke lineaments (Figure 27). Based on the character of the unclassified lineaments, they are interpreted to represent structures formed during D₂-D₄ episodes. The unclassified lineaments were recognized predominantly from the geophysical data by their curvi-linear geometry, and their low-angle truncation of form lines. As discussed in Section 3.2, these lineaments may represent the internal fabric of the rock units including the more intense fabric along ductile or brittle-ductile shear zones. These structures are interpreted to define semi-continuous, curvi-linear zones of ductile or brittle-ductile deformation in the Kabinakagami Lake greenstone belt, however it is unclear what they represent along the northern margin of the Strickland Pluton, and within the Pukaskwa batholith, and the Anahareo pluton.

In general, the unclassified lineaments are interpreted as D₂-D₄ which are the oldest generation of interpreted structure (likely Archean) and may locally show some evidence of offset and/or truncation by younger brittle lineaments (Figure 27). Locally, the D₂-D₄ unclassified lineaments may have been reactivated such that they truncate and/or offset D₅-D₆ brittle lineaments. In these cases, the D₂-D₄ unclassified lineaments were reclassified as D₅-D₆ brittle lineaments as they reactivated under a younger regime of brittle deformation. Structures associated with D₁ deformation were not identified in the lineament interpretation.

The interpreted brittle lineaments in the final integrated data set are observed in two broad orientations: northwest, and northeast, with a subordinate north-trending lineament set also identified. Each of the brittle lineament orientations is parallel to subparallel to the Matachewan, Biscotasing, and Marathon dyke orientations. Despite the geometric relationship between dyke and brittle lineaments, the relative ages of the brittle lineaments do not appear to correlate with the age of emplacement of the dykes (i.e., brittle lineaments subparallel to youngest dyke generation do not consistently offset or truncate brittle lineaments subparallel to older dyke generations). Rather, brittle lineaments of all orientations tend to offset and truncate, and are offset and truncated by all other brittle and dyke lineaments. As a result, brittle lineaments could not systematically be differentiated into different generations of brittle deformation, and were therefore classified into the same broad generation of brittle deformation, D₅-D₆.

Of the 249 final integrated dyke lineaments, four distinct dyke populations can be identified, including 164 dyke lineaments corresponding to the 2.473 Ga northwest-trending Matachewan dyke swarm (Buchan and Ernst, 2004), 40 dyke lineaments corresponding to the 2.167 Ga. northeast-trending Biscotasing dyke swarm (Hamilton et al., 2002), 33 dyke lineaments corresponding to the 2.121 Ga. north-trending Marathon dyke swarm (Buchan et al., 1996; Hamilton et al., 2002), and 12 dyke lineaments corresponding to the 1.238 Ga. west northwest-trending Sudbury dyke swarm (Krogh et al., 1987). As discussed, dyke lineaments may locally truncate and offset, and may be

truncated and offset by all possible orientations of brittle lineaments. Considering these possible relationships, one or several of the following scenarios are possible:

- Dyke emplacement preceded the interpreted brittle faulting, and brittle faults subsequently exploited weaknesses developed in subparallel orientations;
- Dyke swarms exploited and were emplaced along pre-existing faults;
- Dykes and faults were generated coevally in subparallel orientations;
- Brittle faults were reactivated syn- or post-dyke emplacement.

Apart from these timing constraints, there are no additional absolute age constraints for aforementioned phases of deformation.

5.5.1 Mapped Structure and Lineament Relationships

Relatively few faults have been mapped in the White River area (Figure 3), with only five mapped faults within the assessment area. All mapped faults were at least partially reproduced in the lineament interpretation. The relationship of mapped faults relative to the final integrated lineaments can be seen in Figure 27.

A west-northwest-trending, mapped fault is located at the northern extent of Nameigos Lake, within the Kabinakagami Lake greenstone belt and truncating the Pukaskwa batholith against the Strickland pluton. This fault trace is located adjacent and parallel to two west-northwest trending brittle lineaments, however these lineaments only cover the eastern portion of the fault.

A northwest-trending brittle mapped fault is located at the southern extent of Nameigos Lake that is mapped offsetting a thin sliver of the Kabinakagami Lake greenstone belt with a dextral strike-separation. A brittle lineament was interpreted along the southeastern portion of this mapped fault, but was not identified along its northern extent. However, the northern portion of the fault is proximal, and parallel to an interpreted Matachewan dyke, that continues northwest, well beyond the extent of the mapped fault.

A northeast-trending mapped fault crosses the western margin of the assessment area juxtaposing the Pukaskwa batholith against the Strickland pluton. This fault is shown to have sinistral movement by offsetting a thin sliver of mafic metavolcanic rock at the southern extend of the Dayohessarah greenstone belt. The mapped fault is coincident with a series of interpreted brittle lineaments interpreted from the surficial data sets, except at the northeastern extent of the mapped fault.

Within the Anahareo pluton a northwest-trending fault is mapped to the southwest of Anahareo Lake. The mapped trace of this fault ends within the Anahareo pluton. However, this fault is coincident with an interpreted brittle lineament that extends well beyond the extent of the mapped fault and continues for an additional ~10 km to the northwest and ~2 km to the southeast. The portion of the fault that has been mapped is consistent with a brittle lineament segment with a significant DEM expression, whereas the extension to the northwest was interpreted from the geophysical data.

Lastly, a northeast-trending fault has been previously mapped crossing the southeastern corner of the assessment area within the Anahareo pluton. Only a small portion of this mapped fault occurs within the assessment area, and is coincident with a short interpreted brittle lineament interpreted from both the geophysical and surficial data sets.

Multiple dykes had been previously interpreted throughout the White River areas from regional-scale resolution geophysical data (Figure 2; Ontario Geological Survey, 2011). These dykes are generally

coincident with interpreted dyke lineaments, however certain discrepancies exist due to the higher resolution of the geophysical data set used in this assessment. The most noticeable discrepancy is that a single previously interpreted dyke from the regional-scale data is most often recognized as a series of tight-spaced dyke lineaments within the higher resolution geophysical data (Figure 27). This was most evident for northwest-trending Matachewan dykes that often manifested in the high resolution geophysical data as a series of tight-spaced dyke lineaments.

6 Summary of Results

This report documents the source data, workflow, and results from a lineament interpretation of geophysical (magnetic) and surficial (DEM and FRI digital aerial imagery) data sets acquired as part of the Phase 2 preliminary assessment for the White River area. The lineament analysis provides an interpretation of the location and orientation of possible individual brittle, dyke, and unclassified lineaments on the basis of remotely sensed data, and attempts to evaluate their relative timing relationships within the context of the regional geological setting. The workflow involves a three step process that was designed to address the issues of subjectivity and reproducibility. The distribution of lineaments in the area of White River reflects the bedrock structure, resolution of the data sets used, and surficial cover.

Within the White River Phase 2 assessment area, a total of 666 geophysical lineaments, 425 DEM lineaments, and 670 FRI lineaments were interpreted by the two interpreters (RA_1) from their respective data sets. Merging the lineaments derived from the DEM and FRI data resulted in a total of 827 surficial lineaments (RA_2). Merging the surficial lineaments with those derived from the geophysical data resulted in a total of 1225 final integrated lineaments (RA_2).

The reproducibility assessment (RA_1) revealed a moderate to high coincidence between interpreters for all three data sets (i.e., 58% for the geophysical lineaments, 62% for the DEM lineaments, and 74% for the FRI lineaments). The variability between interpreters could be attributed to the resolution of the data sets and the judgement of the expert carrying out the interpretation. In general, longer and higher certainty lineaments were identified more often by both interpreters, as well as dyke lineaments (RA_1 = 69%; which are more easily interpreted due to their distinct geophysical signature).

The coincidence assessment (RA_2) revealed a moderate to low coincidence between surficial lineaments interpreted from the DEM and FRI data sets (i.e., 28% of lineaments were coincident in both surficial data sets). Similarly, the final integrated lineaments revealed a low coincidence between lineaments interpreted from the three data sets (i.e., 9% of lineaments were coincident with all three data sets, 24% of lineaments were coincident in at least one other data set, and 67% of lineaments lacked coincidence with other data sets). The variability between lineaments derived from the different data sets could be attributed to multiple factors, including deeper structures identified in the magnetic data that may not have a surface expression, surficial features that may not extend to depth, features identified in the surficial data that may not possess sufficient magnetic susceptibility contrast to be recognized in the magnetic data, the masking of surface expressions of magnetic lineaments by the presence of overburden, and the differing resolution of the various data sets. Similar to the reproducibility assessment (RA_1), longer and higher certainty lineaments were more often coincident in the various data sets.

An analysis of lineament orientations revealed an overall consistency between the orientations of lineaments identified in the various data sets, which suggests that lineaments interpreted from all three data sets are identifying the same sets of structures. Lineament orientations within the White River area reveal three dominant trends: northwest, northeast, and east-northeast, with an additional minor north trend. Of these lineament orientations, the northwest- and northeast-trending lineaments are well-defined in all data sets. The northwest, north, and northeast lineament orientations are distributed throughout the White River Phase 2 assessment area, and correspond to dyke lineaments of the Matachewan, Marathon, and Biscotasing dyke swarms, respectively, and subparallel brittle

lineaments. Brittle and dyke lineaments occur both as clusters of tight-spaced lineaments and in isolation.

Evaluation of lineament length data for the geophysical brittle and dyke, surficial, and final integrated lineaments reveals roughly the same distribution, where the majority of lineaments are less than 5 km in length. In general, the geophysical brittle and dyke, and final integrated lineament sets contain more long lineaments relative to the integrated surficial lineaments due to the style in which bedrock structures are manifested within these data sets. Lineaments that were reproduced in all three data sets (RA_2=3), and lineaments with the highest certainty value (3) typically represent the longest lineaments (i.e., greater than 5 km). Long surficial, brittle, and dyke lineaments trend predominantly northwest, and northeast, corresponding to the Matachewan and Biscotasing dyke sets, respectively, and subparallel brittle structures. Long surficial lineaments trend dominantly towards the northeast, which is also coincident with the orientation of glaciation.

The geophysical lineament density of brittle, and dyke lineaments throughout all subareas reveal a relatively uniform lineament density, with few discrete zones of elevated and lower lineament density throughout. Zones of elevated lineament density occur within all geological units and are typically the result of clusters of tight-spaced brittle and (or) dyke lineaments, and the intersection of different orientations of lineament clusters. Unclassified lineament density plots reveal several distinct ductile or brittle-ductile domains, including a strong northeast- to east-northeast trending domain coincident with the Kabinakagami Lake greenstone belt, and curvi-linear zones subparallel to the margins of the Strickland pluton and the Pukaskwa batholith.

The integrated surficial lineament density throughout the White River assessment area also showed variable lineament density, with broad but well-defined areas of lower density, and multiple zones of elevated lineament density. Similar to the geophysical data, zones of elevated lineament densities typically occur along or at the intersection of tight-spaced northwest- and northeast-trending surficial lineaments, however, the highest surficial lineament density is correlated with a set of curvi-linear lineaments near the centre of the assessment area, within the Pukaskwa batholith. The density of surficial lineaments is in part related to the presence of overburden that may obscure the interpretation of surficial lineaments related to bedrock structures. For example, limited surficial lineaments were interpreted northeast of Gourlay Lake and proximal to Nameigos Lake where large expanses of organic terrain, glaciolacustrine sediments, and glacial outwash deposits are present.

The final integrated lineament density throughout the White River assessment area is very similar to geophysical and surficial lineament density analyses. Lineament density analyses of the final integrated brittle and dyke lineaments reveal a variable lineament density with multiple well defined zones of elevated lineament density, including throughout most of the Strickland pluton (with the exception of proximal to the north margin of the pluton in the northwest of the assessment area), and throughout much of the Anahareo pluton. Similar to the other data sets, zones of high lineament density correspond to tight-spaced northeast- and northwest-trending brittle and dyke lineaments, and the intersection of these lineament clusters. For unclassified lineaments, lineament density is nearly identical to the results of the geophysical density analyses, revealing multiple isolated domains of elevated lineament density, including a strong northeast- to east-northeast trending ductile or brittle-ductile domain coincident with the Kabinakagami Lake greenstone belt, and curvi-linear zones subparallel to the margins of the Strickland pluton and the Pukaskwa batholith.

Six main regionally distinguishable deformation episodes (D₁-D₆) are recognized in the White River Phase 2 assessment area, and can be used to constraint the relative age relationships of the interpreted lineaments. The final interpreted lineaments can be classified within the structural history into successive stages of ductile, brittle-ductile and brittle deformation, including 196 D₂-D₄

(unclassified) lineaments and 780 D₅-D₆ (brittle) lineaments. A total of 249 dyke lineaments were also interpreted throughout the assessment area.

D₂-D₄ unclassified lineaments are interpreted to represent ductile or brittle-ductile shear zones and were recognized predominantly from the geophysical data by their curvi-linear character and the truncation of form lines. These lineaments may represent the internal fabric of the rock units including the more intense fabric along ductile or brittle-ductile shear zones. Unclassified lineaments define distinct zones within the assessment area. As the unclassified lineaments are the oldest generation of interpreted structure, they are often offset and or truncated by younger brittle lineaments. Locally the unclassified lineaments are also reactivated, in which case they are classified as D₅-D₆ brittle lineaments.

D₅-D₆ brittle lineaments are observed in two dominant orientations: northwest, and northeast, with a subordinate north-trending lineament set also identified. These orientations are subparallel to the Matachewan, Biscotasing, and Marathon dyke orientations. Brittle lineaments of all orientations are observed to offset and truncate, and be offset and truncated by all other brittle and dyke lineament orientations. As a result, brittle lineaments cannot systematically be differentiated into different generations. Therefore, all brittle lineaments were classified into the same broad D₅-D₆ generation of brittle deformation.

Interpreted brittle lineaments are at least partially coincident with all mapped faults within and intersecting the White River Phase 2 assessment area. Multiple dykes had been previously interpreted throughout the White River areas from regional-scale resolution geophysical data. These dykes are generally coincident with interpreted dyke lineaments such that a single previously interpreted dyke from the regional-scale data is most often recognized as a series of tight-spaced dyke lineaments within the higher resolution geophysical data.

Of the 249 final integrated dyke lineaments, four distinct dyke populations can be identified, including 164 dyke lineaments corresponding to the 2.473 Ga northwest-trending Matachewan dyke swarm, 40 dyke lineaments corresponding to the 2.167 Ga. northeast-trending Biscotasing dyke swarm, 33 dyke lineaments corresponding to the 2.121 Ga. north-trending Marathon dyke swarm, and 12 dyke lineaments corresponding to the 1.238 Ga. west northwest-trending Sudbury dyke swarm. Dyke lineaments locally truncate and offset, and are truncated and offset by all orientations of brittle lineaments.

7 References

- AECOM, 2014a: Phase 1 Geoscientific Desktop Preliminary Assessment of Potential Suitability for Siting a Deep Geological Repository for Canada's Used Nuclear Fuel. Township of White River, Ontario. Report prepared for NWMO, November 2014. APM-REP-06144-0083. Report available at www.nwmo.ca
- AECOM, 2014b: Phase 1 Geoscientific Desktop Preliminary Assessment Terrain and Remote Sensing Study. Township of White River, Ontario. Report prepared for NWMO, November 2014. APM-REP-06144-0084. Report available at www.nwmo.ca
- Barnett, P.J. 1992. Quaternary Geology of Ontario; In: Geology of Ontario, Ontario Geological Survey, Special Volume 4, Part 2, p.1010–1088.
- Beakhouse, G.P. and Lin, S. 2006. Tectonic significance of the Pukaskwa batholith with the Hemlo and Mishibishu greenstone belts; Ontario Geological Survey, Open File Report 6192, p.7-1 to 7-7.
- Beakhouse, G.P., Lin, S. and Kamo, S.L. 2011. Magnetic and tectonic emplacement of the Pukaskwa batholith, Superior Province, Ontario, Canada; Can. Journal of Earth Science, v.48, p.187-204.
- Berman, R.G., Easton, R.M. and Nadeau, L. 2000. A New Tectonometamorphic Map of the Canadian Shield: Introduction; The Canadian Mineralogist, v. 38, p.277-285.
- Berman, R.G., Sanborn-Barrie, M., Stern, R.A. and Carson, C.J. 2005. Tectonometamorphism at ca. 2.35 and 1.85 Ga: In: the Rae Domain, western Churchill Province, Nunavut, Canada: Insights from structural, metamorphic and in situ geochronological analysis of the southwestern Committee Bay Belt; The Canadian Mineralogist, v. 43, p.409-442.
- Bleeker, W. and Hall, B. 2007. The Slave Craton: Geology and metallogenic evolution; In Goodfellow, W.D., ed., Mineral Deposits of Canada: A Synthesis of Major Deposit-Types, District Metallogeny, the Evolution of Geological Provinces, and Exploration Methods: Geological Association of Canada, Mineral Deposits Division, Special Publication No. 5, p.849-879
- Bokelmann, G.H.R. 2002. Which forces drive North America?, Geology, v.30, p.1027-1030
- Bokelmann, G.H.R. and Silver, P.G. 2002. Shear Stress at the Base of Shield Lithosphere. Geophysical Research Letters, v. 29, p.61-64
- Breaks, F.W. and Bond, W.D. 1993. The English River Subprovince – An Archean Gneiss Belt: Geology, geochemistry and associated mineralization; Ontario Geological Survey, Open File Report 5846, v. 1, 483p.
- Brown, A., Everitt, R.A., Martin C.D. and Davison, C.C. 1995. Past and future fracturing In AECL research areas in the Superior Province of the Canadian Precambrian Shield, with emphasis on the Lac Du Bonnet Batholith; Whiteshell Laboratories, Pinawa, Manitoba

- Buchan, K.L. and Ernst, R.E. 2004. Diabase dyke swarms and related units in Canada and adjacent regions. Geological Survey of Canada, Map 2022A, scale 1:5,000,000.
- Buchan, K.L., Halls, H.C. and Mortensen, J.K. 1996. Paleomagnetism, U-Pb geochronology, and geochemistry of Marathon dykes, Superior Province, and comparison with the Fort Frances swarm. Canadian Journal of Earth Sciences, v. 33, pp. 1583-1595.
- Corfu, F. and Muir, T.L. 1989. The Hemlo-Heron Bay greenstone belt and Hemlo Au-Mo deposit, Superior Province, Ontario, Canada: 1. Sequence of igneous activity determined by zircon U-Pb geochronology; Chemical Geology, vol. 79, p.183-200.
- Corfu, F. and Stott, G.M. 1996. Hf isotopic composition and age constraints on the evolution of the Archean central Uchi Subprovince, Ontario, Canada. Precambrian Research, v.78, p. 53-63
- Corfu, F., Stott, G.M. and Breaks, F.W. 1995. U-Pb geochronology and evolution of the English River subprovince, an Archean low P – high T metasedimentary belt in the Superior Province. Tectonics, v.14, p.1220-1233
- Corrigan, D., Galley, A.G. and Pehrsson, S. 2007. Tectonic evolution and metallogeny of the southwestern Trans-Hudson Orogen, in Goodfellow, W.D., ed., Mineral Deposits of Canada: A Synthesis of Major Deposit-Types, District Metallogeny, the Evolution of Geological Provinces, and Exploration Methods: Geological Association of Canada, Mineral Deposits Division, Special Publication No. 5, p.881-902.
- Davis, D.W., and Lin, S. 2003. Unraveling the geologic history of the Hemlo Archean gold deposit, Superior Province, Canada; a U-Pb geochronological study; Economic Geology and the Bulletin of the Society of Economic Geologists, 98, p.51–67.
- Easton, R.M. 2000a. Metamorphism of the Canadian Shield, Ontario, Canada. I. The Superior Province; The Canadian Mineralogist, v. 38, p.287-317.
- Easton, R.M. 2000b. Metamorphism of the Canadian Shield, Ontario, Canada. II. Proterozoic metamorphic history; The Canadian Mineralogist, v. 38, p.319-344.
- Ernst, R.E. and Buchan, K.L. 1993. Paleomagnetism of the Abitibi dyke swarm, southern Superior Province, and implications for the Logan Loop; Canadian Journal of Earth Sciences, v. 30, p.1886-1897.
- Fenwick, K.G. 1966. Dayohessarah Lake area, Algoma District; Ontario Department of Mines, Map 2129, scale 1:26,720
- Fenwick, K.G. 1967. Geology of the Dayohessarah Lake area, District of Algoma; Ontario Department of Mines, Geological Report 49, 16p.
- Forte, A., Moucha, R., Simmons, N., Grand, S., and Mitrovica, J., 2010. Deep-mantle contributions to the surface dynamics of the North American continent. Tectonophysics, v. 481, p. 3–15.
- Fraser, J.A. and Heywood, W.W. (editors) 1978. Metamorphism in the Canadian Shield; Geological Survey of Canada, Paper 78-10, 367p.

- Gartner, J.F. and McQuay, D.F. 1980a. Obakamiga Lake Area (NTS 42F/SW). Districts of Algoma and Thunder Bay; Ontario Geological Survey, Northern Ontario Engineering Geology Terrain Study 45, 16p., Accompanied by Map 5084, scale 1:100,000.
- Gartner, J.F. and McQuay, D.F. 1980b. Kabinakagami Lake Area (NTS 42C/NE), District Algoma; Ontario Geological Survey, Northern Ontario Engineering Geology Terrain Study 62, 14p., Accompanied by Map 5095, scale 1:100,000.
- Geddes R.S. and Kristjansson, F.J. 1986. Quaternary geology of the White River area, Districts of Thunder Bay and Algoma; Ontario Geological Survey, Map P.2988, Geological Series-Preliminary Map. scale 1:50,000.
- Geddes R.S. and Kristjansson, F.J. 2009. Quaternary Geology of the White River Area, northern Ontario; Ontario Geological Survey, Map 2682, scale 1:50,000.
- Geddes, R.S., Bajc, A.F. and Kristjansson, F.J. 1985. Quaternary Geology of the Hemlo Region, District of Thunder Bay; In: Summary of Field Work, 1985, Ontario Geological Survey, Ontario Geological Survey, Miscellaneous Paper 126, p.151-154.
- Haimson, B.C. 1990. Scale effects in rock stress measurements. In Proceedings international workshop on scale effects in rock masses, Loen, AA Balkema, Rotterdam, p.89-101.
- Halls, H.C., Stott, G.M., Ernst, R.E. and Davis, D.W., 2006. A Paleoproterozoic mantle plume beneath the Lake Superior region; p.23-24 In: Institute on Lake Superior Geology, 52nd Annual Meeting Sault Ste Marie, Ontario, Part 1, Program and Abstracts.
- Hamilton, M.A., David, D.W., Buchan, K.L. and Halls H.C. 2002. Precise U-Pb dating of reversely magnetized Marathon diabase dykes and implications for emplacement of giant dyke swarms along the southern margin of the Superior Province, Ontario. Geological Survey of Canada, Current Research 2002-F6, 10p.
- Jackson, S.L. 1998. Stratigraphy, structure and metamorphism; Part 1, p.1--58, in S.L. Jackson, G.P. Beakhouse and D.W. Davis, Geological Setting of the Hemlo Gold Deposit; an Interim Progress Report, Ontario Geological Survey, Open File Report 5977, 121p.
- Jolly, W.T. 1978. Metamorphic history of the Archean Abitibi Belt; In: Metamorphism in the Canadian Shield; Geological Survey of Canada, Paper 78-10, p.63-78.
- Kraus, J. and Menard, T. 1997. A thermal gradient at constant pressure: Implications for low- to medium-pressure metamorphism in a compressional tectonic setting, Flin Flon and Kisseynew domains, Trans-Hudson Orogen, Central Canada; The Canadian Mineralogist, v. 35, p.1117-1136.
- Krogh, T.E., Corfu, F., Davis, D.W., Dunning, G.R., Heaman, L.M., Kamo, S.L., Mashado, N., Greenhough, J.D. and Nakamura, E. 1987. Precise U-Pb isotopic ages of diabase dykes and mafic to ultramafic rocks using trace amounts of baddeleyite and zircon; In: Mafic Dyke Swarms, Geological Association of Canada, Special Paper 34, p.147-152.
- Lin, S. 2001. Stratigraphic and Structural Setting of the Hemlo Gold Deposit, Ontario, Canada. Economic Geology, v. 96, pp. 477–507.

- Lin, S. and Beakhouse, G.P. 2013. Synchronous vertical and horizontal tectonism at late stages of Archean cratonization and genesis of Hemlo gold deposit, Superior craton, Ontario, Canada; *Geology*, v. 41; no. 3; p.359–362.
- Mehnert, K.R. 1968. *Migmatites and the origin of granitic rocks*; Elsevier, Amsterdam, 391p.
- Menard, T. and Gordon, T.M. 1997. Metamorphic P-T paths from the Eastern Flin Flon Belt and Kisseynew Domain, Snow Lake, Manitoba; *The Canadian Mineralogist*, v. 35, p. 1093-1115.
- Milne, V.G., 1968. *Geology of the Black River area, District of Thunder Bay*; Ontario Department of Mines, Geological Report 72, 68p.
- Milne, V.G., Giblin, P.E., Bennett, G., Thurston, P.C., Wolfe, W.J., Giguere, J.F., Leahy, E.J. and Rupert, R.J. 1972. Manitouwadge-Wawa sheet, geological compilation series, Algoma, Cochrane, Sudbury and Thunder Bay districts; Ontario Geological Survey, M2220, scale 1:253,440 or 1 inch to 4 miles.
- Muir, T.L. 2003. Structural evolution of the Hemlo greenstone belt in the vicinity of the world-class Hemlo gold deposit. *Canadian Journal of Earth Sciences*, vol. 40, pp. 395-430.
- Nur, A. 1982. The origin of tensile fractures. *Journal of Structural Geology*, v. 4, p. 31-40.
- NWMO (Nuclear Waste Management Organization), 2014. Geoscientific Desktop Preliminary Assessment of Potential Suitability for Siting a Deep Geological Repository for Canada's Used Nuclear Fuel. Township of White River, Ontario. NWMO Report Number: APM-REP-06144-0083.
- OMNR (Ontario Ministry of Natural Resources), 2009. *Forest Information Manual – Forest Resources Inventory Technical Specifications*.
- Ontario Ministry of Northern Development, Mines and Forestry, 2005, *The Northern Ontario Engineering Geology Terrain Study (NOEGTS)*
- Ontario Geological Survey 1999. Single master gravity and aeromagnetic data for Ontario, ASCII, Excel® and Access® formats; Ontario Geological Survey, Geophysical Data Set 1035.
- Ontario Geological Survey (OGS), 2011. 1:250 000 scale bedrock geology of Ontario; Ontario Geological Survey, Miscellaneous Release–Data 126 - Revision 1.
- Osmani, I.A. 1991. Proterozoic mafic dyke swarms in the Superior Province of Ontario. in *Geology of Ontario*, Ontario Geological Survey, Special Volume 4, Part 1, pp. 661-681
- Pease, V., Percival, J., Smithies, H., Stevens, G. and Van Kranendonk, M. 2008. When did plate tectonics begin? Evidence from the orogenic record; In: Condie, K.C. and Pease, V., eds., *When Did Plate Tectonics Begin on Earth?*; Geological Society of America Special Paper 440, p.199-228.
- Percival, J.A., Sanborn-Barrie, M., Skulski, T., Stott, G.M., Helmstaedt, H. and White, D.J. 2006. Tectonic evolution of the western Superior Province from NATMAP and Lithoprobe studies; *Can. J. Earth Sciences* v.43, p.1085-1117.

- Peterson, V.L., and Zaleski, E. 1999. Structural history of the Manitouwadge greenstone belt and its volcanogenic Cu-Zn massive sulphide deposits, Wawa Subprovince, south-central Superior Province; *Can. Jour. of Earth Sciences*, V36, p.605-625.
- Polat, A. 1998. Geodynamics of the Late Archean Wawa Subprovince greenstone belts, Superior Province, Canada. PhD Thesis, Department of Geological Sciences, University of Saskatchewan, Saskatoon, 249p.
- Polat, A., Kerrich, R. and Wyman, D.A. 1998. The late Archean Schreiber–Hemlo and White River–Dayohessarah greenstone belts, Superior Province: collages of oceanic plateaus, oceanic arcs, and subduction–accretion complexes. *Tectonophysics*, 289, 295–326.
- Powell, W.G., Carmichael, D.M. and Hodgson, C.J. 1993. Thermobarometry in a subgreenschist to greenschist transition in metabasites of the Abitibi greenstone belt, Superior Province, Canada; *J. Metamorphic Geology*, v.11, p.165-178.
- Santaguida, F. 2001. Precambrian geology compilation series – White River sheet; Ontario Geological Survey, Map 2666, scale 1:250,000.
- Sawyer, E.W. 2008. Atlas of Migmatites; The Canadian Mineralogist Special Publication 9; Mineralogical Association of Canada, NRC Research Press, Ottawa. 371p
- Schandl, E.S., Davis, D.W., Gorton, M.P., and Wasteneys, I.A. 1991. Geochronology of hydrothermal alteration around volcanic-hosted massive sulphide deposits in the Superior Province; Ontario Geological Survey, Miscellaneous Paper 156, p.105-120.
- SGL (Sander Geophysics Limited) 2017. Phase 2 Geoscientific Preliminary Assessment, Acquisition, Processing and Interpretation of High-Resolution Airborne Geophysical Data, Township of White River and Area, Ontario. NWMO Report Number: APM-REP-01332-0209.
- Siragusa, G.M. 1977. Geology of the Kabinakagami Lake area, District of Algoma; Ontario Division of Mines, Geoscience Report 159, 39p., accompanied by Map 2355, scale 1:63,360 or 1 inch to 1 mile.
- Siragusa, G.M. 1978. Geology of the Esnagi Lake area, District of Algoma; Ontario Geological Survey, Geoscience Report 176, 50p., accompanied by Map 2382, scale 63,360 or 1 inch to 1 mile
- SRK, 2013a. Phase 1 Geoscientific Desktop Preliminary Assessment, Lineament Interpretation, Township of Schreiber, Ontario. NWMO Report Number: APM-REP-06144-0038.
- SRK, 2013b. Phase 1 Geoscientific Desktop Preliminary Assessment, Lineament Interpretation, Township of Ear Falls. NWMO Report Number: APM-REP-06144-0022.
- SRK, 2014a. Phase 1 Geoscientific Desktop Preliminary Assessment, Lineament Interpretation, Township of Manitouwadge. NWMO Report Number: APM-REP-06144-0078.
- SRK, 2014b. Phase 1 Geoscientific Desktop Preliminary Assessment, Lineament Interpretation, Township of White River. NWMO Report Number: APM-REP-06144-0086.

- SRK, 2015a. Phase 2 Geoscientific Desktop Preliminary Assessment, Lineament Interpretation, Township of Creighton. NWMO Report Number: APM-REP-06145-0011.
- SRK, 2015b. Phase 2 Geoscientific Desktop Preliminary Assessment, Lineament Interpretation, Township of Schreiber. NWMO Report Number: APM-REP-06145-0007.
- SRK, 2015c. Phase 2 Geoscientific Desktop Preliminary Assessment, Lineament Interpretation, Township of Ignace. NWMO Report Number: APM-REP-06145-0003
- Stott, G., Mahoney, K.L. and Zwiers, W.G. 1995a. Precambrian geology of the Dayohessarah Lake area (north); Ontario Geological Survey, Preliminary Map P.3309, scale 1:20,000.
- Stott, G., Mahoney, K.L. and Zwiers, W.G. 1995b. Precambrian geology of the Dayohessarah Lake area (central); Ontario Geological Survey, Preliminary Map P.3310, scale 1:20,000.
- Stott, G., Mahoney, K.L. and Zwiers, W.G. 1995c. Precambrian geology of the Dayohessarah Lake area (south); Ontario Geological Survey, Preliminary Map P.3311, scale 1:20,000.
- Stott, G.M. 1999. Precambrian geology of the Dayohessarah Lake area, White River, Ontario; Ontario Geological Survey, Open File Report 5984, 54p.
- Streckeisen, A. L., 1976. Classification of the common igneous rocks by means of their chemical composition: a provisional attempt; Neues Jahrbuch fr Mineralogie, Monatshefte, 1976 H. 1, p.1-15.
- Williams, H. R., G.M. Stott, K.B. Heather, T.L. Muir and R.P. Sage. 1991. Wawa Subprovince. in Geology of Ontario, Ontario Geological Survey, Special Volume 4, Part 1, pp. 485-525.
- Williams, H.R. and Breaks, F.W. 1989. Geological studies in the Manitouwadge-Hornepayne area; Ontario Geological Survey, Miscellaneous Paper 146, p.79-91.
- Williams, H.R. and F.W. Breaks, 1996. Geology of the Manitouwadge-Hornepayne region, Ontario; Ontario Geological Survey, Open File Report 5953, 138p.
- Zaleski, E. and Peterson, V.L. 1993. Geology of the Manitouwadge greenstone belt, Ontario; Geological Survey of Canada, Open File 2753, scale 1:25,000
- Zaleski, E., Peterson, V.L., and van Breemen, O. 1994. Structure and tectonics of the Manitouwadge greenstone belt and the Wawa-Quetico subprovince boundary, Superior province, northwestern Ontario; In: Current Research 1994-C; Geological Survey of Canada, p.237-247.
- Zaleski, E., Peterson, V.L., and van Breemen, O. 1995. Geological and age relationships of the margins of the Manitouwadge greenstone belt and the Wawa-Quetico subprovince boundary, northwestern Ontario; in: Current Research 1995-C, Geological Survey of Canada, p.35-44.
- Zaleski, E., van Breemen O. and Peterson, V.L. 1999. Geological evolution of the Manitouwadge greenstone belt and the Wawa-Quetico subprovince boundary, Superior Province, Ontario, constrained by U-Pb zircon dates of supracrustal and plutonic rocks; Canadian Journal of Earth Sciences, Vol. 36, p.945-966.

Zoback, M.L., 1992. First- and second-order patterns of stress in the lithosphere: the world stress map project; *Journal of Geophysical. Research*, 97, p.11,703-11,728.

APPENDIX A – Additional Supporting Figures

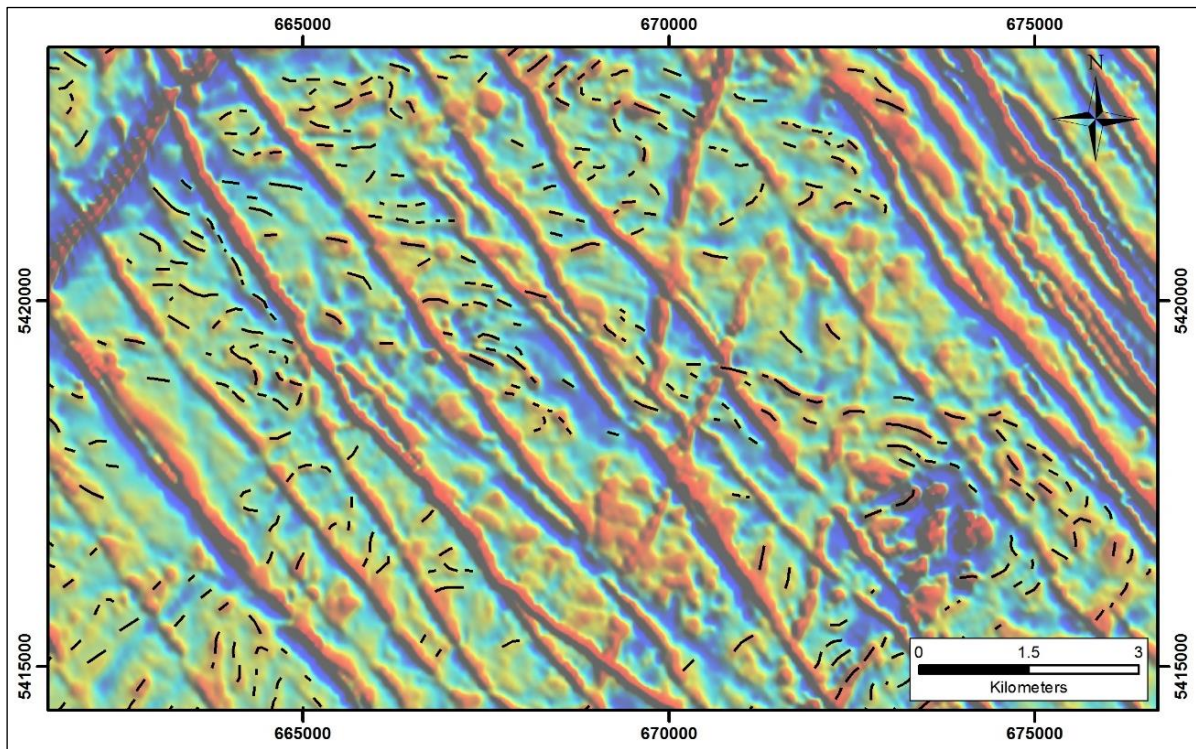


Figure A1: Example of Form Lines from the White River Area

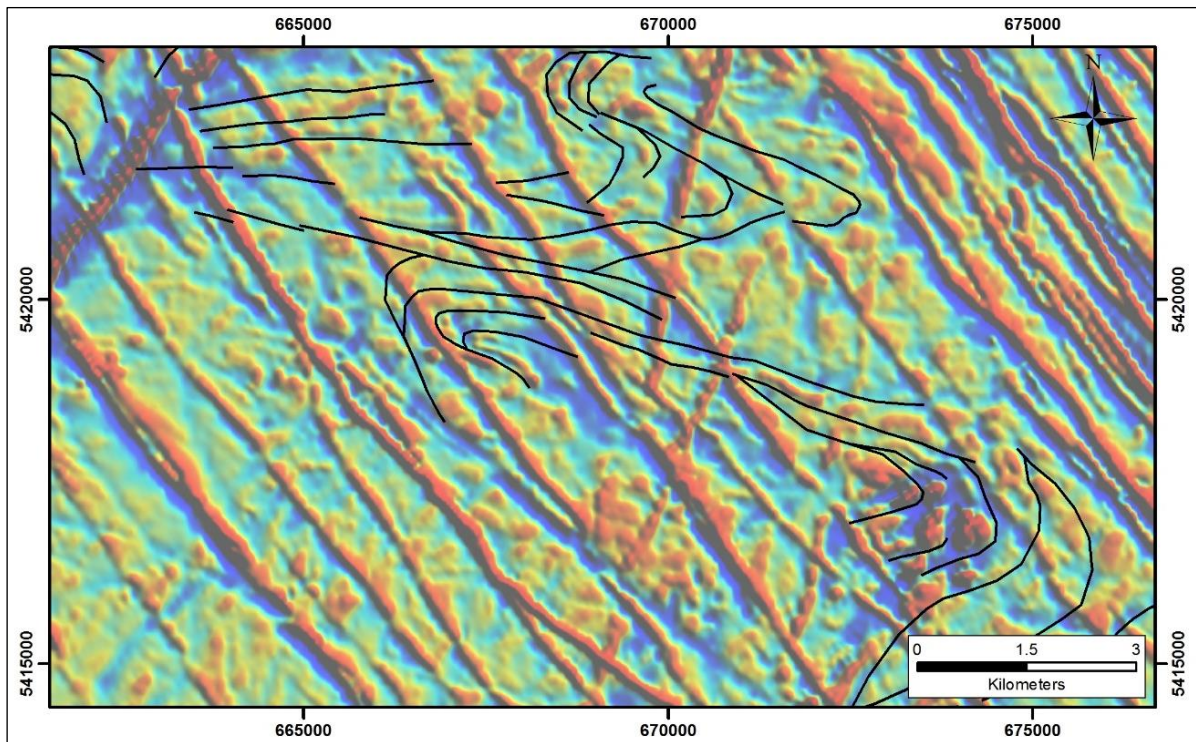


Figure A2: Example of Unclassified Lineaments from the White River Area

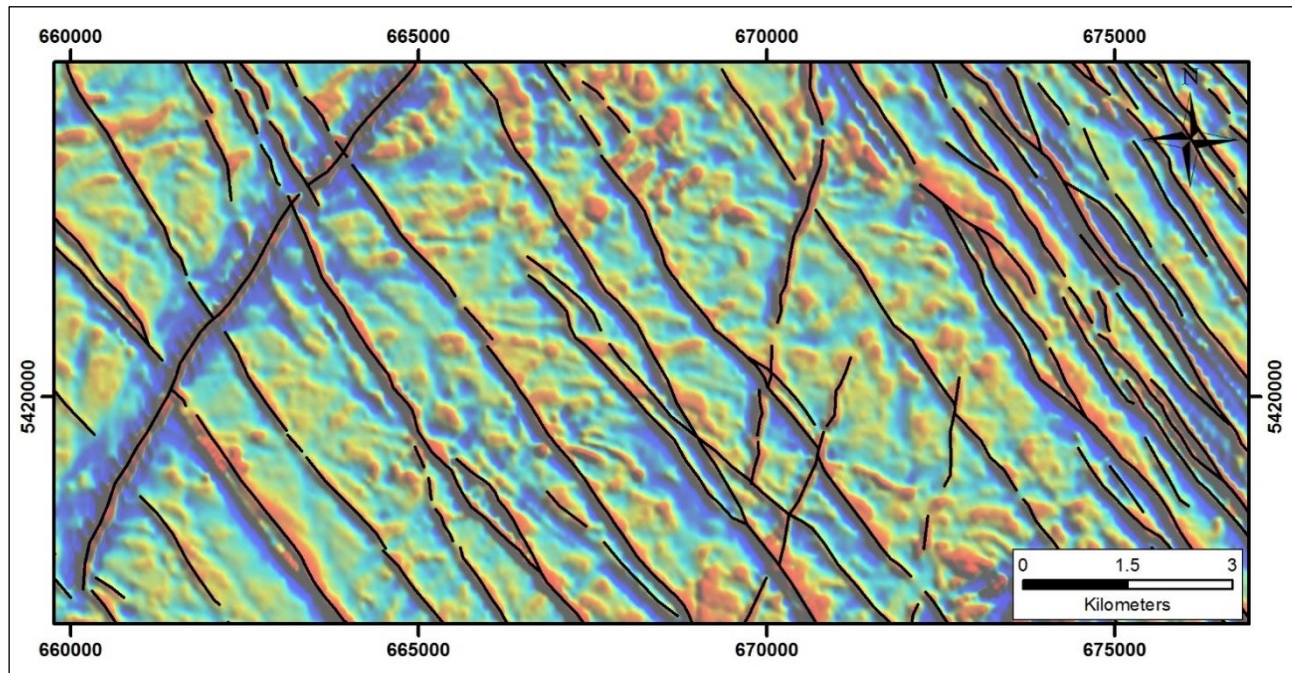


Figure A3: Example of Dyke Lineaments from the White River Area

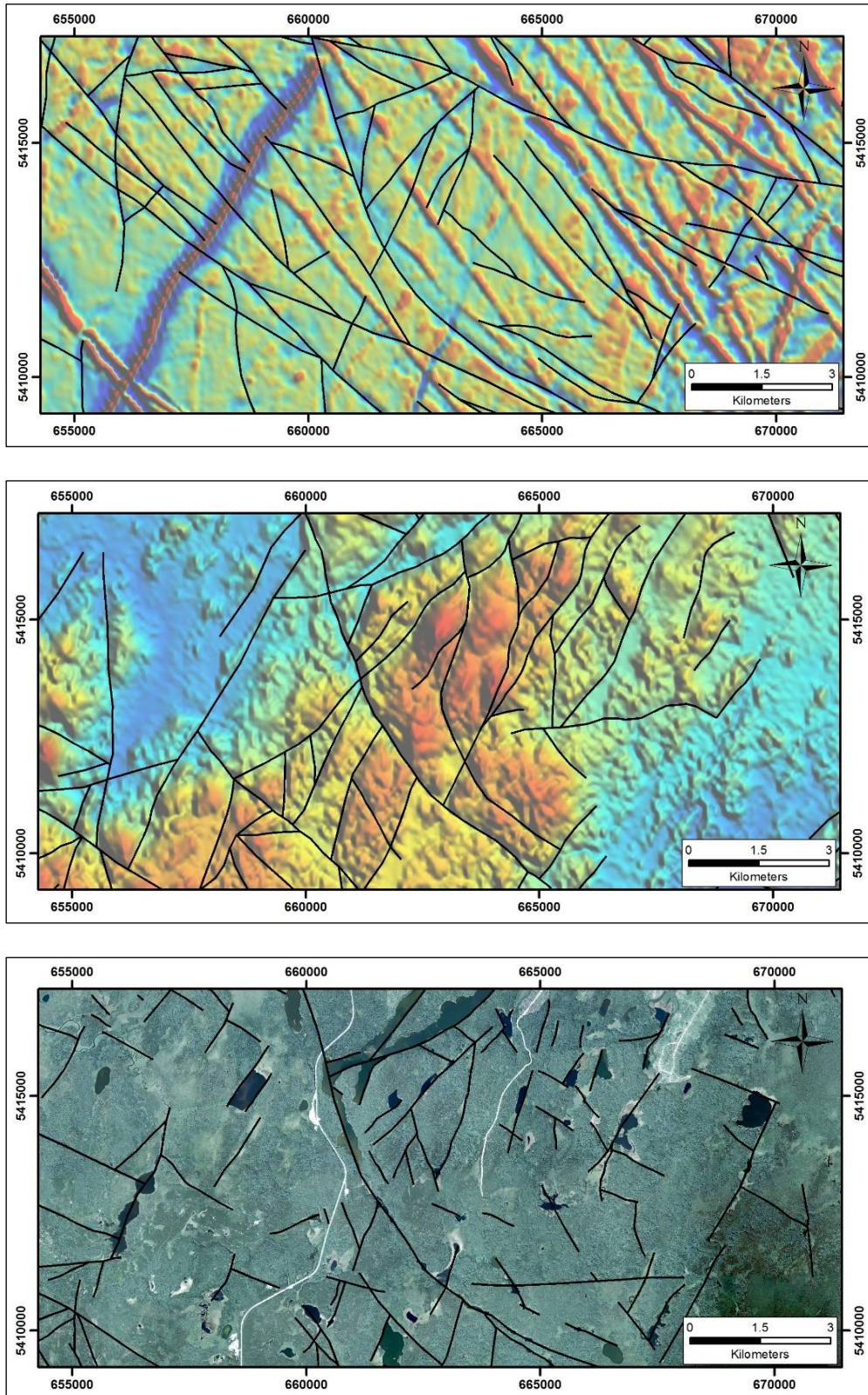


Figure A4: Example of Brittle Lineaments from the Same Location in the White River Area
Top, middle and bottom show brittle lineaments manifested in magnetic, DEM and FRI data sets, respectively.

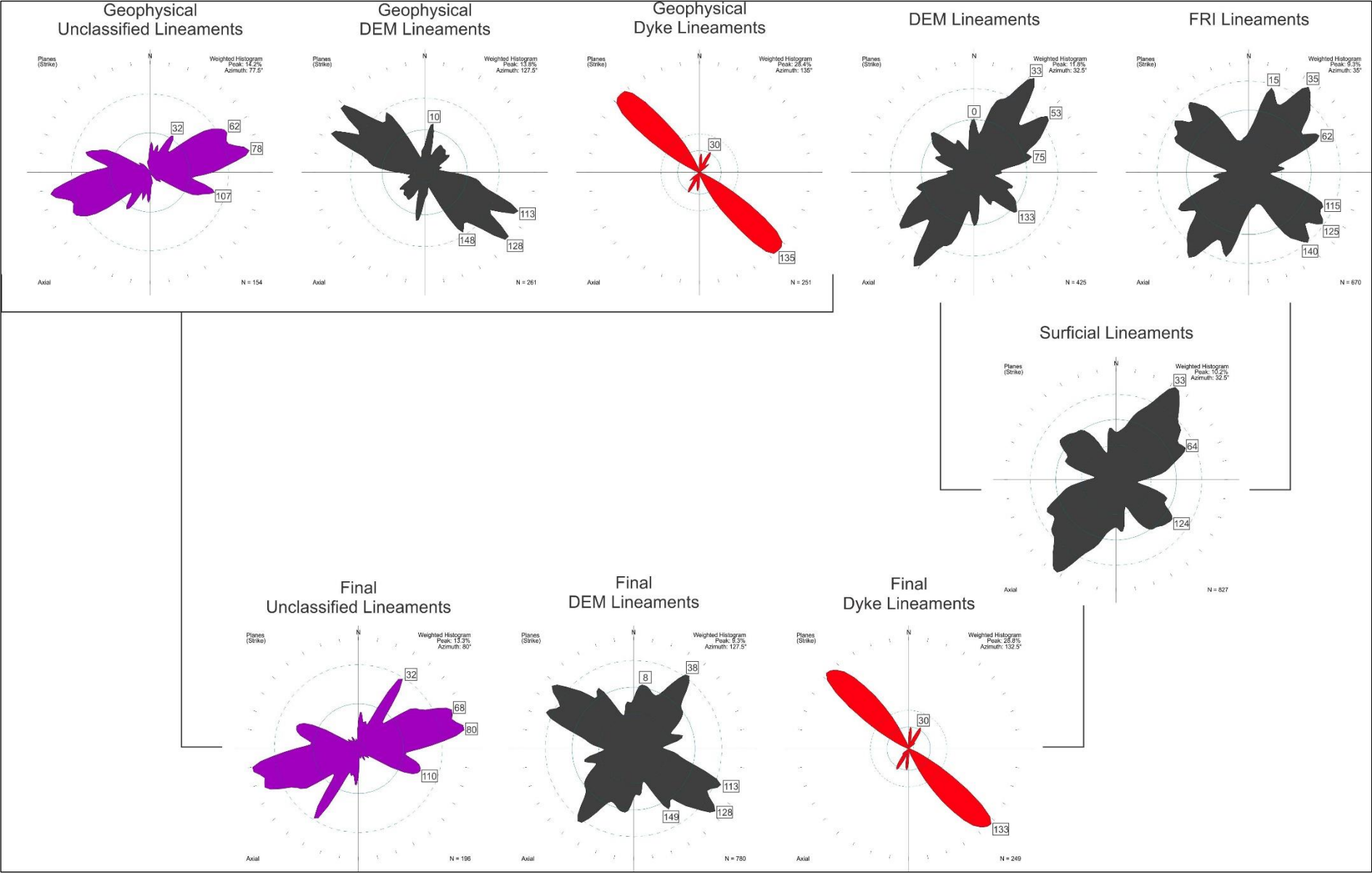


Figure A5: Summary of Lineament Orientations for White River Phase 2 Assessment Area

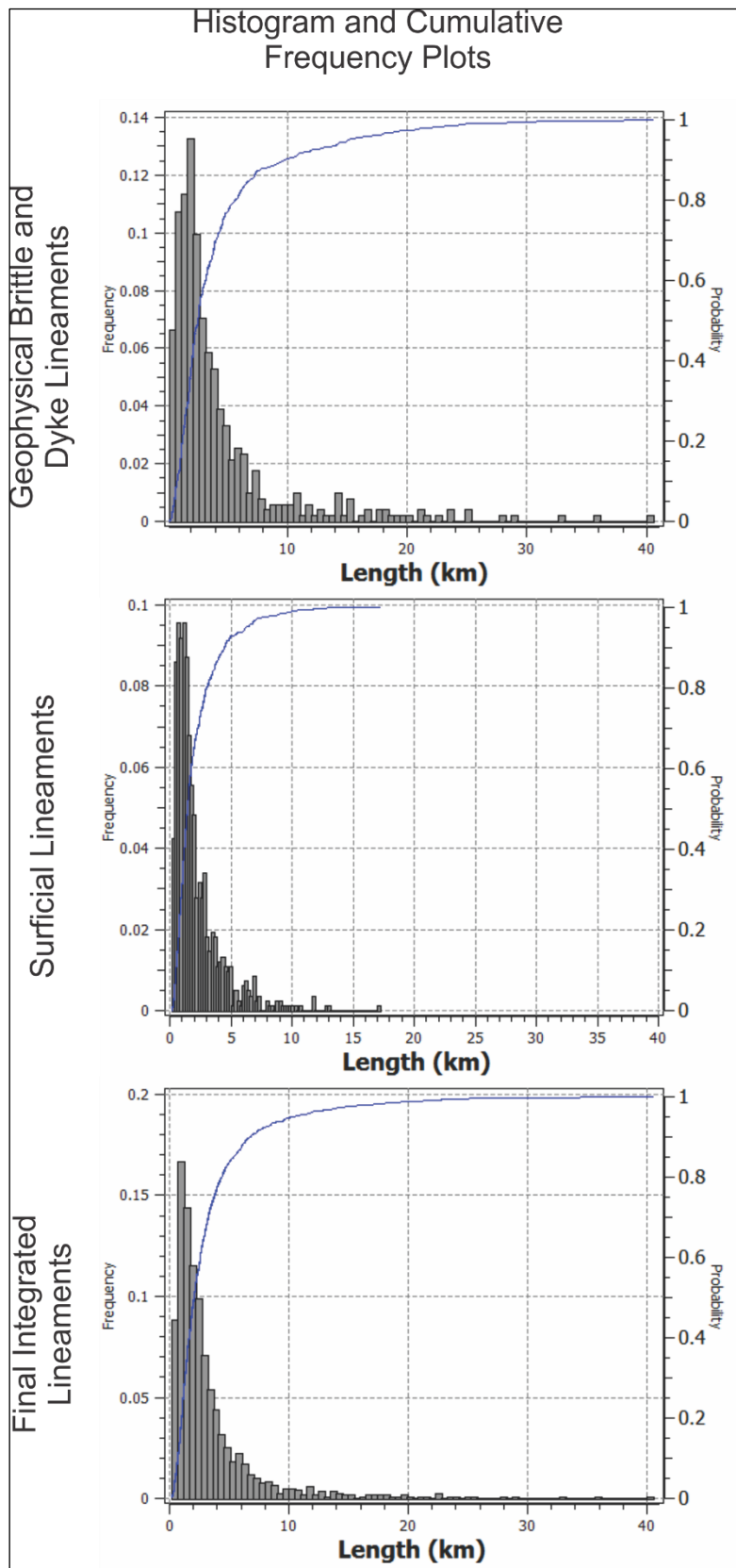


Figure A6: Summary of Length Statistics for the White River Phase 2 Assessment Area

APPENDIX B – Summary of Lineament Statistics

Table B1: Summary of Geophysical Lineament Statistics

	All Lineaments	Unclassified	Brittle	Dyke
Total Number of Lineaments	666	154	261	251
Max Length (kilometres)	40.53	16.87	33.02	40.53
Minimum Length (kilometres)	0.19	0.6	0.28	0.19
Median Length (kilometres)	2.68	3.05	2.6	2.52
Mean Length (kilometres)	4.2	3.81	3.51	5.16
Certainty 1 (number)	114	38	57	19
Certainty 1 (percent)	17%	25%	22%	8%
Certainty 2 (number)	288	91	130	67
Certainty 2 (percent)	43%	59%	50%	27%
Certainty 3 (number)	264	25	74	165
Certainty 3 (percent)	40%	16%	28%	66%
RA1 = 2 (number)	383	71	138	174
RA1 = 2 (percent)	58%	46%	53%	69%
RA1 = 1 (number)	283	83	123	77
RA1 = 1 (percent)	42%	54%	47%	31%

Table B2: Summary of DEM Lineament Statistics

	All Lineaments
Total Number of Lineaments	425
Max Length (kilometres)	15.98
Minimum Length (kilometres)	0.38
Median Length (kilometres)	2.42
Mean Length (kilometres)	3.085
Certainty 1 (number)	143
Certainty 1 (percent)	34%
Certainty 2 (number)	215
Certainty 2 (percent)	50%
Certainty 3 (number)	67
Certainty 3 (percent)	16%
RA1 = 2 (number)	262
RA1 = 2 (percent)	62%
RA1 = 1 (number)	163
RA1 = 1 (percent)	38%

Table B3: Summary of FRI Lineament Statistics

	All Lineaments
Total Number of Lineaments	670
Max Length (kilometres)	14.23
Minimum Length (kilometres)	0.16
Median Length (kilometres)	1.06
Mean Length (kilometres)	1.43
Certainty 1 (number)	369
Certainty 1 (percent)	55%
Certainty 2 (number)	261
Certainty 2 (percent)	39%
Certainty 3 (number)	40
Certainty 3 (percent)	6%
RA1 = 2 (number)	493
RA1 = 2 (percent)	74%
RA1 = 1 (number)	177
RA1 = 1 (percent)	26%

Table B4: Summary of Integrated Surficial Lineament Statistics

	All Lineaments
Total Number of Lineaments	827
Max Length (kilometres)	17.18
Minimum Length (kilometres)	0.17
Median Length (kilometres)	1.45
Mean Length (kilometres)	2.12
Certainty 1 (number)	391
Certainty 1 (percent)	47%
Certainty 2 (number)	351
Certainty 2 (percent)	42%
Certainty 3 (number)	85
Certainty 3 (percent)	10%
RA2 = 2 (number)	232
RA2 = 2 (percent)	28%
RA2 = 1 (number)	595
RA2 = 1 (percent)	72%

Table B5: Summary of Final Integrated Lineament Statistics

	All Lineaments	Unclassified	Brittle	Dyke
Total Number of Lineaments	1225	196	780	249
Max Length (kilometres)	40.53	17.14	33.01	40.53
Minimum Length (kilometres)	0.17	0.56	0.17	0.19
Median Length (kilometres)	2.06	2.73	1.81	2.53
Mean Length (kilometres)	3.29	3.56	2.61	5.19
Certainty 1 (number)	371	51	301	19
Certainty 1 (percent)	30%	26%	39%	8%
Certainty 2 (number)	518	104	348	66
Certainty 2 (percent)	42%	53%	45%	27%
Certainty 3 (number)	336	41	131	164
Certainty 3 (percent)	27%	21%	17%	66%
RA2 = 3 (number)	105	24	60	21
RA2 = 3 (percent)	9%	12%	8%	8%
RA2 = 2 (number)	297	49	211	37
RA2 = 2 (percent)	24%	25%	27%	15%
RA2 = 1 (number)	823	123	509	191
RA2 = 1 (percent)	67%	63%	65%	77%

Table B6: Summary of Final Integrated Brittle and Dyke Lineament Length Statistics

	Mean length (kilometres)	Median length (kilometres)
Certainty 1	1.48	1.18
Certainty 2	2.51	2.11
Certainty 3	6.48	4.52
RA2 = 3	8.27	6.12
RA2 = 2	4.20	3.01
RA2 = 1	2.33	1.53

Figures

Figure 1: Location and Overview of the White River Area

Figure 2: Bedrock Geology of the White River Area

Figure 3: Terrain Features of the White River Area

Figure 4: Pole Reduced Magnetic Data (First Vertical Derivative) of the White River Area

Figure 5: Digital Elevation Data of the White River Area

Figure 6: Forest Resource Inventory Digital Aerial Imagery of the White River Area

Figure 7: Form Lines from Pole Reduced Magnetic Data of the White River Area

Figure 8: Interpreted Lineaments from Pole Reduced Magnetic Data of the White River Area

Figure 9: Interpreted Lineaments from Digital Elevation Data of the White River Area

Figure 10: Interpreted Lineaments from Forest Resource Inventory (FRI) Imagery of the White River Area

Figure 11: Interpreted Lineaments from Surficial Data of the White River Area

Figure 12: Interpreted Lineaments from Pole Reduced Magnetic Data of the White River Area

Figure 13: Select Final Integrated Lineaments of the White River Area

Figure 14: Interpreted Brittle and Dyke Lineaments from Pole Reduced Magnetic Data (by Length) of the White River Area

Figure 15: Interpreted Lineaments (by Length) from Surficial Data of the White River Area

Figure 16: Final Integrated Lineaments (by Length) of the White River Area

Figure 17: Lineament Density for Interpreted Brittle and Dyke Lineaments from Pole Reduced Magnetic Data of the White River Area

Figure 18: Lineament Density for All Interpreted Lineaments from Pole Reduced Magnetic Data of the White River Area

Figure 19: Lineament Density for Interpreted Lineaments from Surficial Data of the White River Area

Figure 20: Lineament Density for Final Integrated Brittle and Dyke Lineaments of the White River Area

Figure 21: Lineament Density for All Final Integrated Lineaments of the White River Area

Figure 22: Lineament Intersection Density for Interpreted Brittle and Dyke Lineaments from Pole Reduced Magnetic Data of the White River Area

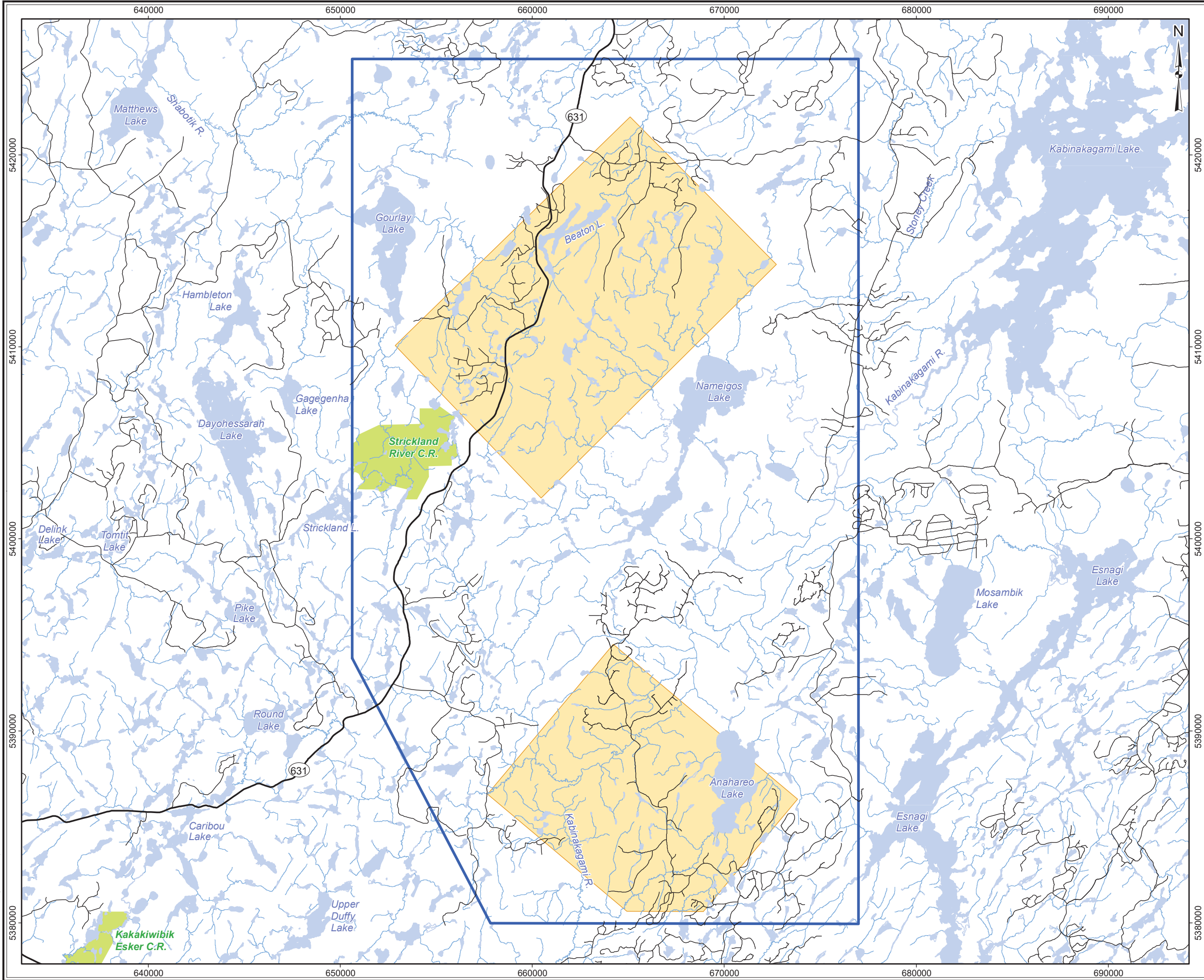
Figure 23: Lineament Intersection Density for All Interpreted Lineaments from Pole Reduced Magnetic Data of the White River Area

Figure 24: Lineament Intersection Density for Interpreted Surficial Lineaments of the White River Area

Figure 25: Lineament Intersection Density for Final Integrated Brittle and Dyke Lineaments of the White River Area

Figure 26: Lineament Intersection Density for All Final Integrated Lineaments of the White River Area

Figure 27: Lineament Relative Age Relationships of the White River Area



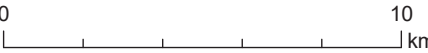
LEGEND

- Phase 2 Assessment Area
- Major Road
- Minor Road
- Watercourse
- Waterbody
- Conservation Reserve
- Withdrawal Area



REFERENCE

Base Data: Land Information Ontario (obtained 2015);
CanVec Topography (obtained 2015)



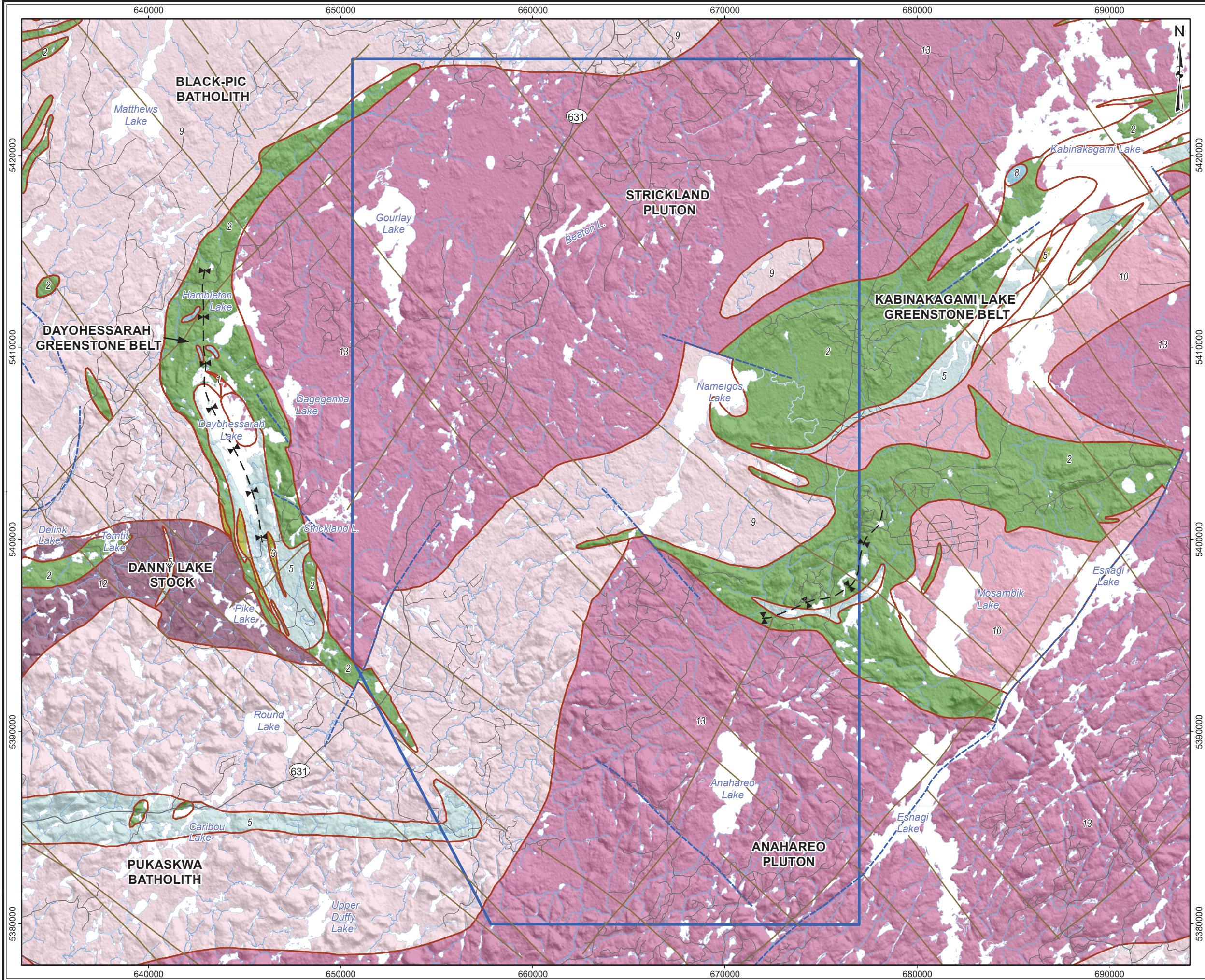
PROJECT Phase 2 Structural Lineament Interpretation
White River Area, Ontario

TITLE
**Location and Overview
of the White River Area**

DESIGN	KR	02 SEP 2014
GIS	JA	23 SEP 2016
CHECK	SC	23 SEP 2016
REVIEW	JPS	23 SEP 2016

Figure 1

REVISION 5
UTM ZONE 16N
NAD 1983
1:190,000



LEGEND

- Phase 2 Assessment Area
- Major Road
- Minor Road
- Watercourse
- Waterbody
- Bedrock Geology**
 - Fold (syncline)
 - Fault
 - Dyke
 - Geological Boundary
 - 13: Granite-granodiorite
 - 12: Diorite-monzonite- granodiorite
 - 10: Foliated tonalite suite
 - 9: Gneissic tonalite suite
 - 8: Gabbro
 - 5: Metasedimentary rocks
 - 3: Felsic and intermediate metavolcanic rocks
 - 2: Mafic metavolcanic Rocks

REFERENCE

Base Data: Land Information Ontario (obtained 2015);
CanVec Topography (obtained 2015)

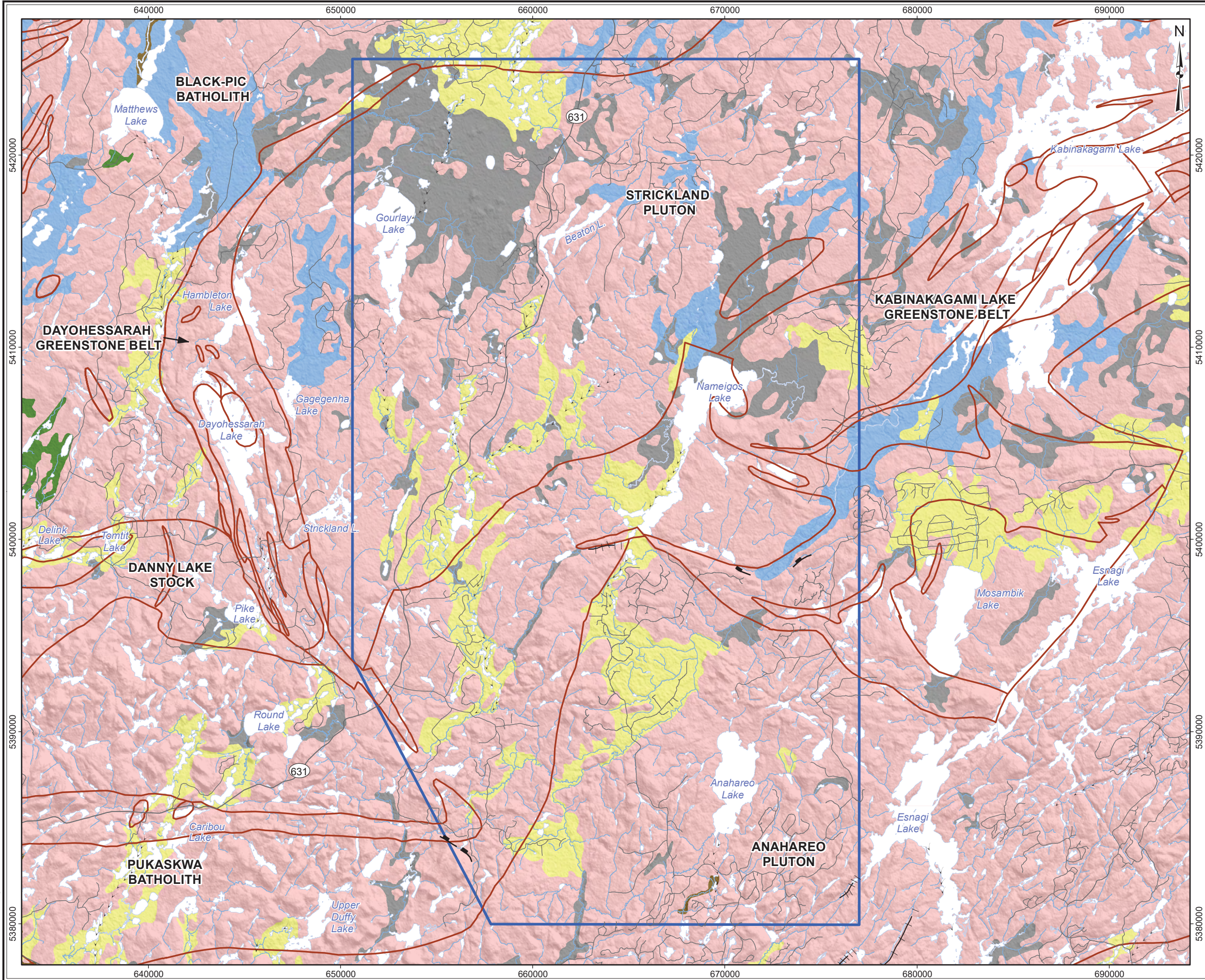
Bedrock Geology: MRD126-REV1 (Ontario Geological Survey, 2011);
Ontario Geological Survey Map 2666 (Santaguida, 2001).

0 10 km

PROJECT Phase 2 Structural Lineament Interpretation
White River Area, Ontario

TITLE **Bedrock Geology
of the White River Area**

DESIGN	KR	02 SEP 2014	Figure 2	REVISION 4
GIS	JA	23 SEP 2016		UTM ZONE 16N
CHECK	SC	23 SEP 2016		NAD 1983
REVIEW	JPS	23 SEP 2016		1:190,000



LEGEND

- Phase 2 Assessment Area
- Major Road
- Minor Road
- Watercourse
- Waterbody
- Geological Boundary

Surficial Geology

- Escarpment
- Esker
- Steep-walled valley
- Moraine
- Glacial outwash, esker
- Glaciolacustrine plain
- Alluvial
- Organics
- Bedrock

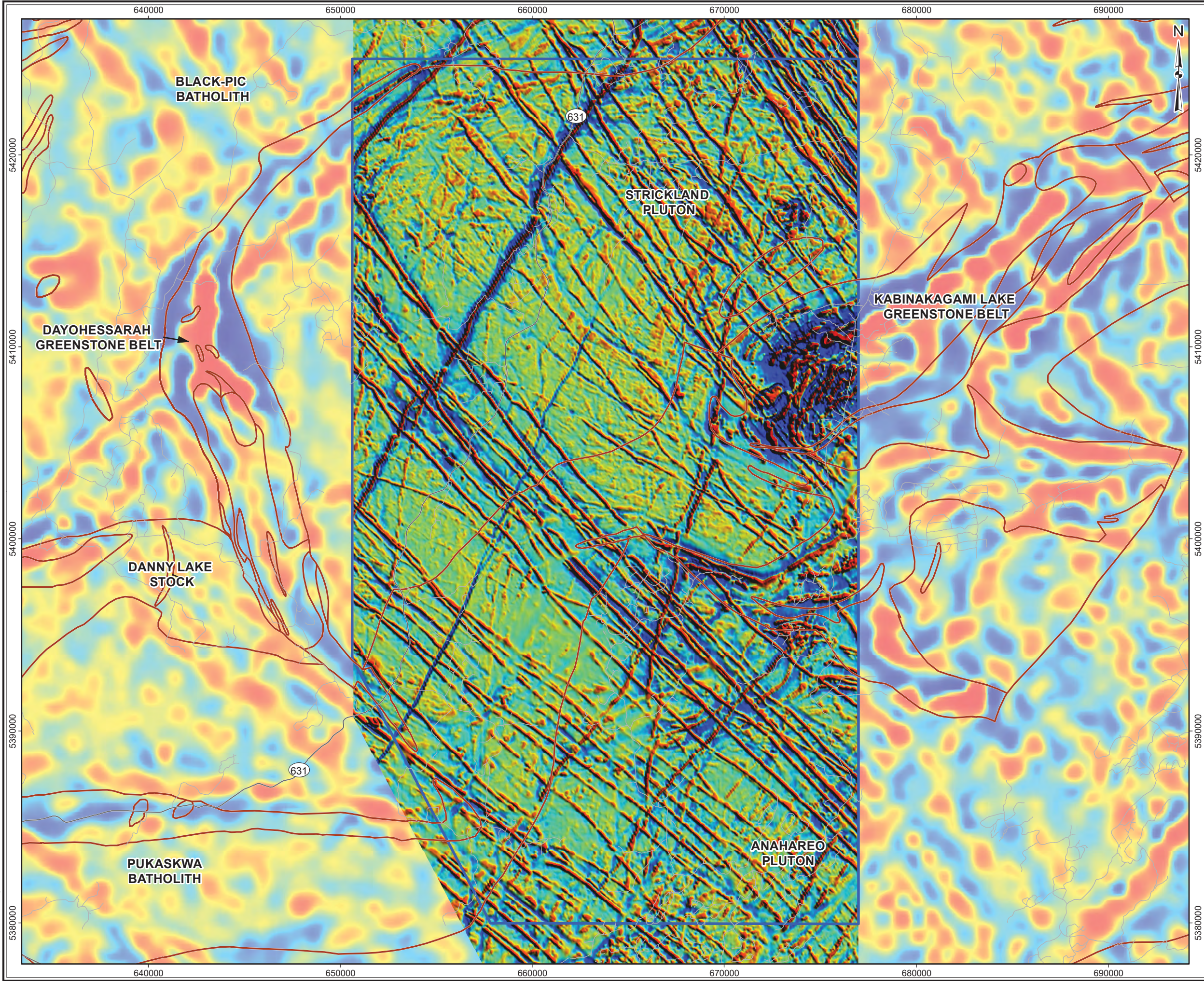
REFERENCE

Base Data: Land Information Ontario (obtained 2015);
CanVec Topography (obtained 2015)

Surficial Geology: MRD-160 (Digital Northern Ontario Engineering
Geology Terrain Study, 2005)

0 10 km

PROJECT				Phase 2 Structural Lineament Interpretation White River Area, Ontario	
TITLE				Terrain Features of the White River Area	
DESIGN	KR	02 SEP 2014	Figure 3	REVISION 4	
GIS	JA	23 SEP 2016		UTM ZONE 16N	
CHECK	SC	23 SEP 2016		NAD 1983	
REVIEW	JPS	23 SEP 2016		1:190,000	



LEGEND

- Phase 2 Assessment Area
- Major Road
- Minor Road
- Geological Boundary

Magnetic Intensity (nT/km)

4,288

-3,197

REFERENCE

Base Data: Land Information Ontario (obtained 2015);
CanVec Topography (obtained 2015)

Background Regional Geophysics: Single Master Gravity and
Aeromagnetic Data for Ontario (Ontario Geological Survey, 1999)

Detailed Geophysics: Pole Reduced Magnetic Data
(First Vertical Derivative) (SGL, 2017)

0

10

km

PROJECT

Phase 2 Structural Lineament Interpretation
White River Area, Ontario

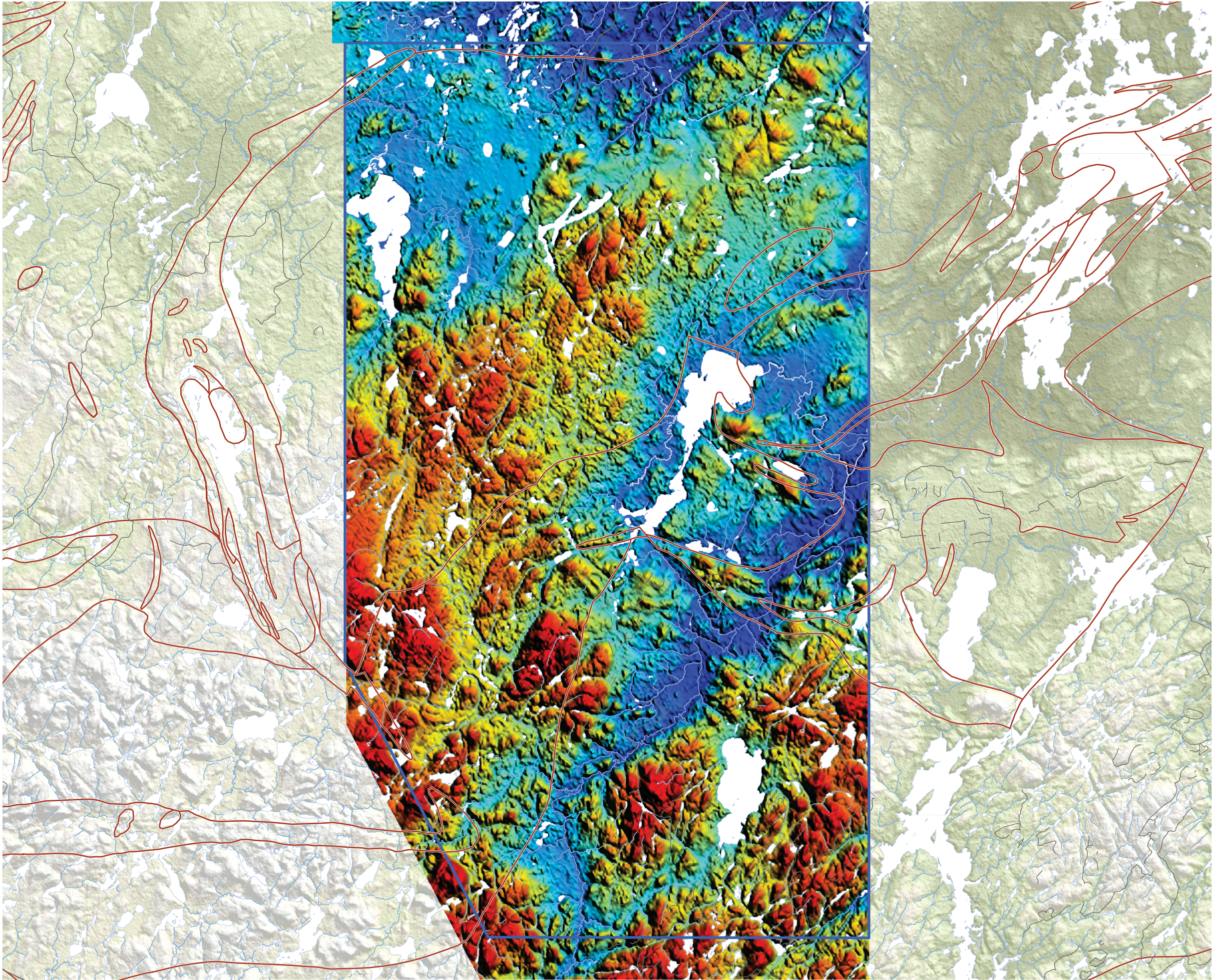
TITLE

**Pole Reduced Magnetic Data (First Vertical Derivative)
of the White River Area**

DESIGN	KR	02 SEP 2014
GIS	JA	23 SEP 2016
CHECK	SC	23 SEP 2016
REVIEW	JPS	23 SEP 2016

Figure 4

REVISION 4
UTM ZONE 16N
NAD 1983
1:190,000




REFERENCE

Base Data: Land Information Ontario (obtained 2015);
CanVec Topography (obtained 2015)

Background Relief: 1 Arc-Second Digital Elevation Model (SRTM, 2000)

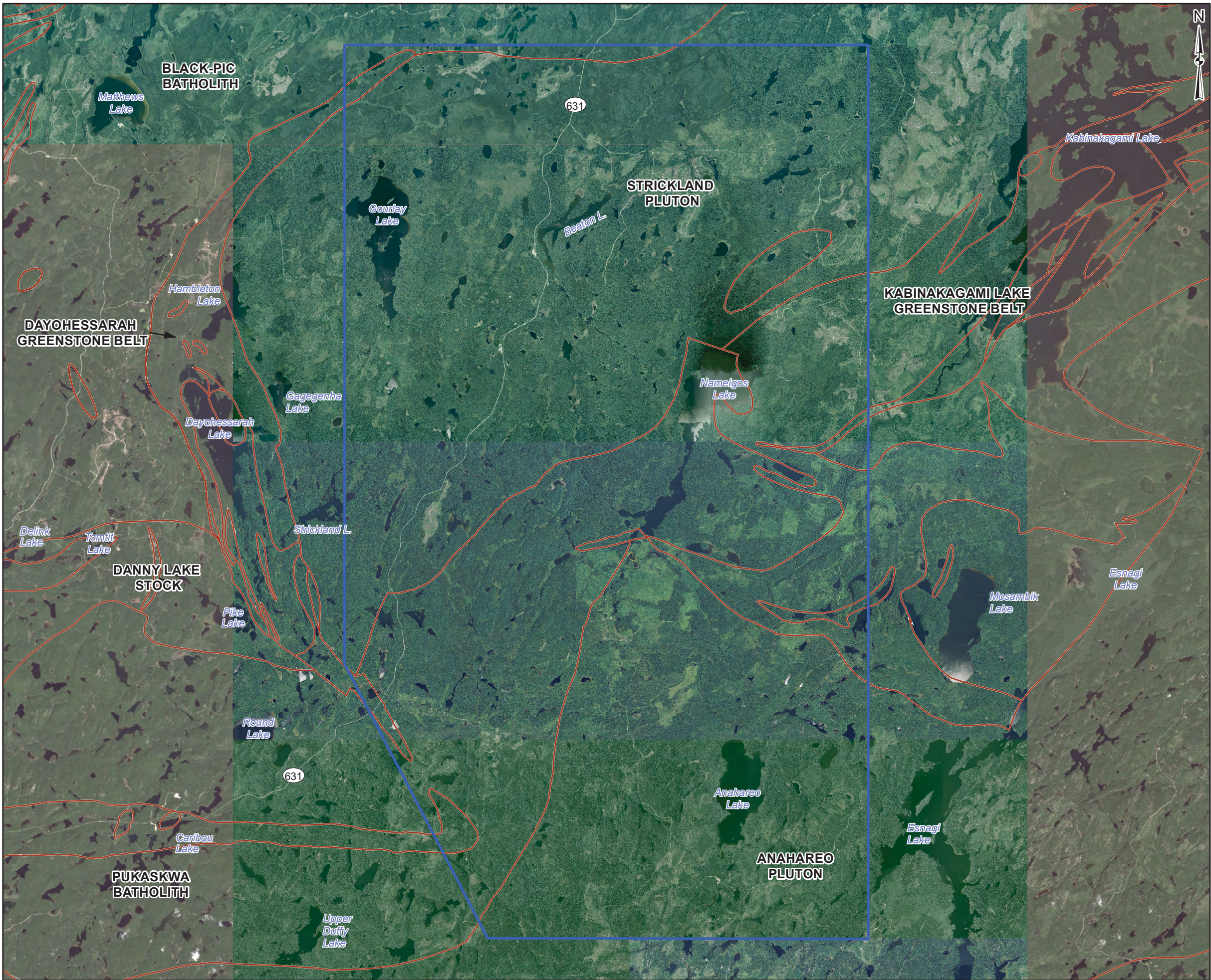
Detailed Relief: Digital Elevation Model (SGL, 2017)




Phase 2 Structural Lineament Interpretation
White River Area, Ontario


Digital Elevation Data
of the White River Area

DESIGN	KR	02 SEP 2014	Figure 5	REVISION 4
GIS	JA	23 SEP 2016		UTM ZONE 16N
CHECK	SC	23 SEP 2016		NAD 1983
REVIEW	JPS	23 SEP 2016		1:190,000



LEGEND

 Phase 2 Assessment Area

 Geological Boundary

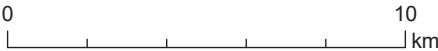



REFERENCE

Base Data: Land Information Ontario (obtained 2015);
CanVec Topography (obtained 2015)

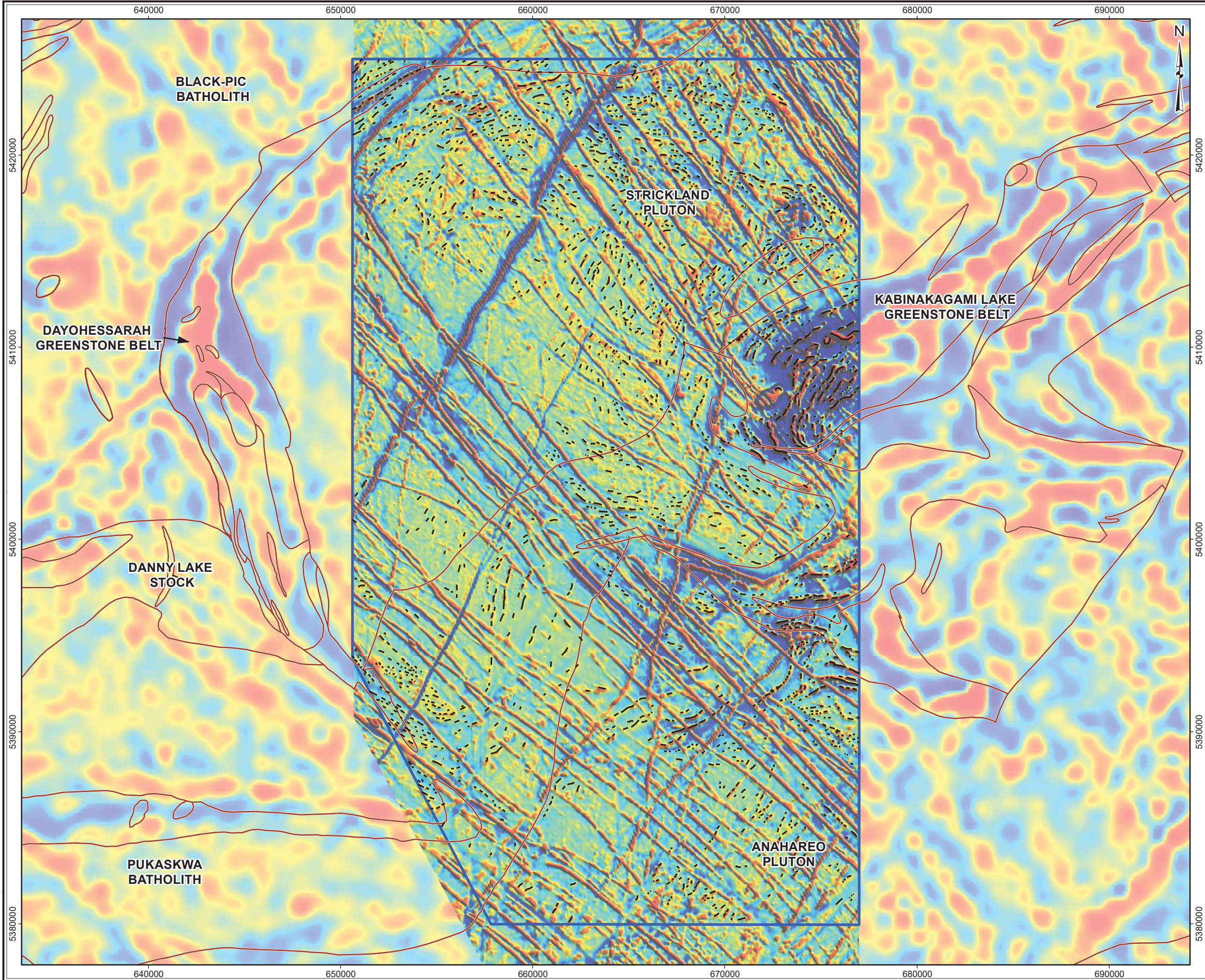
Background Imagery: Pan-sharpened LandSAT-8 (LP DAAC, 2015)

Detailed Imagery: Forest Resource Inventory Digital Aerial Imagery
(Land Information Ontario, 2007-2011)





PROJECT				Phase 2 Structural Lineament Interpretation White River Area, Ontario	
TITLE				Forest Resource Inventory Digital Aerial Imagery of the White River Area	
DESIGN	KR	02 SEP 2014	Figure 6	REVISION 4	
GIS	JA	23 SEP 2016		UTM ZONE 16N	
CHECK	SC	23 SEP 2016		NAD 1983	
REVIEW	JPS	23 SEP 2016		1:190,000	



LEGEND

- Phase 2 Assessment Area
- Geological Boundary
- Form Line

Magnetic Intensity (nT/km)

4,288

-3,197

Thunder Bay
CAN
USA
Wawa
Lake Superior
Sault-Ste. Marie
Sudbury

REFERENCE

Base Data: Land Information Ontario (obtained 2015); CanVec Topography (obtained 2015)

Background Regional Geophysics: Single Master Gravity and Aeromagnetic Data for Ontario (Ontario Geological Survey, 1999)

Detailed Geophysics: Pole Reduced Magnetic Data (First Vertical Derivative) (SGL, 2017)

010 km

srk consulting

PROJECT

Phase 2 Structural Lineament Interpretation
White River Area, Ontario

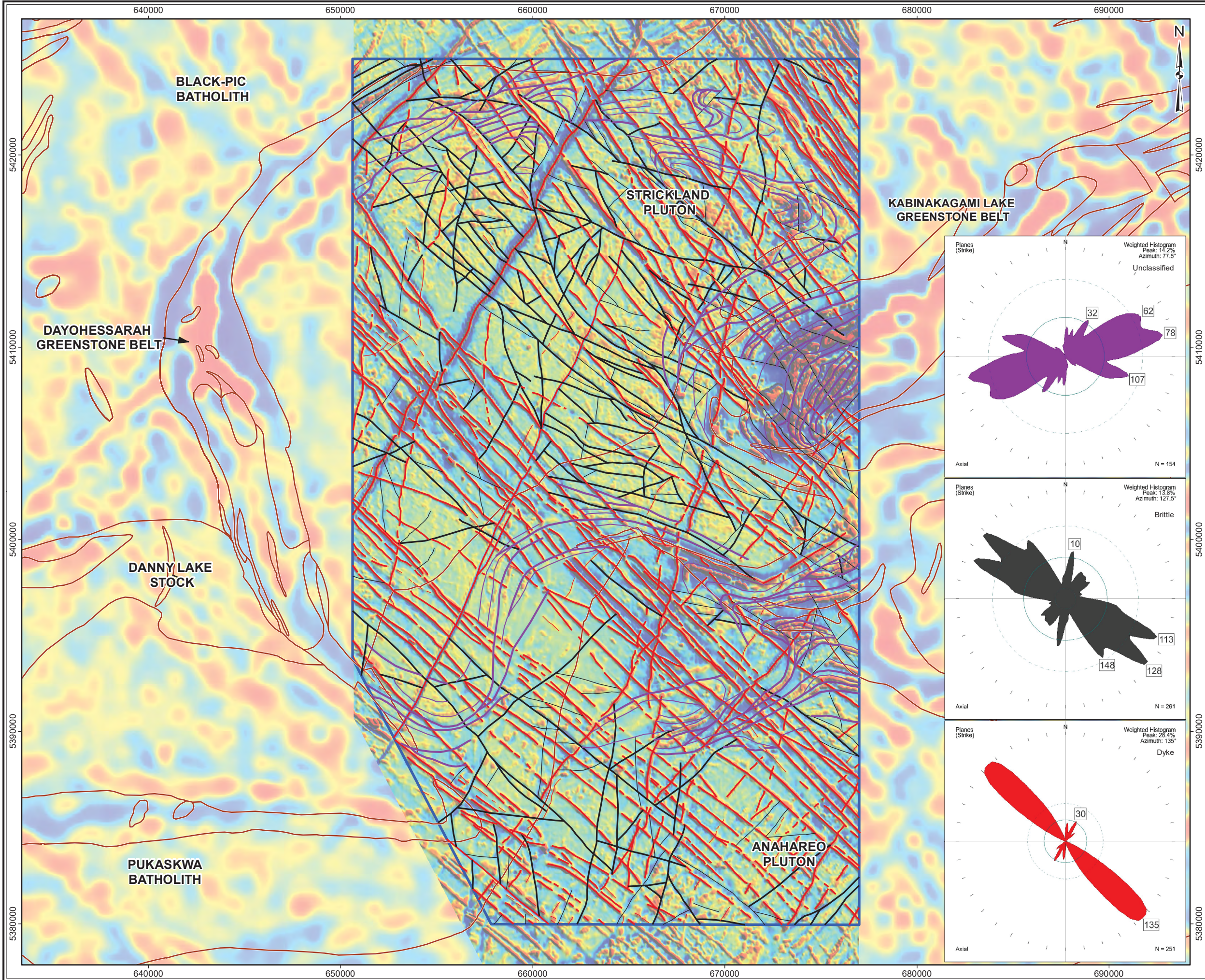
TITLE

**Form Lines
from Pole Reduced Magnetic Data
of the White River Area**

DESIGN	KR	02 SEP 2014
GIS	JA	23 SEP 2016
CHECK	SC	23 SEP 2016
REVIEW	JPS	23 SEP 2016

Figure 7

REVISION 4
UTM ZONE 16N
NAD 1983
1:190,000



LEGEND

Phase 2 Assessment Area

Geological Boundary

Unclassified Lineament (RA1)

1

2

Brittle Lineament (RA 1)

1

2

Dyke Lineament (RA 1)

1

2

Magnetic Intensity (nT/km)

4,288

-3,197

REFERENCE

Base Data: Land Information Ontario (obtained 2015); CanVec Topography (obtained 2015)

Background Regional Geophysics: Single Master Gravity and Aeromagnetic Data for Ontario (Ontario Geological Survey, 1999)

Detailed Geophysics: Pole Reduced Magnetic Data (First Vertical Derivative) (SGL, 2017)

0 10 km

srk consulting

PROJECT: Phase 2 Structural Lineament Interpretation
White River Area, Ontario

TITLE: Interpreted Lineaments from Pole Reduced Magnetic Data of the White River Area

DESIGN	KR	02 SEP 2014
GIS	JA	11 APR 2017
CHECK	SC	11 APR 2017
REVIEW	JPS	11 APR 2017

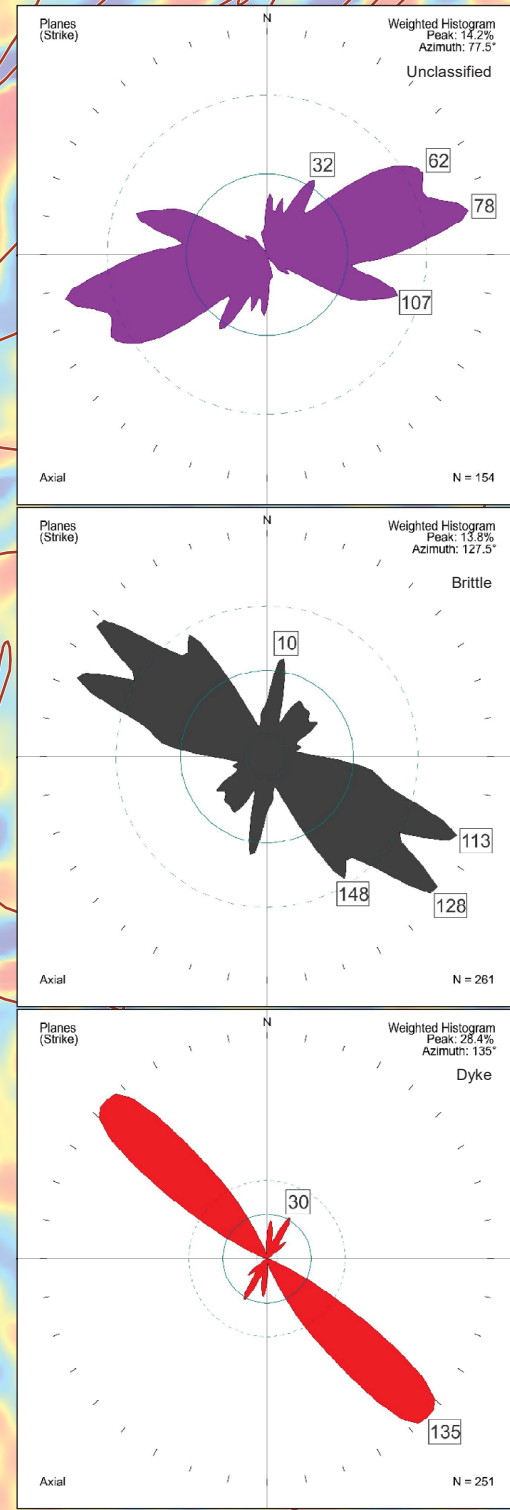
REVISION 5

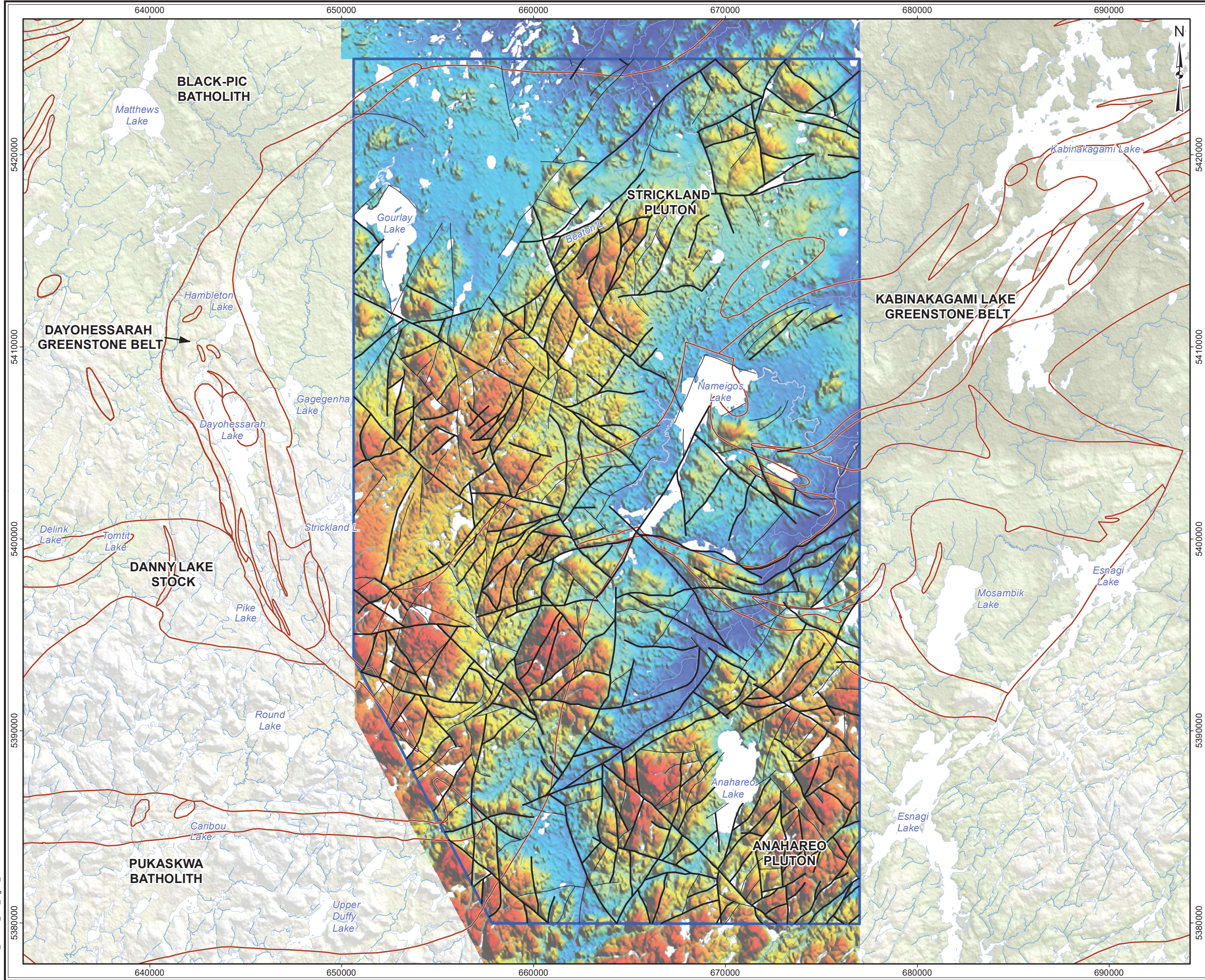
UTM ZONE 16N

NAD 1983

1:190,000

Figure 8





LEGEND

- Phase 2 Assessment Area
- Watercourse
- Waterbody
- Geological Boundary
- DEM Lineament (RA1)**
 - 1
 - 2

Elevation (masl)
315 563

Planes (Strike)

0 33 53 75 133

Axial N = 425

Thunder Bay Wawa Sault Ste. Marie Sudbury

CAN USA Lake Superior

REFERENCE

Base Data: Land Information Ontario (obtained 2015);
CanVec Topography (obtained 2015)

Background Relief: 1 Arc-Second Digital Elevation Model (SRTM, 2000)

Detailed Relief: Digital Elevation Model (SGL, 2017)

0 10 km

srk consulting

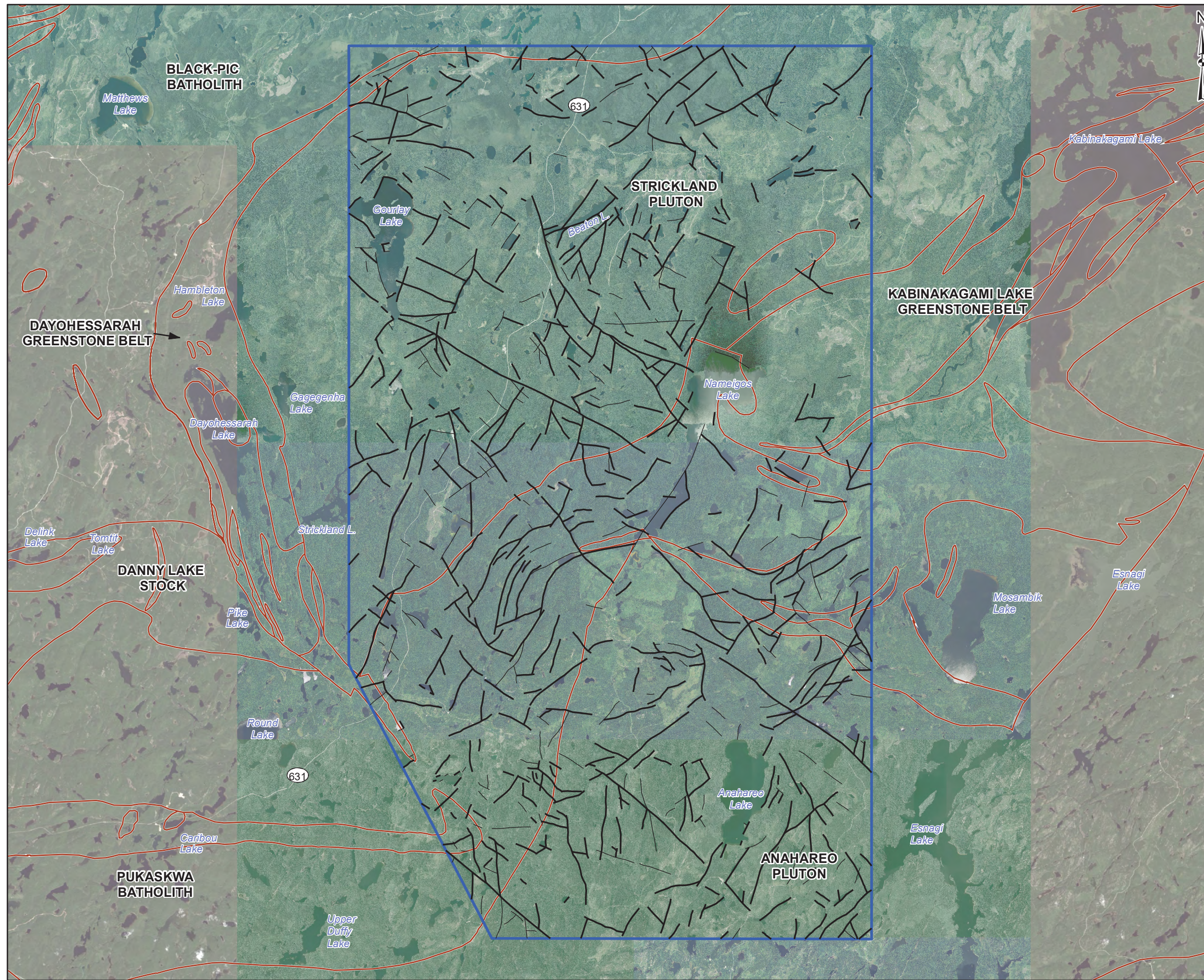
PROJECT Phase 2 Structural Lineament Interpretation
White River Area, Ontario

TITLE **Interpreted Lineaments from Digital Elevation Data
of the White River Area**

DESIGN	KR	02 SEP 2014
GIS	JA	11 APR 2017
CHECK	SC	11 APR 2017
REVIEW	JPS	11 APR 2017

Figure 9

REVISION 5
UTM ZONE 16N
NAD 1983
1:190,000



LEGEND

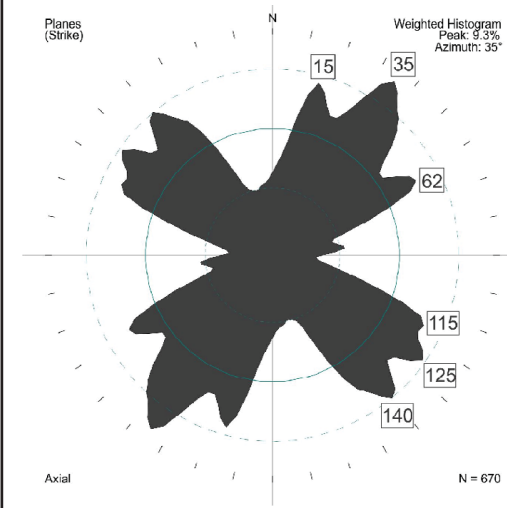
Phase 2 Assessment Area

Geological Boundary

FRI Lineament (RA1)

1

2



REFERENCE

Base Data: Land Information Ontario (obtained 2015);
CanVec Topography (obtained 2015)

Background Imagery: Pan-sharpened Landsat-8 (LP DAAC, 2015)

Detailed Imagery: Forest Resource Inventory Digital Aerial Imagery (OMNR, 2009)

0 10 km

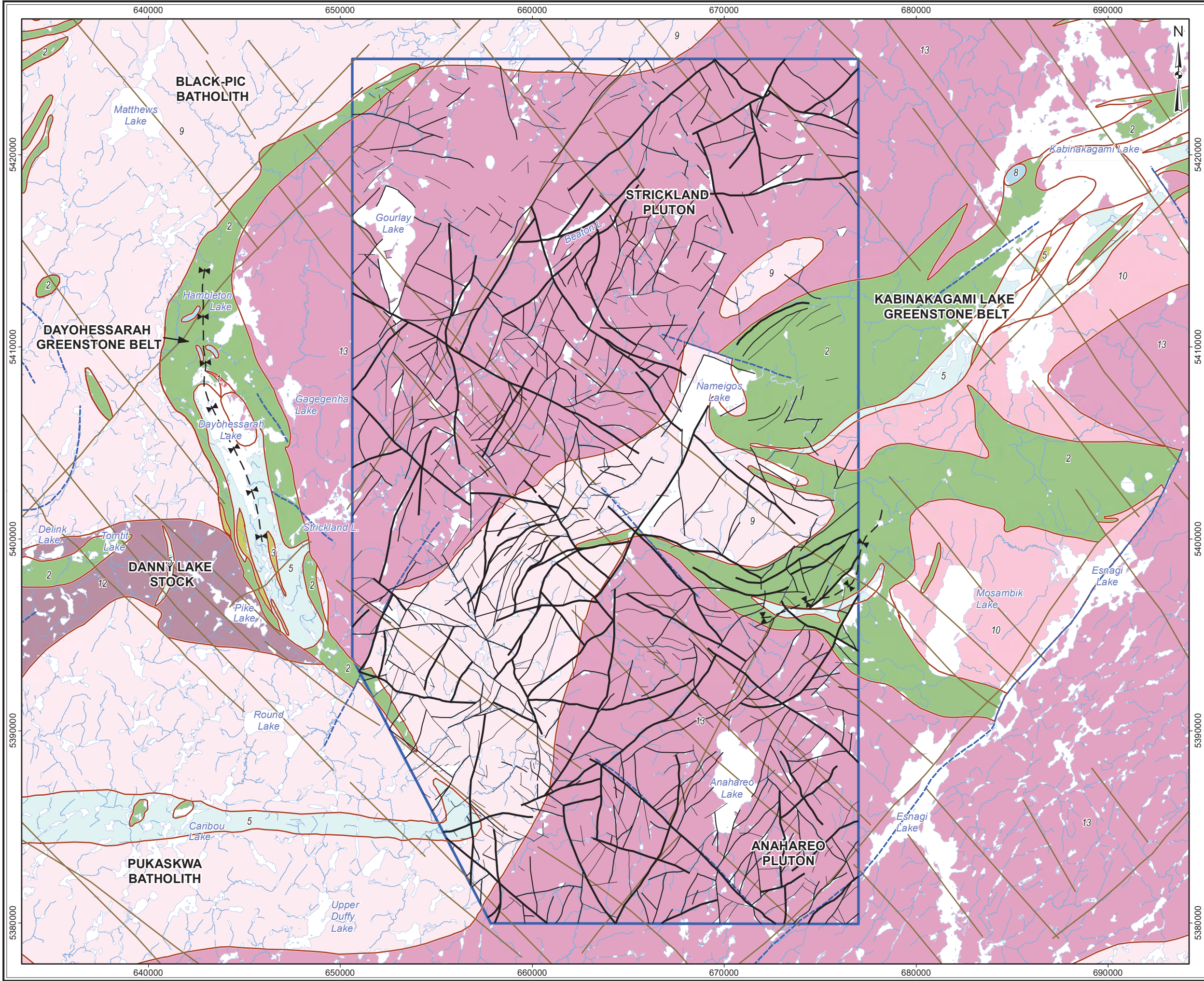
PROJECT Phase 2 Structural Lineament Interpretation
White River Area, Ontario

TITLE **Interpreted Lineaments
from Forest Resource Inventory (FRI) Imagery
of the White River Area**

DESIGN	KR	02 SEP 2014
GIS	JA	11 APR 2017
CHECK	SC	11 APR 2017
REVIEW	JPS	11 APR 2017

Figure 10

REVISION 5
UTM ZONE 16N
NAD 1983
1:190,000



LEGEND

Phase 2 Assessment Area

Watercourse

Waterbody

Bedrock Geology

Fold (syncline)

Mapped Fault

Mapped Dyke

Geological Boundary

13: Granite-granodiorite

12: Diorite-monzonite- granodiorite

10: Foliated tonalite suite

9: Gneissic tonalite suite

8: Gabbro

5: Metasedimentary rocks

3: Felsic and intermediate metavolcanic rocks

2: Mafic metavolcanic Rocks

Surficial Lineament

Certainty 1

Certainty 2

Certainty 3

Planes (Strike)

Weighted Histogram

Peak: 10.2%

Azimuth: 32.5°

33

64

124

North Arrow

Scale Bar: 0 to 10 km

REFERENCE

Base Data: Land Information Ontario (obtained 2015); CanVec Topography (obtained 2015)

Bedrock Geology: MRD126-REV1 (Ontario Geological Survey, 2011); Ontario Geological Survey Map 2666 (Santaguida, 2001).

srk consulting

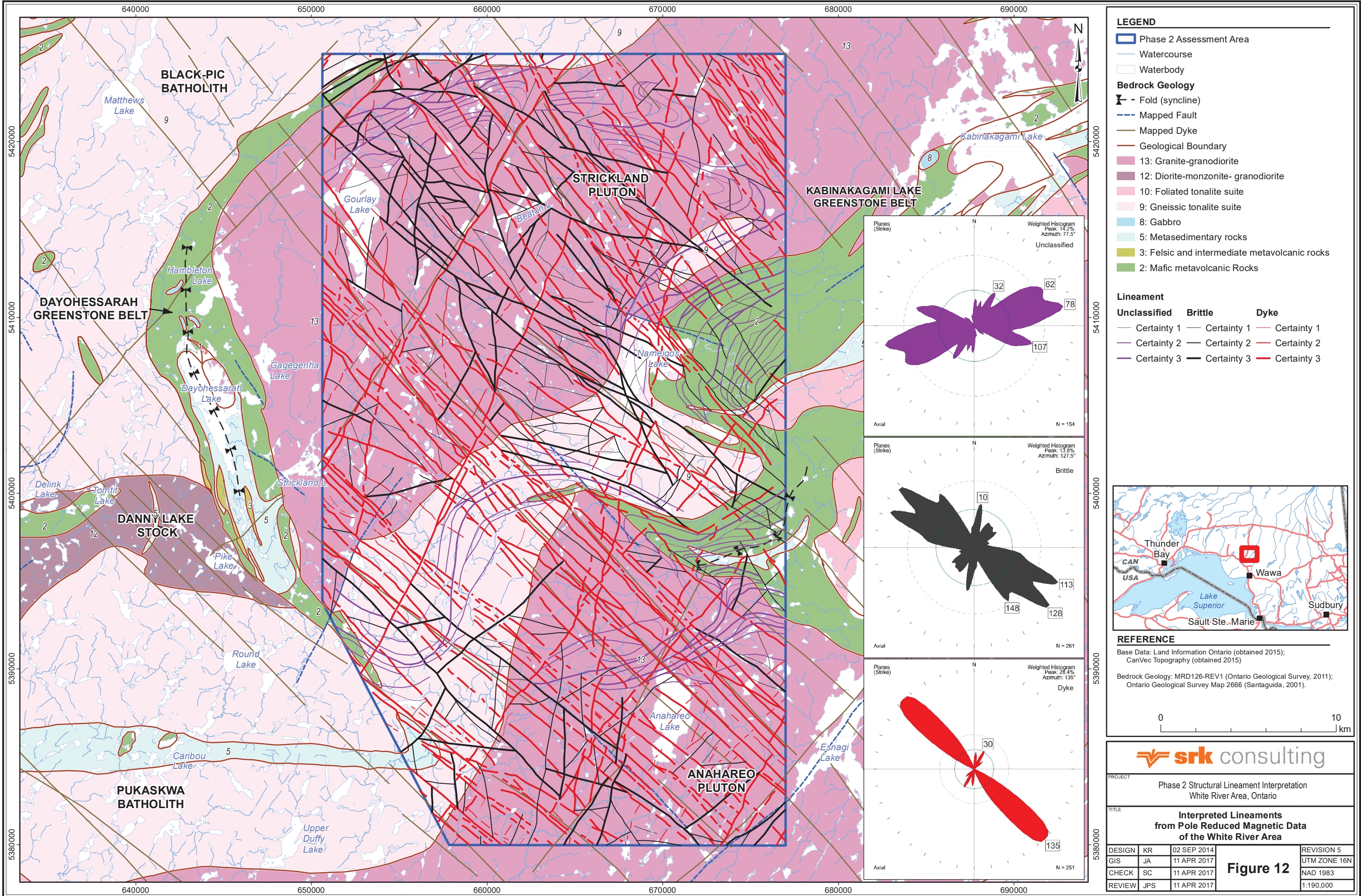
PROJECT: Phase 2 Structural Lineament Interpretation
White River Area, Ontario

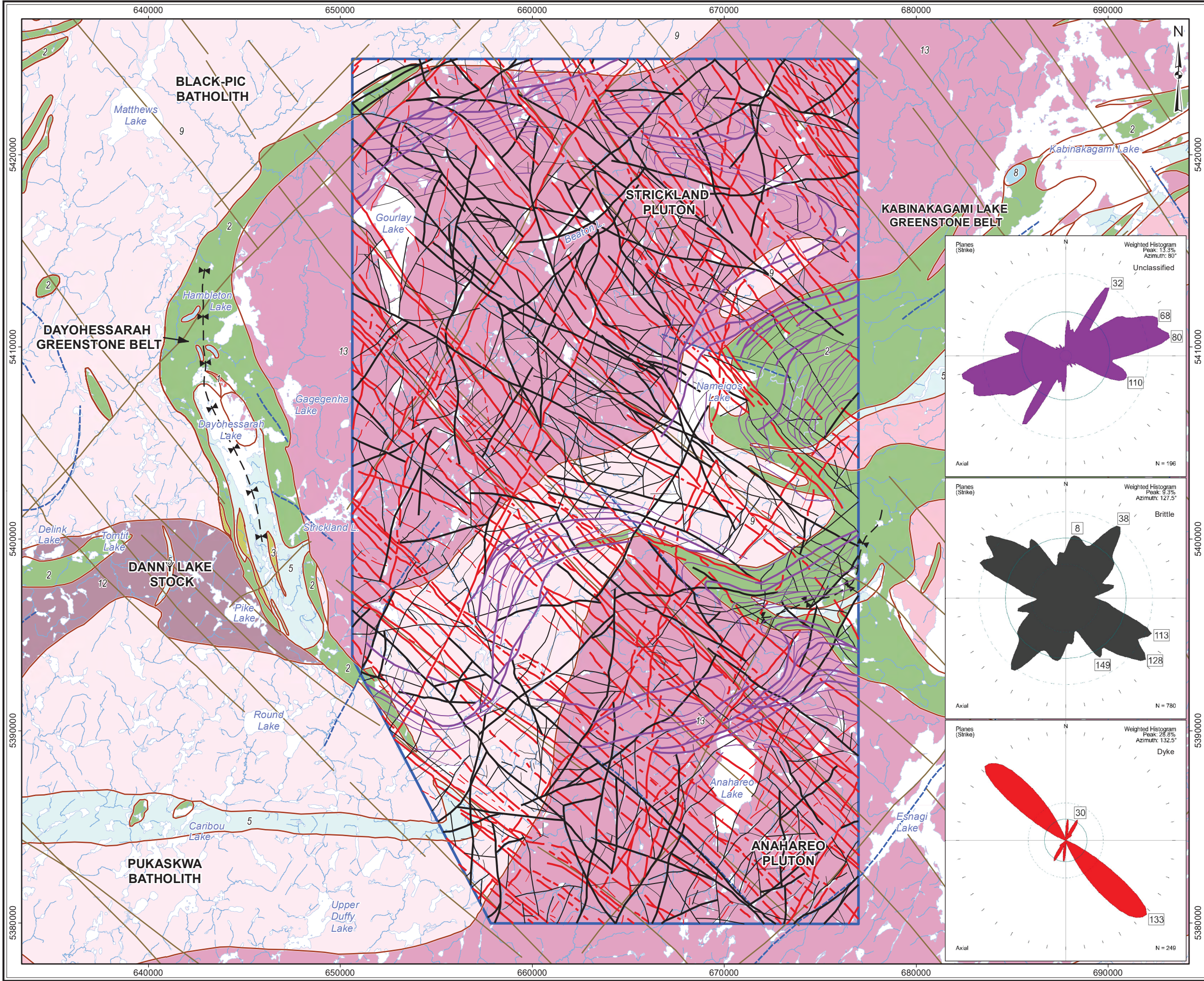
TITLE: **Interpreted Lineaments from Surficial Data of the White River Area**

DESIGN	KR	02 SEP 2014
GIS	JA	11 APR 2017
CHECK	SC	11 APR 2017
REVIEW	JPS	11 APR 2017

Figure 11

REVISION 5
UTM ZONE 16N
NAD 1983
1:190,000





LEGEND

Phase 2 Assessment Area

Watercourse

Waterbody

Bedrock Geology

Fold (syncline)

Mapped Fault

Mapped Dyke

Geological Boundary

13: Granite-granodiorite

12: Diorite-monzonite- granodiorite

10: Foliated tonalite suite

9: Gneissic tonalite suite

8: Gabbro

5: Metasedimentary rocks

3: Felsic and intermediate metavolcanic rocks

2: Mafic metavolcanic Rocks

Lineament

Unclassified	Brittle	Dyke
Certainty 1	Certainty 1	Certainty 1
Certainty 2	Certainty 2	Certainty 2
Certainty 3	Certainty 3	Certainty 3

REFERENCE

Base Data: Land Information Ontario (obtained 2015);
CanVec Topography (obtained 2015)

Bedrock Geology: MRD126-REV1 (Ontario Geological Survey, 2011);
Ontario Geological Survey Map 2666 (Santaguida, 2001).

0 10 km

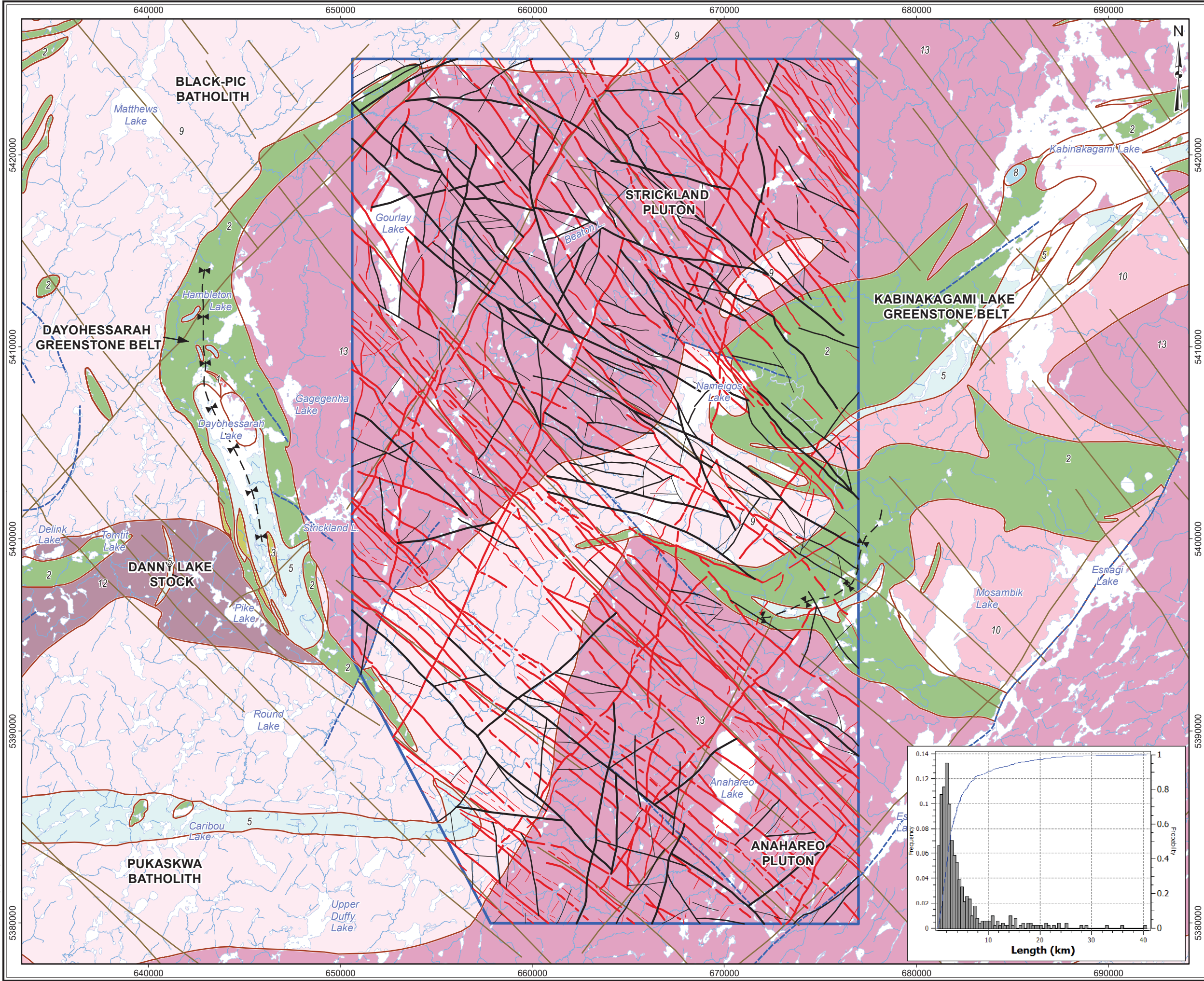
PROJECT Phase 2 Structural Lineament Interpretation
White River Area, Ontario

TITLE **Final Integrated Lineaments
of the White River Area**

DESIGN	KR	02 SEP 2014
GIS	JA	11 APR 2017
CHECK	SC	11 APR 2017
REVIEW	JPS	11 APR 2017

Figure 13

REVISION 6
UTM ZONE 16N
NAD 1983
1:190,000



LEGEND

Phase 2 Assessment Area

Watercourse

Waterbody

Bedrock Geology

- Fold (syncline)

Mapped Fault

Mapped Dyke

Geological Boundary

13: Granite-granodiorite

12: Diorite-monzonite- granodiorite

10: Foliated tonalite suite

9: Gneissic tonalite suite

8: Gabbro

5: Metasedimentary rocks

3: Felsic and intermediate metavolcanic rocks

2: Mafic metavolcanic Rocks

Brittle Lineament

<1 km

1 - 2.5

2.5 - 5

>5 km

Dyke Lineament

<1 km

1 - 2.5

2.5 - 5

>5 km

REFERENCE
Base Data: Land Information Ontario (obtained 2015);
CanVec Topography (obtained 2015)

Bedrock Geology: MRD126-REV1 (Ontario Geological Survey, 2011);
Ontario Geological Survey Map 2666 (Santaguida, 2001).

0

10

km

srk consulting

PROJECT

Phase 2 Structural Lineament Interpretation
White River Area, Ontario

TITLE

Interpreted Brittle and Dyke Lineaments
from Pole Reduced Magnetic Data (by Length)
of the White River Area

DESIGN

KR

02 SEP 2014

GIS

JA

23 SEP 2016

CHECK

SC

23 SEP 2016

REVIEW

JPS

23 SEP 2016

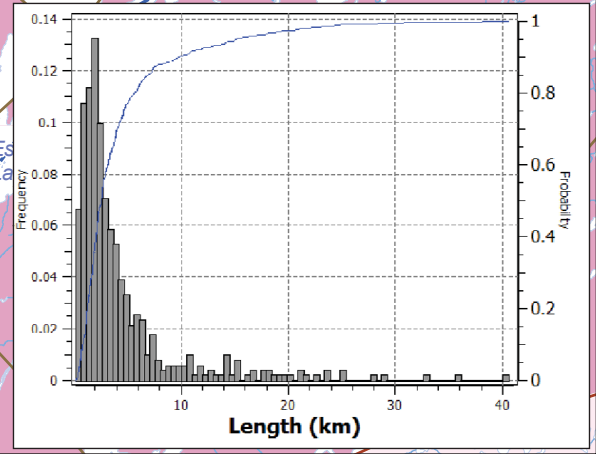
REVISION 2

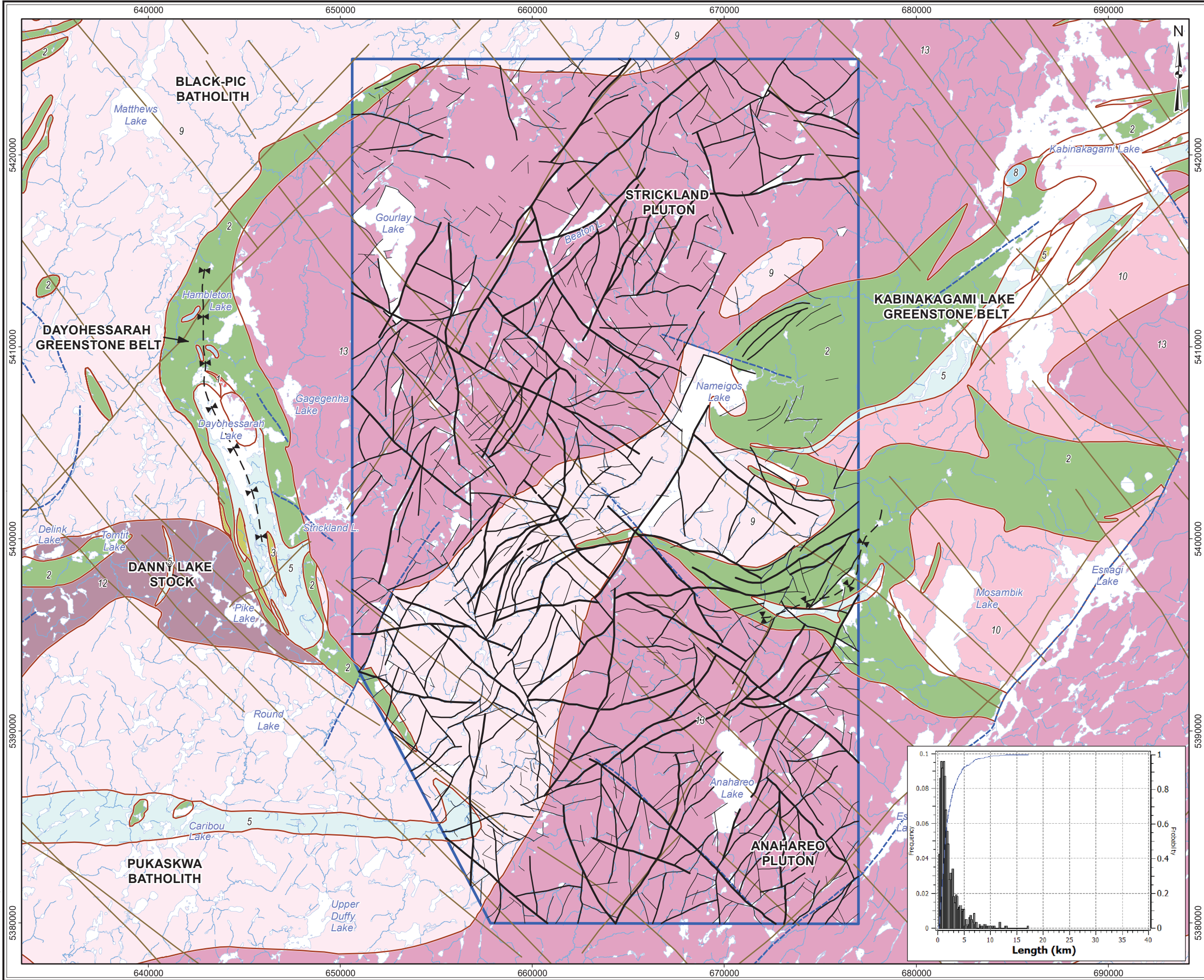
UTM ZONE 16N

NAD 1983

1:190,000

Figure 14





LEGEND

Phase 2 Assessment Area

Watercourse

Waterbody

Bedrock Geology

- Fold (syncline)

Mapped Fault

Mapped Dyke

Geological Boundary

13

Granite-granodiorite

12

Diorite-monzonite- granodiorite

10

Foliated tonalite suite

9

Gneissic tonalite suite

8

Gabbro

5

Metasedimentary rocks

3

Felsic and intermediate metavolcanic rocks

2

Mafic metavolcanic Rocks

Surficial Lineament

<1 km

1 - 2.5

2.5 - 5

>5 km

REFERENCE
Base Data: Land Information Ontario (obtained 2015);
CanVec Topography (obtained 2015)

Bedrock Geology: MRD126-REV1 (Ontario Geological Survey, 2011);
Ontario Geological Survey Map 2666 (Santaguida, 2001).

0100000

0200000

0300000

0400000

0500000

0600000

0700000

0800000

0900000

1000000

1100000

1200000

1300000

1400000

1500000

1600000

1700000

1800000

1900000

2000000

2100000

2200000

2300000

2400000

2500000

2600000

2700000

2800000

2900000

3000000

3100000

3200000

3300000

3400000

3500000

3600000

3700000

3800000

3900000

4000000

4100000

4200000

4300000

4400000

4500000

4600000

4700000

4800000

4900000

5000000

5100000

5200000

5300000

5400000

5500000

5600000

5700000

5800000

5900000

6000000

6100000

6200000

6300000

6400000

6500000

6600000

6700000

6800000

6900000

7000000

7100000

7200000

7300000

7400000

7500000

7600000

7700000

7800000

7900000

8000000

8100000

8200000

8300000

8400000

8500000

8600000

8700000

8800000

8900000

9000000

9100000

9200000

9300000

9400000

9500000

9600000

9700000

9800000

9900000

10000000

10100000

10200000

10300000

10400000

10500000

10600000

10700000

10800000

10900000

11000000

11100000

11200000

11300000

11400000

11500000

11600000

11700000

11800000

11900000

12000000

12100000

12200000

12300000

12400000

12500000

12600000

12700000

12800000

12900000

13000000

13100000

13200000

13300000

13400000

13500000

13600000

13700000

13800000

13900000

14000000

14100000

14200000

14300000

14400000

14500000

14600000

14700000

14800000

14900000

15000000

15100000

15200000

15300000

15400000

15500000

15600000

15700000

15800000

15900000

16000000

16100000

16200000

16300000

16400000

16500000

16600000

16700000

16800000

16900000

17000000

17100000

17200000

17300000

17400000

17500000

17600000

17700000

17800000

17900000

18000000

18100000

18200000

18300000

18400000

18500000

18600000

18700000

18800000

18900000

19000000

19100000

19200000

19300000

19400000

19500000

19600000

19700000

19800000

19900000

20000000

20100000

20200000

20300000

20400000

20500000

20600000

20700000

20800000

20900000

21000000

21100000

21200000

21300000

21400000

21500000

21600000

21700000

21800000

21900000

22000000

22100000

22200000

22300000

22400000

22500000

22600000

22700000

22800000

22900000

23000000

23100000

23200000

23300000

23400000

23500000

23600000

23700000

23800000

23900000

24000000

24100000

24200000

24300000

24400000

24500000

24600000

24700000

24800000

24900000

25000000

25100000

25200000

25300000

25400000

25500000

25600000

25700000

25800000

25900000

26000000

26100000

26200000

26300000

26400000

26500000

26600000

26700000

26800000

26900000

27000000

27100000

27200000

27300000

27400000

27500000

27600000

27700000

27800000

27900000

28000000

28100000

28200000

28300000

28400000

28500000

28600000

28700000

28800000

28900000

29000000

29100000

29200000

29300000

29400000

29500000

29600000

29700000

29800000

29900000

30000000

30100000

30200000

30300000

30400000

30500000

30600000

30700000

30800000

30900000

31000000

31100000

31200000

31300000

31400000

31500000

31600000

31700000

31800000

31900000

32000000

32100000

32200000

32300000

32400000

32500000

32600000

32700000

32800000

32900000

33000000

33100000

33200000

33300000

33400000

33500000

33600000

33700000

33800000

33900000

34000000

34100000

34200000

34300000

34400000

34500000

34600000

34700000

34800000

34900000

35000000

35100000

35200000

35300000

35400000

35500000

35600000

35700000

35800000

35900000

36000000

36100000

36200000

36300000

36400000

36500000

36600000

36700000

36800000

36900000

37000000

37100000

37200000

37300000

37400000

37500000

37600000

37700000

37800000

37900000

38000000

38100000

38200000

38300000

38400000

38500000

38600000

38700000

38800000

38900000

39000000

39100000

39200000

39300000

39400000

39500000

39600000

39700000

39800000

39900000

40000000

40100000

40200000

40300000

40400000

40500000

40600000

40700000

40800000

40900000

41000000

41100000

41200000

41300000

41400000

41500000

41600000

41700000

41800000

41900000

42000000

42100000

42200000

42300000

42400000

42500000

42600000

42700000

42800000

42900000

43000000

43100000

43200000

43300000

43400000

43500000

43600000

43700000

43800000

43900000

44000000

44100000

44200000

44300000

44400000

44500000

44600000

44700000

44800000

44900000

45000000

45100000

45200000

45300000

45400000

45500000

45600000

45700000

45800000

45900000

46000000

46100000

46200000

46300000

46400000

46500000

46600000

46700000

46800000

46900000

47000000

47100000

47200000

47300000

47400000

47500000

47600000

47700000

47800000

47900000

48000000

48100000

48200000

48300000

48400000

48500000

48600000

48700000

48800000

48900000

49000000

49100000

49200000

49300000

49400000

49500000

49600000

49700000

49800000

49900000

50000000

50100000

50200000

50300000

50400000

50500000

50600000

50700000

50800000

50900000

51000000

51100000

51200000

51300000

51400000

51500000

51600000

51700000

51800000

51900000

52000000

52100000

52200000

52300000

52400000

52500000

52600000

52700000

52800000

52900000

53000000

53100000

53200000

53300000

53400000

53500000

53600000

53700000

53800000

53900000

54000000

54100000

54200000

54300000

54400000

54500000

54600000

54700000

54800000

54900000

55000000

55100000

55200000

55300000

55400000

55500000

55600000

55700000

55800000

55900000

56000000

56100000

56200000

56300000

56400000

56500000

56600000

56700000

56800000

56900000

57000000

57100000

57200000

57300000

57400000

57500000

57600000

57700000

57800000

57900000

58000000

58100000

58200000

58300000

58400000

58500000

58600000

58700000

58800000

58900000

59000000

59100000

59200000

59300000

59400000

59500000

59600000

59700000

59800000

59900000

60000000

60100000

60200000

60300000

60400000

60500000

60600000

60700000

60800000

60900000

61000000

61100000

61200000

61300000

61400000

61500000

61600000

61700000

61800000

61900000

62000000

62100000

62200000

62300000

62400000

62500000

62600000

62700000

62800000

62900000

63000000

63100000

63200000

63300000

63400000

63500000

63600000

63700000

63800000

63900000

64000000

64100000

64200000

64300000

64400000

64500000

64600000

64700000

64800000

64900000

65000000

65100000

65200000

65300000

65400000

65500000

65600000

65700000

65800000

65900000

66000000

66100000

66200000

66300000

66400000

66500000

66600000

66700000

66800000

66900000

67000000

67100000

67200000

67300000

67400000

67500000

67600000

67700000

67800000

67900000

68000000

68100000

68200000

68300000

68400000

68500000

68600000

68700000

68800000

68900000

69000000

69100000

69200000

69300000

69400000

69500000

69600000

69700000

69800000

69900000

70000000

70100000

70200000

70300000

70400000

70500000

70600000

70700000

70800000

70900000

71000000

71100000

71200000

71300000

71400000

71500000

71600000

71700000

71800000

71900000

72000000

72100000

72200000

72300000

72400000

72500000

72600000

72700000

72800000

72900000

73000000

73100000

73200000

73300000

73400000

73500000

73600000

73700000

73800000

73900000

74000000

74100000

74200000

74300000

74400000

74500000

74600000

74700000

74800000

74900000

75000000

75100000

75200000

75300000

75400000

75500000

75600000

75700000

75800000

75900000

76000000

76100000

76200000

76300000

76400000

76500000

76600000

76700000

76800000

76900000

77000000

77100000

77200000

77300000

77400000

77500000

77600000

77700000

77800000

77900000

78000000

78100000

78200000

78300000

78400000

78500000

78600000

78700000

78800000

78900000

79000000

79100000

79200000

79300000

79400000

79500000

79600000

79700000

79800000

79900000

80000000

80100000

80200000

80300000

80400000

80500000

80600000

80700000

80800000

80900000

81000000

81100000

81200000

81300000

81400000

81500000

81600000

81700000

81800000

81900000

82000000

82100000

82200000

82300000

82400000

82500000

82600000

82700000

82800000

82900000

83000000

83100000

83200000

83300000

83400000

83500000

83600000

83700000

83800000

83900000

84000000

84100000

84200000

84300000

84400000

84500000

84600000

84700000

84800000

84900000

85000000

85100000

85200000

85300000

85400000

85500000

85600000

85700000

85800000

85900000

86000000

86100000

86200000

86300000

86400000

86500000

86600000

86700000

86800000

86900000

87000000

87100000

87200000

87300000

87400000

87500000

87600000

87700000

87800000

87900000

88000000

88100000

88200000

88300000

88400000

88500000

88600000

88700000

88800000

88900000

89000000

89100000

89200000

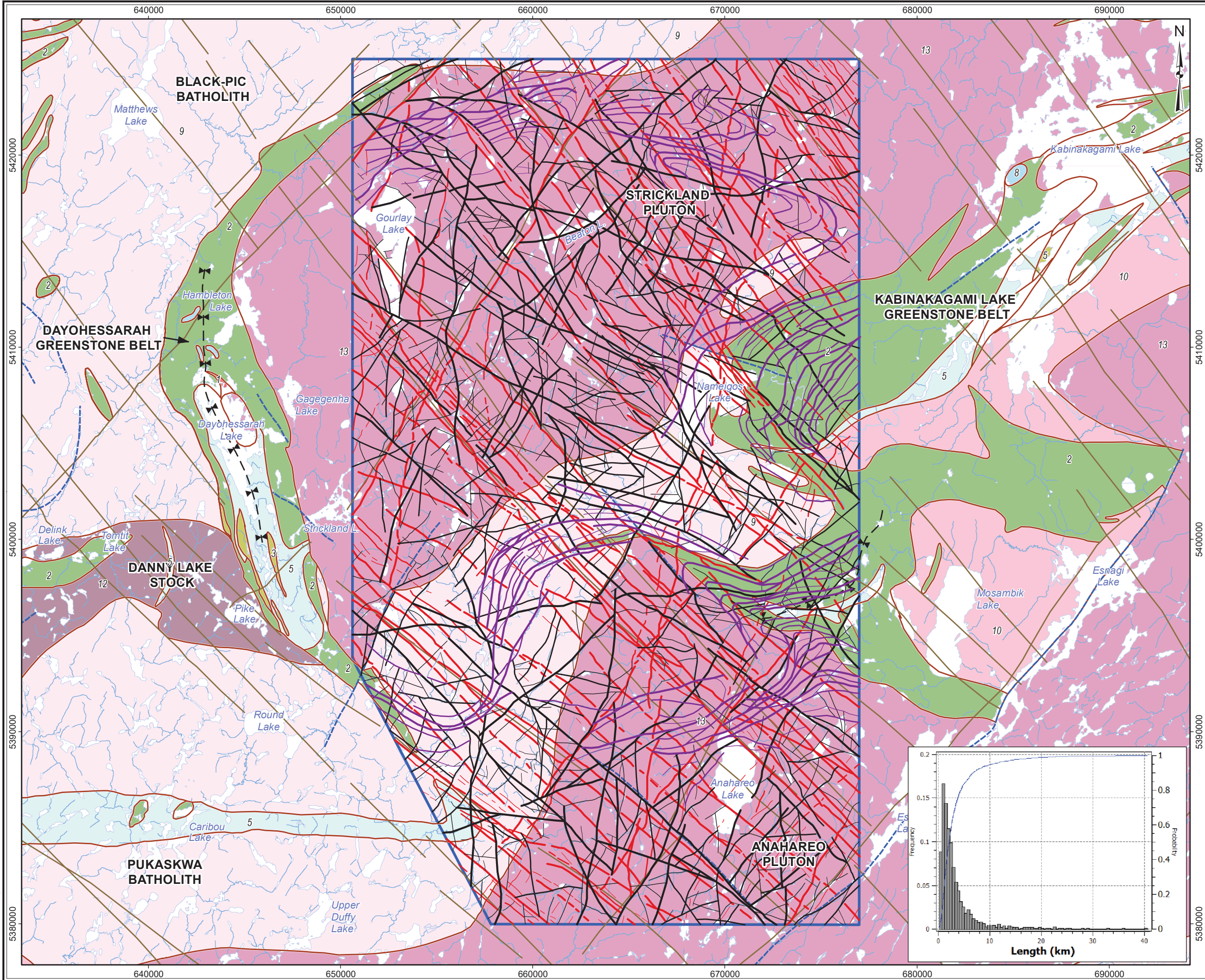
89300000

89400000

89500000

89600000

897000



LEGEND

Phase 2 Assessment Area

Watercourse

Waterbody

Bedrock Geology

Fold (syncline)

Mapped Fault

Mapped Dyke

Geological Boundary

13: Granite-granodiorite

12: Diorite-monzonite- granodiorite

10: Foliated tonalite suite

9: Gneissic tonalite suite

8: Gabbro

5: Metasedimentary rocks

3: Felsic and intermediate metavolcanic rocks

2: Mafic metavolcanic Rocks

Lineament

Unclassified

Brittle

Dyke

<1 km

1 - 2.5

2.5 - 5

>5 km

<1 km

1 - 2.5

2.5 - 5

>5 km

<1 km

1 - 2.5

2.5 - 5

>5 km

REFERENCE

Base Data: Land Information Ontario (obtained 2015);
CanVec Topography (obtained 2015)

Bedrock Geology: MRD126-REV1 (Ontario Geological Survey, 2011);
Ontario Geological Survey Map 2666 (Santaguida, 2001).

010 km

PROJECT

Phase 2 Structural Lineament Interpretation
White River Area, Ontario

TITLE

Final Integrated Lineaments (by Length)
of the White River Area

DESIGN	KR	02 SEP 2014
GIS	JA	23 SEP 2016
CHECK	SC	23 SEP 2016
REVIEW	JPS	23 SEP 2016

REVISION 2

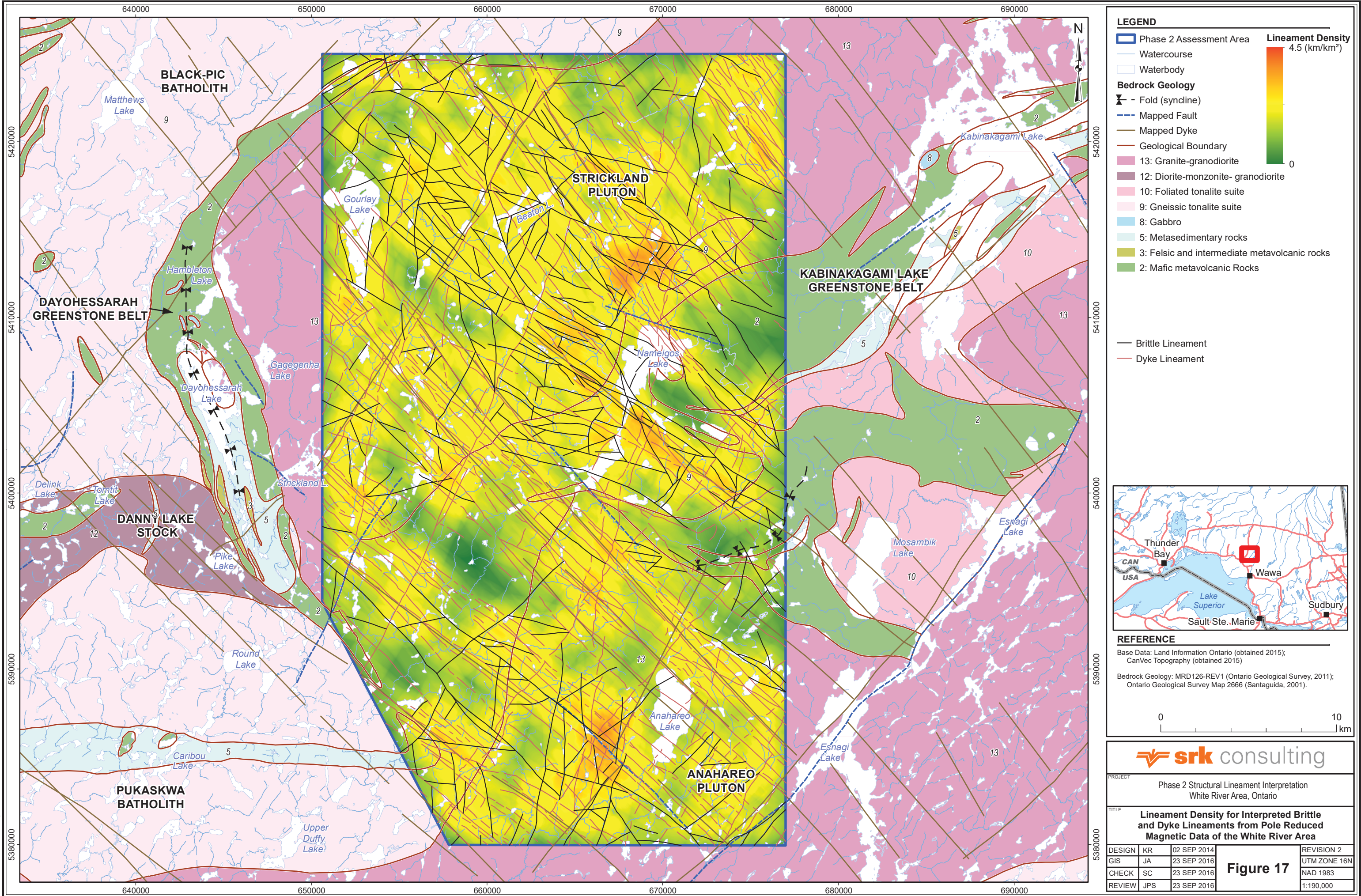
UTM ZONE 16N

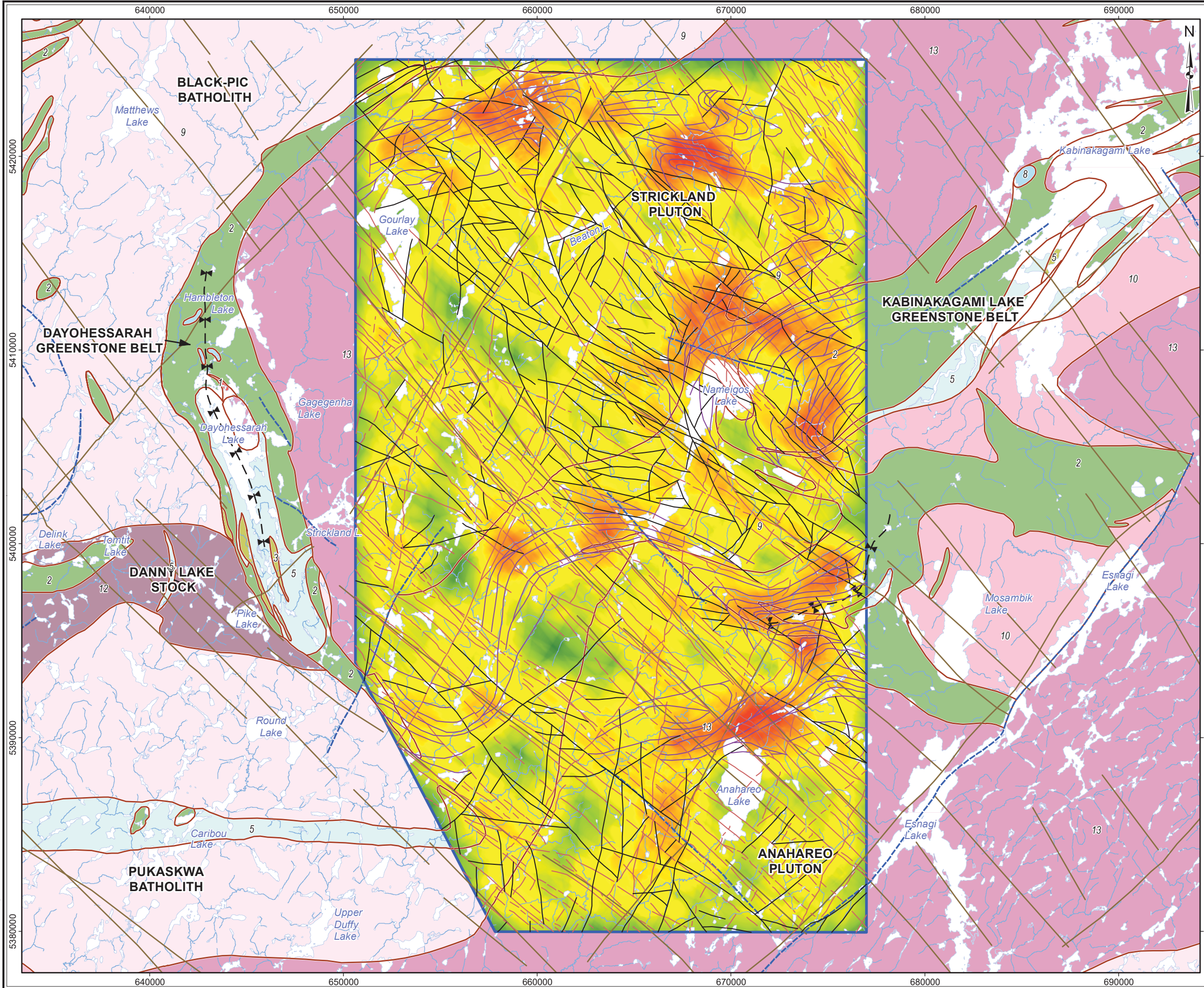
NAD 1983

1:190,000

Figure 16

File: SRK_NWMO_WR_Fig17_mBDLinDens





LEGEND

Phase 2 Assessment Area

Watercourse

Waterbody

Bedrock Geology

- Fold (syncline)

Mapped Fault

Mapped Dyke

Geological Boundary

13: Granite-granodiorite

12: Diorite-monzonite- granodiorite

10: Foliated tonalite suite

9: Gneissic tonalite suite

8: Gabbro

5: Metasedimentary rocks

3: Felsic and intermediate metavolcanic rocks

2: Mafic metavolcanic Rocks

Unclassified Lineament

Brittle Lineament

Dyke Lineament

Lineament Density

4.5 (km/km²)

0

REFERENCE

Base Data: Land Information Ontario (obtained 2015);
CanVec Topography (obtained 2015)

Bedrock Geology: MRD126-REV1 (Ontario Geological Survey, 2011);
Ontario Geological Survey Map 2666 (Santaguida, 2001).

PROJECT

Phase 2 Structural Lineament Interpretation
White River Area, Ontario

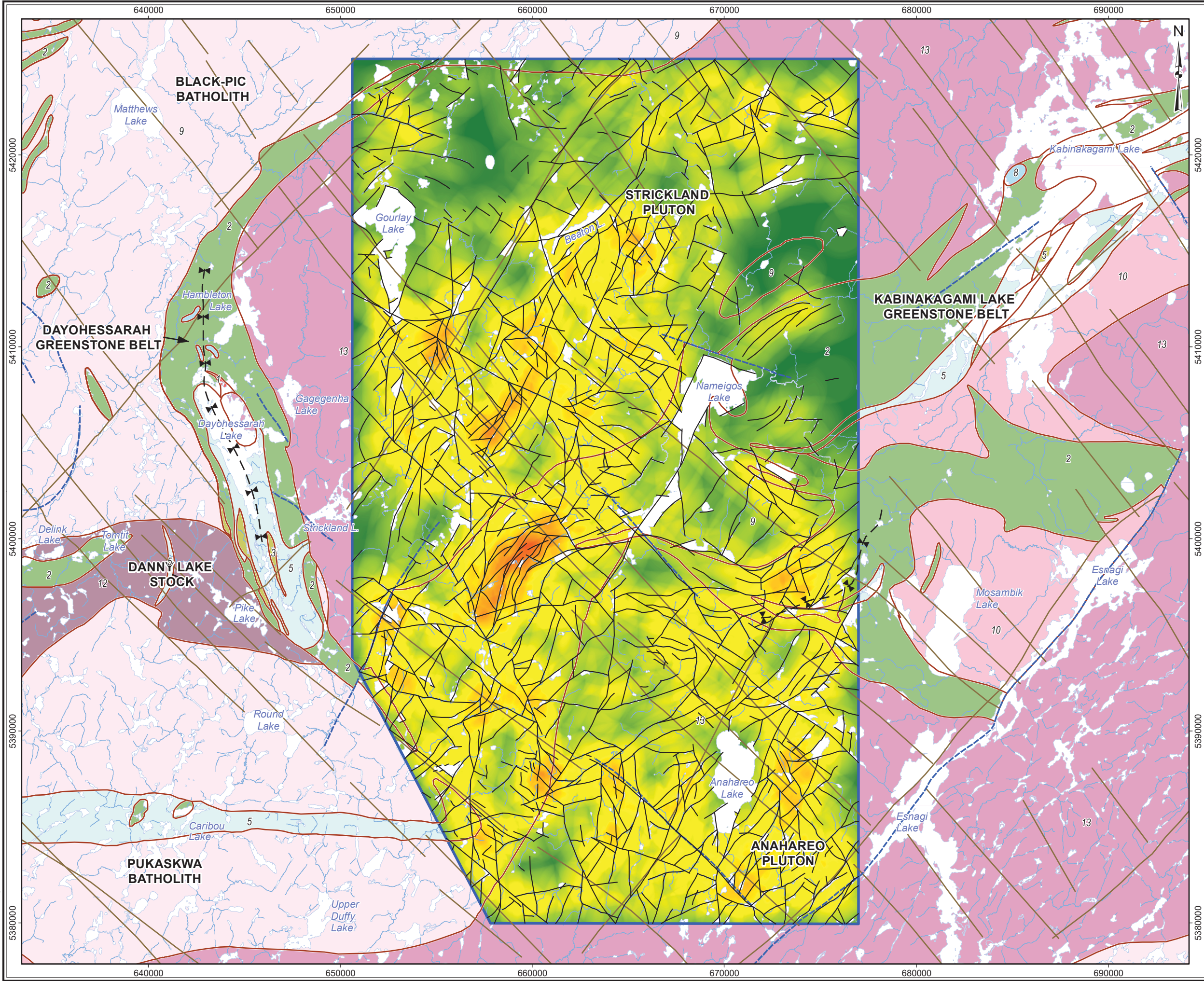
TITLE

**Lineament Density for All Interpreted
Lineaments from Pole Reduced
Magnetic Data of the White River Area**

DESIGN	KR	02 SEP 2014	REVISION 2 UTM ZONE 16N NAD 1983 1:190,000
GIS	JA	23 SEP 2016	
CHECK	SC	23 SEP 2016	
REVIEW	JPS	23 SEP 2016	

Figure 18

File: SRK_NWMO_WR_Fig19_slinDens



LEGEND

Phase 2 Assessment Area

Watercourse

Waterbody

Bedrock Geology

Fold (syncline)

Mapped Fault

Mapped Dyke

Geological Boundary

13: Granite-granodiorite

12: Diorite-monzonite- granodiorite

10: Foliated tonalite suite

9: Gneissic tonalite suite

8: Gabbro

5: Metasedimentary rocks

3: Felsic and intermediate metavolcanic rocks

2: Mafic metavolcanic Rocks

Lineament Density

4 (km/km²)

0

Surficial Lineament

REFERENCE

Base Data: Land Information Ontario (obtained 2015);
CanVec Topography (obtained 2015)

Bedrock Geology: MRD126-REV1 (Ontario Geological Survey, 2011);
Ontario Geological Survey Map 2666 (Santaguida, 2001).

0

10

km

srk consulting

PROJECT

Phase 2 Structural Lineament Interpretation
White River Area, Ontario

TITLE

Lineament Density for Interpreted Lineaments
from Surficial Data of the White River Area

DESIGN	KR	02 SEP 2014
GIS	JA	23 SEP 2016
CHECK	SC	23 SEP 2016
REVIEW	JPS	23 SEP 2016

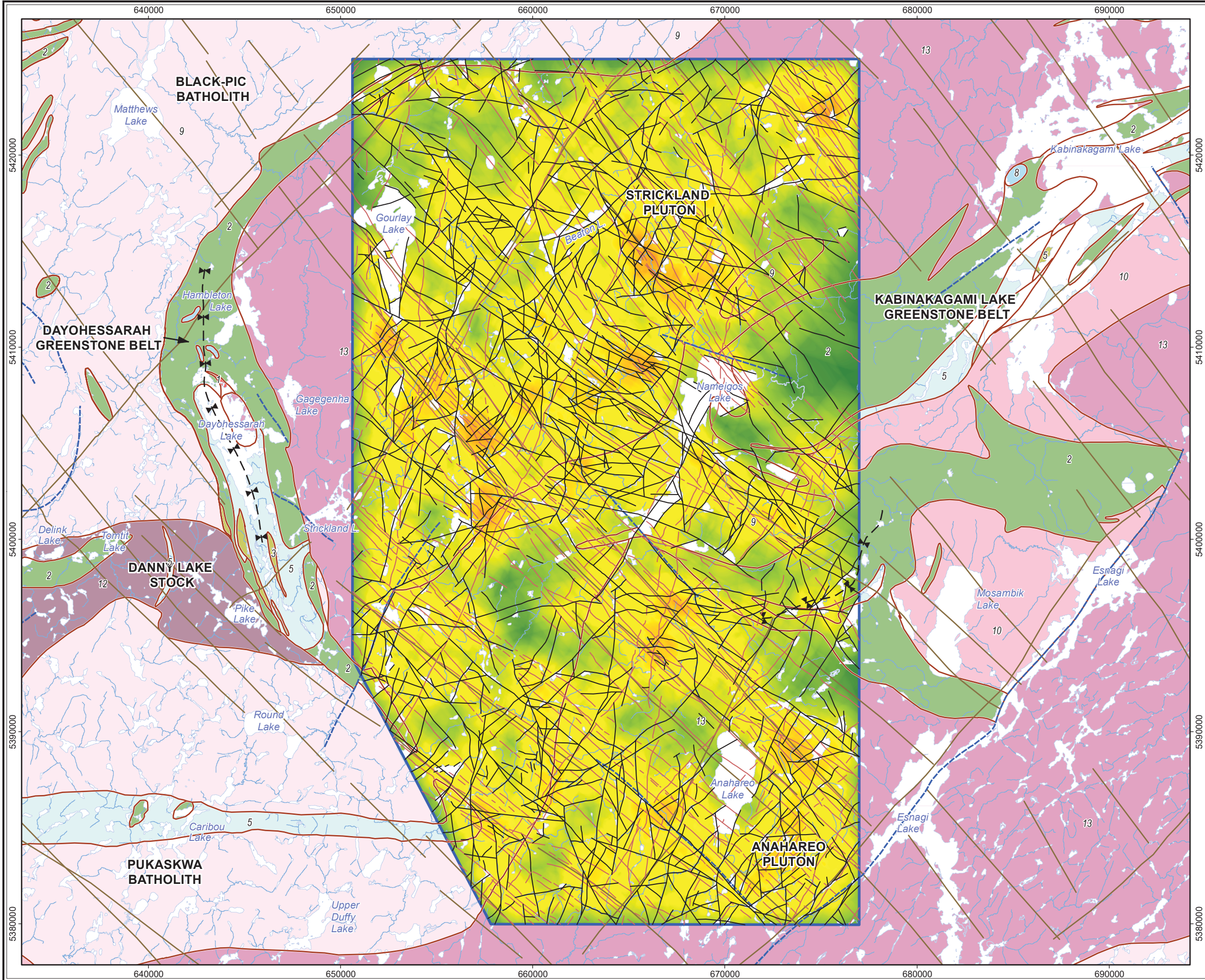
REVISION 2

UTM ZONE 16N

NAD 1983

1:190,000


Figure 19



REFERENCE

Base Data: Land Information Ontario (obtained 2015);
CanVec Topography (obtained 2015)

Bedrock Geology: MRD126-REV1 (Ontario Geological Survey, 2011);
Ontario Geological Survey Map 2666 (Santaguida, 2001).



PROJECT

Phase 2 Structural Lineament Interpretation
White River Area, Ontario

TITLE

DESIGN	KR	02 SEP 2014
GIS	JA	23 SEP 2016
CHECK	SC	23 SEP 2016
REVIEW	JPS	23 SEP 2016

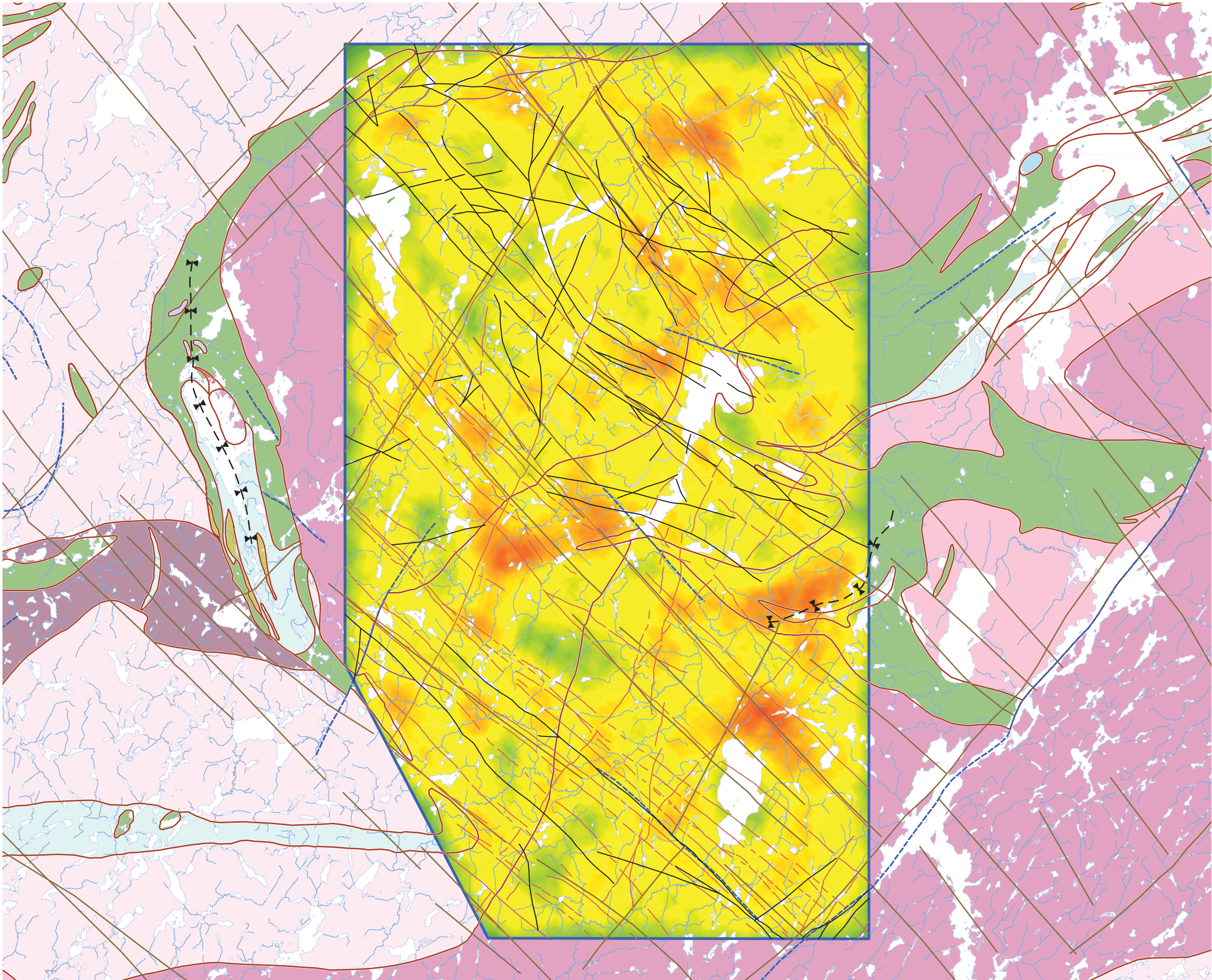
REVISION 2

UTM ZONE 16N

NAD 1983

1:190,000

Figure 20



REFERENCE

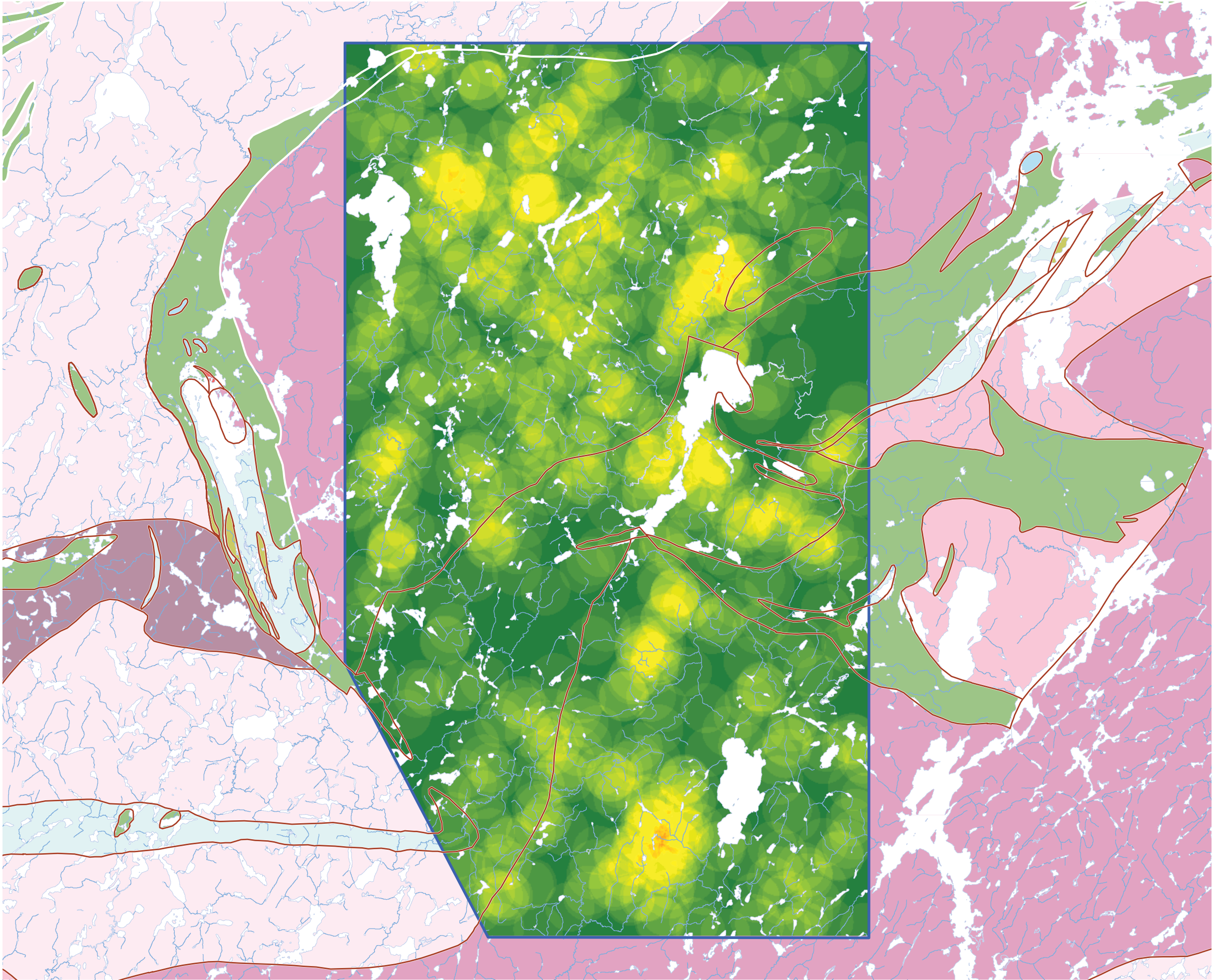
Base Data: Land Information Ontario (obtained 2015);
CanVec Topography (obtained 2015)

Bedrock Geology: MRD126-REV1 (Ontario Geological Survey, 2011);
Ontario Geological Survey Map 2666 (Santaguida, 2001).



Phase 2 Structural Lineament Interpretation
White River Area, Ontario

DESIGN	KR	02 SEP 2014	Figure 21	REVISION 2
GIS	JA	23 SEP 2016		UTM ZONE 16N
CHECK	SC	23 SEP 2016		NAD 1983
REVIEW	JPS	23 SEP 2016		1:190,000



REFERENCE

Base Data: Land Information Ontario (obtained 2015);
CanVec Topography (obtained 2015)

Bedrock Geology: MRD126-REV1 (Ontario Geological Survey, 2011);
Ontario Geological Survey Map 2666 (Santaguida, 2001).



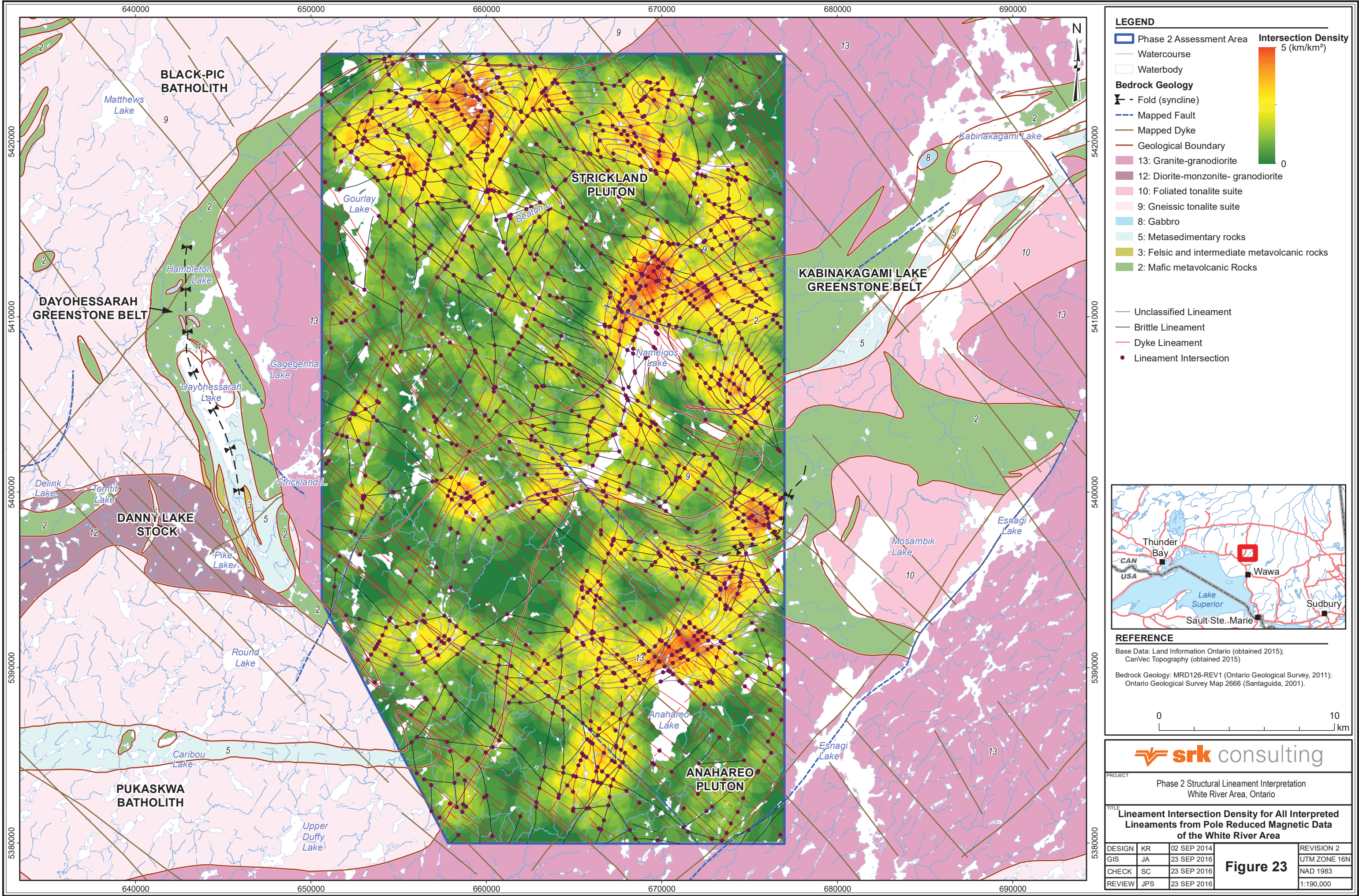
Phase 2 Structural Lineament Interpretation
White River Area, Ontario

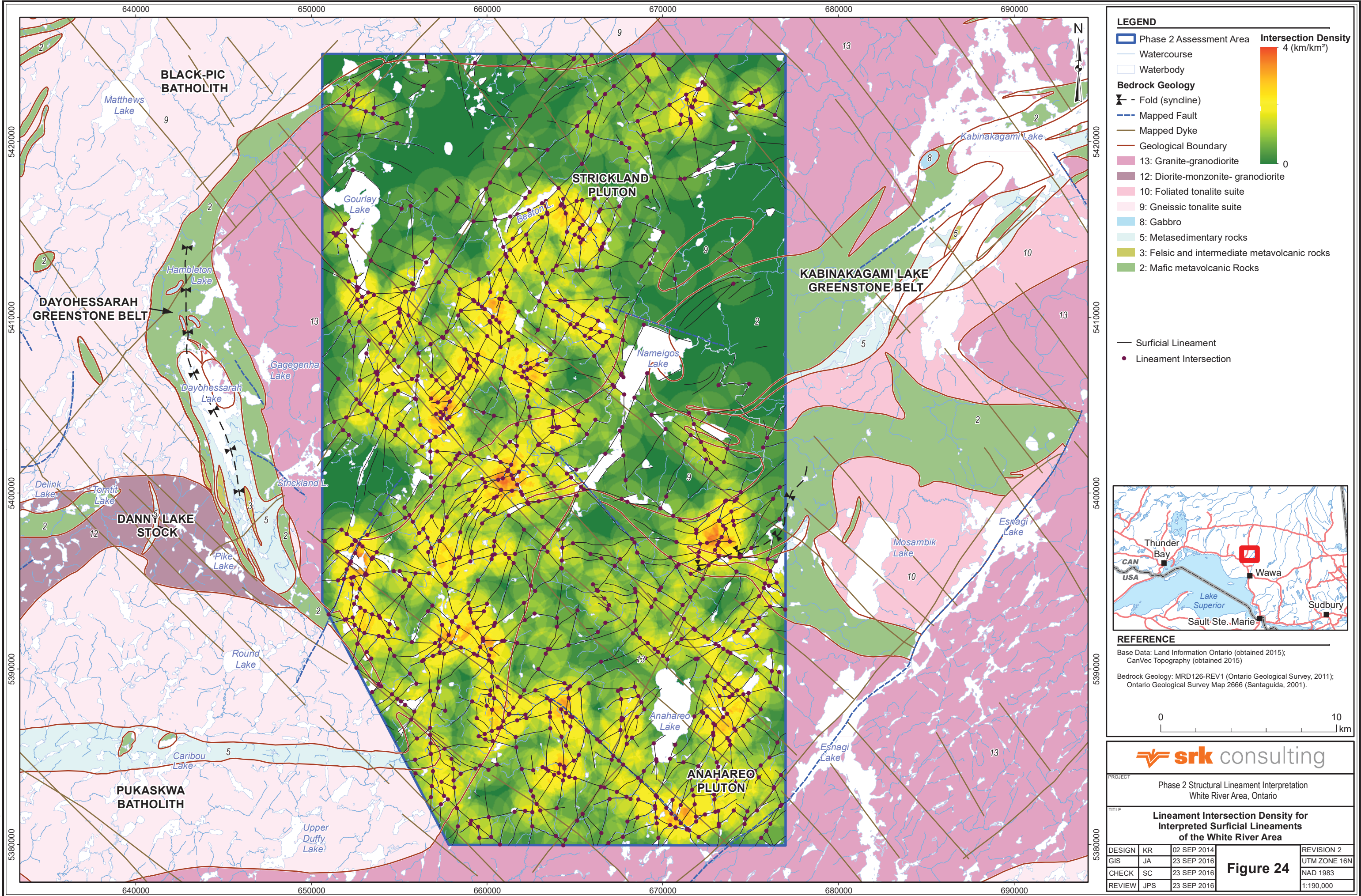
DESIGN	KR	02 SEP 2014
GIS	JA	23 SEP 2016
CHECK	SC	23 SEP 2016
REVIEW	JPS	23 SEP 2016

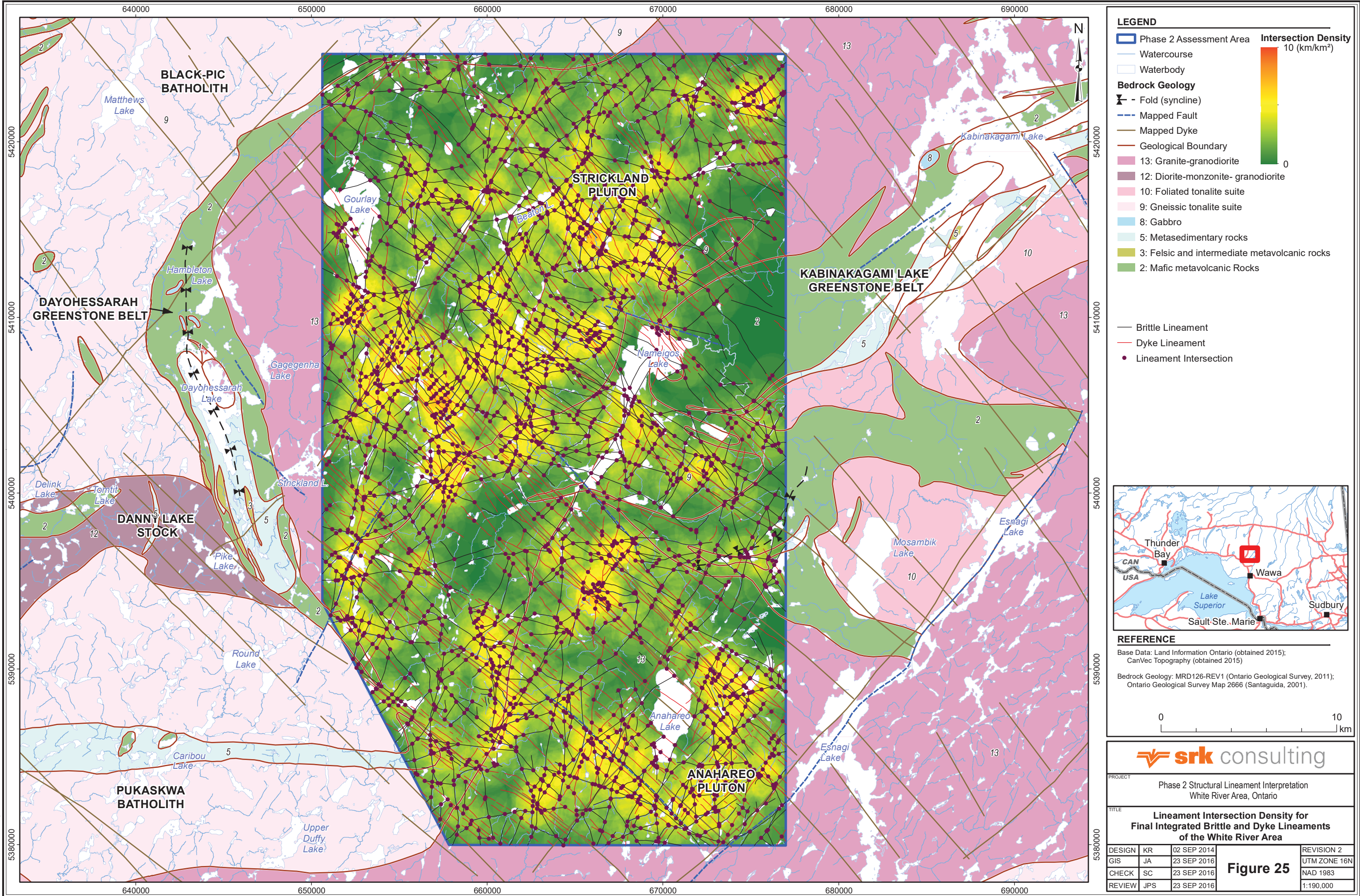
Figure 22

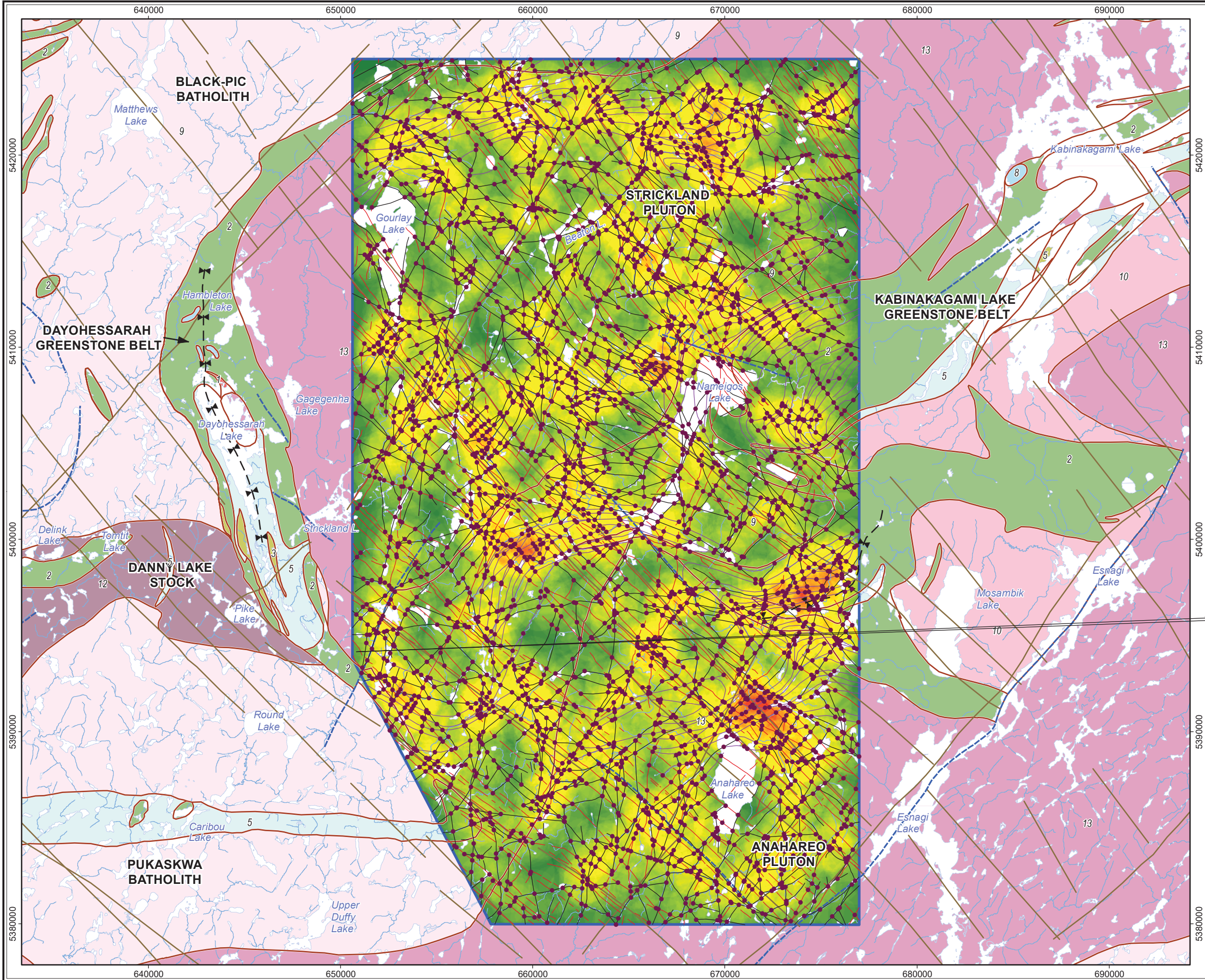
REVISION 2
UTM ZONE 16N
NAD 1983
1:190,000

File: SRK_NWMO_WR_Fig23_mUBD_intDens









REFERENCE

Base Data: Land Information Ontario (obtained 2015);
CanVec Topography (obtained 2015)

Bedrock Geology: MRD126-REV1 (Ontario Geological Survey, 2011);
Ontario Geological Survey Map 2666 (Santaguida, 2001).

PROJECT

Phase 2 Structural Lineament Interpretation
White River Area, Ontario

TITLE

DESIGN	KR	02 SEP 2014
GIS	JA	23 SEP 2016
CHECK	SC	23 SEP 2016
REVIEW	JPS	23 SEP 2016

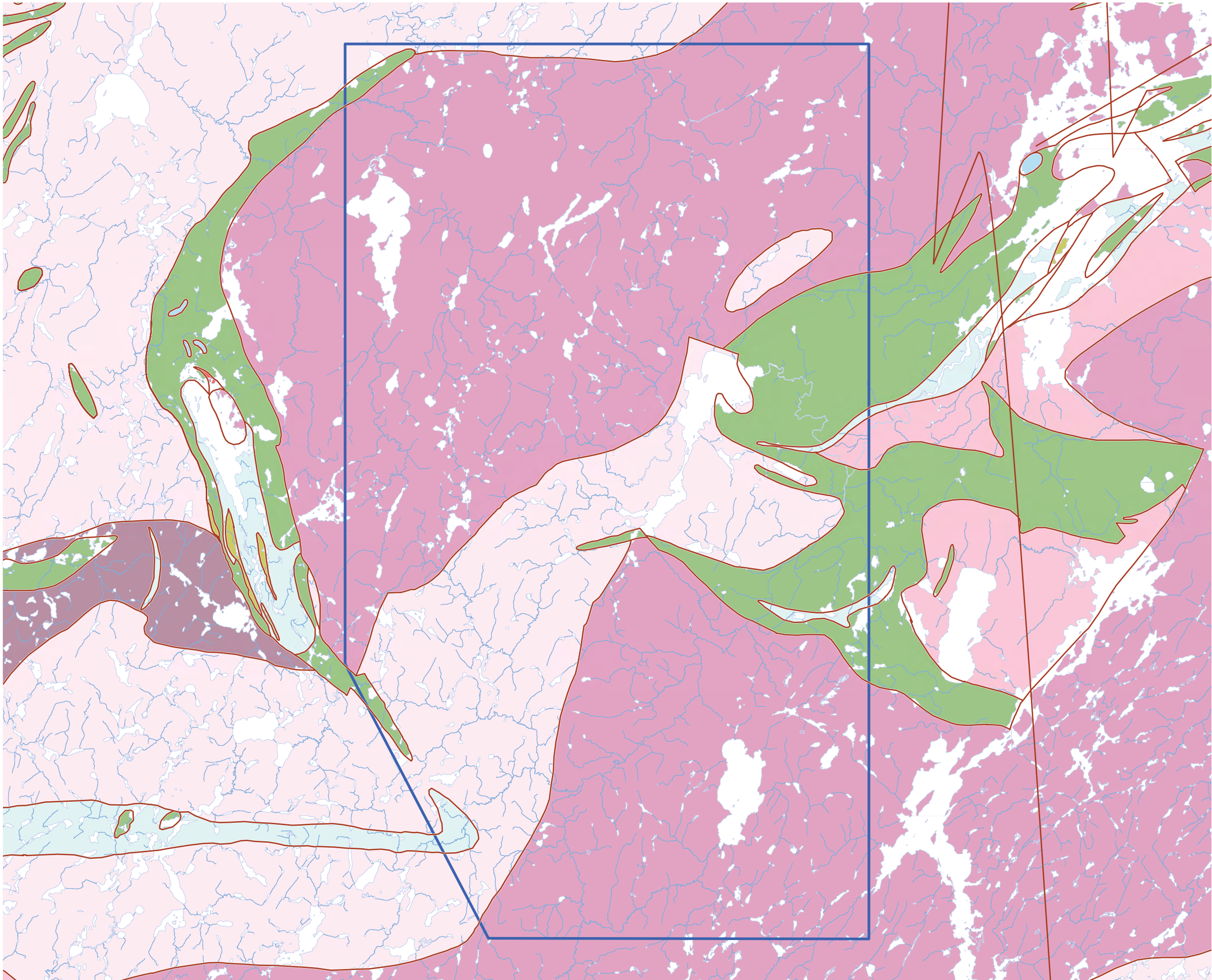
REVISION 2

UTM ZONE 16N

NAD 1983

1:190,000

Figure 26



REFERENCE

Base Data: Land Information Ontario (obtained 2015);
CanVec Topography (obtained 2015)

Bedrock Geology: MRD126-REV1 (Ontario Geological Survey, 2011);
Ontario Geological Survey Map 2666 (Santaguida, 2001).



Phase 2 Structural Lineament Interpretation
White River Area, Ontario

DESIGN	KR	02 SEP 2014
GIS	JA	11 APR 2017
CHECK	SC	11 APR 2017
REVIEW	JPS	11 APR 2017

Figure 27

REVISION 6
UTM ZONE 16N
NAD 1983
1:190,000